UNIVERSIDADE FEDERAL DE PERNAMBUCO
CENTRO DE CIÊNCIAS EXATAS E DA NATUREZA
PROGRAMA DE PÓS-GRADUAÇÃO EM FÍSICA

MIGUEL ROLANDOVICH O'REILLY LUKIN

Diffusion process of a random particle in a one-dimensional finite interval in the Fock space approach

Recife

2020

MIGUEL ROLANDOVICH O'REILLY LUKIN

Diffusion process of a random particle in a one-dimensional finite interval in the Fock space approach

Thesis presented to the Graduate Program in Physics at the Federal University of Pernambuco, as a partial requirement for obtaining the title of Doctor in Physics.

Concentration area: Theoretical and computational physics.

Supervisor: Prof. Dr. Ernesto Carneiro Pessoa Raposo

Co-supervisor: Prof. Dr. Hugo de Andrade Araújo

Recife

2020

Catalogação na fonte
Bibliotecária Mariana de Souza Alves CRB4-2105

L954d Lukin, Miguel Rolandovich O'reilly
Diffusion process of a random particle in a one-dimensional finite interval in the Fock space approach / Miguel Rolandovich O'reilly Lukin. – 2020.
107f.: il., fig.

Orientador: Ernesto Carneiro Pessoa Raposo.
Tese (Doutorado) – Universidade Federal de Pernambuco. CCEN, Física, Recife, 2020.
Inclui referências e apêndices.

1. Física Teórica e Computacional. 2. Caminhante aleatório. 3. Difusão normal. 4. Difusão anômala. I. Raposo, Ernesto Carneiro Pessoa. (orientador) II. Título.

530.1 CDD (22. ed.) UFPE-CCEN 2020-202

MIGUEL ROLANDOVICH O'REILLY LUKIN

DIFFUSION PROCESS OF A RANDOM PARTICLE IN A ONE-DIMENSIONAL FINITE INTERVAL IN THE FOCK SPACE APPROACH

Thesis presented to the Posgraduate Program in Physics at the Federal University of Pernambuco, as a partial requirement for obtaining the title of Doctor in Physics.

Aprovada em: 28/10/2020.

BANCA EXAMINADORA

_____

Prof. Ernesto Carneiro Pessoa Raposo
Orientador
Universidade Federal de Pernambuco

_____

Prof. Paulo Roberto de Araújo Campos
Examinador Interno
Universidade Federal de Pernambuco

_____

Prof. Renê Rodrigues Montenegro Filho
Examinador Interno
Universidade Federal de Pernambuco

_____

Prof. Francisco Anacleto Barros Fidelis de Moura
Examinador Externo
Universidade Federal de Alagoas

_____

Prof. Madras Viswanathan Gandhi Mohan
Examinador Externo
Universidade Federal do Rio Grande do Norte

a DEUS

ACKNOWLEDGEMENTS

Thanks God. To God, all honor and glory.

To my mother, that made possible this journey.

To my tutor, who gave me a lot of opportunities, who never gave up on me, to his immense patience and wisdom. My entire life is not enough to thank you.

To the friends I have and made in Brazil, specially to Jesus, Ammis, Guillermo, Enrique, Javier, Hermes, Yosdan and many more. Thanks to all who somehow help me in this country Brazil where at the first moments gave me a hand, have spoken for me in portuguese because a knew nothing about it.

To all the excellent teachers I had in the physics department at UFPE and even in the other university where I have been, UFPB. My gratitude for contributing in my formation not only as a physicist but as a better man.

To the secretary of the physics department, Alexsandra, a very nice woman, very professional.

To my wife, Enmeline and my son, Ernesto Alejandro. My life is devoted to you two. Thanks for supporting me in the best and the worst moments, for being with me always, even in the distance, and now for joined me here in Brazil.

To this country, that I loved, love and will love forever for give me this chance to study and to learn physics. Thanks to the financial support of FACEPE and latter now to CAPES.

THANKS TO EVERY ONE (just in case I missed anyone, thanks to all).

ABSTRACT

In this work we study the statistical properties of a random walker (RW) in a one-dimensional discrete lattice in different scenarios. In the simplest case, the steps of the RW have fixed length and equal probabilities to hop to the right or to the left, in a lattice with absorbing borders. We apply the Fock space approach to obtain a Schrödinger-like equation from a master equation that describes the transport mechanisms of the random particle and that allows us to write a quasi-Hamiltonian and compute the probability of the RW to be at any position in the lattice after some arbitrary time. The plot of the probability versus position shows, in this simplest case, an expected Gaussian distribution when the borders are still untouched, with a change occurring after the borders are reached. In addition, we compute some quantities like the mean value and standard deviation of the RW position. In a second scenario, we study the RW behavior under a power-law distribution of step lengths, with the power-law exponent controlling the diffusive properties of the RW, from the superdiffusive regime for this variable exponent in the interval (1,3) to the diffusive (normal, Gaussian-like) regime with values greater than 3. In a similar manner, we compute the probability distribution of the RW as a function of the position and time, and the mean value, standard deviation, and survival rate as a function of time. We show that after a few steps the behavior of the survival probability is proportional to the inverse of the square root of time, that obeys the Sparre-Andersen theorem, when the RW can reach only one border, and its long-term asymptotic behavior is given by an exponential decay behavior, when both absorbing borders are touched. Finally, we study the behavior of the RW with Lévy alfa-stable distribution of step lengths. The behavior of the probability distribution of the RW as a function of the position in the lattice is shown, as well as the survival rate and other relevant quantities. Overall, the statistical properties of the Lévy and power-law RWs are found to be similar, as expected. Indeed, the power-law distribution corresponds to the asymptotic limit of the Lévy distribution. Our findings are generally found to be in good agreement with previous results for these types of RW particles obtained under other approaches.

Keywords: Random walk. Normal diffusion. Anomalous diffusion. Fock space approach. Power-law distribution. Lévy alfa-stable distribution.

RESUMO

Estudamos o modelo do caminhante aleatório (RW) em uma rede 1D de N sítios em diferentes cenários usando o formalismo de espaço de Fock. No caso mais simples, o RW é governado por uma distribuição com comprimento fixo de passo e probabilidade igual de saltar para a direita ou para a esquerda de um sitio para outro na rede com bordas absorventes. Também aplicamos a abordagem do espaço Fock para obter uma equação do tipo Schrödinger a partir de uma equação mestra que descreve o mecanismo de transporte do RW e nos permite escrever um quase-hamiltoniano e calcular a probabilidade em qualquer posição da rede após algum tempo arbitrário. O gráfico da probabilidade versus posição mostra uma distribuição gaussiana esperada quando as bordas ainda não são atingidas, com uma mudança ocorrendo depois que as bordas são atingidas. Além disso, calculamos algumas quantidades, como o valor médio e o desvio padrão da posição da partícula. Em um segundo cenário estudamos o comportamento do RW, desta vez sob uma distribuição de Lei de Potência onde o indice expõente muda do regime superdifusivo para valor igual a 2 até os regimes gaussianos para valor igual a 3. De maneira semelhante, calculamos a posição da probabilidade no tempo, o valor médio, o desvio padrão e a taxa de sobrevivência da partícula. Em particular, investigamos o comportamento da taxa de sobrevivência S em função do tempo. Mostramos que, após algumas etapas, o comportamento de S é função do inverso da raiz quadrada do tempo, que obedece ao teorema de Sparre-Andersen, e seu comportamento assintótico a longo prazo é dado por um decaimento exponencial. Finalmente, estudamos o comportamento do RW com uma distribuição Lévy alfa estável. E apresentado, ao gráfico para a probabilidade em função da posição na rede e também são calculadas as demais quantidades.

Palavras-chaves: Caminhante aleatório. Difusão normal. Difusão anômala. Abordagem no espaço de Fock. Distribuição da lei de potência. Distribuição de Lévy alfa-estável.

LIST OF FIGURES

CONTENTS

1 INTRODUCTION

« Look deep into nature, and then you will understand everything better. »

Albert Einstein

Resumo do capítulo.

Esta tese consta de seis capítulos. Inicialmente, apresentamos um capítulo introdutório de conceitos básicos tais como a definição do problema da busca aleatória, o teorema central do limite e também uma generalização deste para casos de funções densidade de probabilidade com primeiros momentos divergentes. Além disso, mencionamos os tipos de difusões subdivididas em difusão normal e anômala, e finalmente temos também uma seção para a apresentação da família de distribuições α-estáveis de Lévy.

O Capítulo 2 é dedicado à discussão do formalismo do espaço Fock como uma ferramenta matemática comumente usada na mecânica quântica e que pode ser estendida a processos estocásticos clássicos. Mostraremos que o espaço de Fock também é adequado para abordar o problema da busca aleatória sob uma perspectiva diferente, com aplicação a três distribuições de probabilidade de tamanhos de passos, a saber: distribuição tipo delta de Dirac com comprimento de passo fixo, distribuição com decaimento lei de potência e distribuições de Lévy.

O terceiro capítulo contém os resultados de um exemplo de caminhada aleatória realizada em um intervalo unidimensional com posições discretas e sítios absorventes nas bordas, onde é estudado o comportamento de um caminhante saltando de um sítio para outro com tamanho fixo de passos.

No Capítulo 4 são apresentados os resultados do comportamento estatístico de um caminhante aleatório cujos tamanhos de passos seguem uma distribuição do tipo lei de potência, analisado para diferentes valores do exponente μ que determina o tipo de difusão (normal ou superdifusivo) da caminhada aleatória.

O Capítulo 5 reúne os resultados de um caminhante aleatório cujos tamanhos de passos são regidos por uma distribuição α-estável de Lévy, mostrando o comportamento estatístico do processo para o índice de Lévy $\alpha \in (0,2]$. Esses resultados foram publicados recentemente no artigo [Araújo et al. 2020].

Finalmente, o último capítulo apresenta as conclusões deste trabalho e as perspectivas para projetos posteriores.

Dois apêndices são também incluídos contendo cálculos auxiliares que, por serem muito específicos e detalhados, seriam mais adequados se apresentados separadamente do texto principal da tese.

1.1 THE RANDOM SEARCH PROBLEM

The problem of random searches encompasses a variety of phenomena. To mention a few examples, we can cite the search for lost or forgotten keys [Bénichou et al. 2011], looking for and capturing criminals by the police [Viswanathan et al. 2011], heartbeat rate studies to detect cardiac problems and related diseases [Peng et al. 1993], and the animal foraging theory [Hallam and (eds.) 1986, Viswanathan et al. 2011]. In particular, we focus our attention to random searches in the context of animal foraging.

The problem of random search is defined as the quest for the most efficient strategy to be adopted when one is searching for randomly distributed sites with a limited view of the search space. The strategy depends on the probability $P(\ell)d\ell$ of giving a step length of size $[\ell, \ell + d\ell)$, where $P(\ell)$ is the probability density function (PDF) of step lengths. The efficiency of the search is generally defined as [Viswanathan et al. 2011, Neto 2012]

$$\eta = \frac{\texttt{number of sites found}}{\texttt{total distance traveled}}. \tag{1.1}$$

As the name indicates, we are dealing with a process that is not deterministic, i.e., it is random and depends on many factors or variables related to the components of the random search. The searcher can be the predator in the case of an animal searching for food, and the target can be the prey, which could be another animal or other source of nourishment like plants, grass, etc. These agents could have or not information about the environment. In fact, the knowledge *a priori* of where to find food should influence the outcome of the search [Viswanathan et al. 2011]. Also, there are a number of variables involving physiological capacities, that could be translated, e.g., into the lower or higher expenditure of energy to reach the goals of the search. As for the targets, they could be abundant or scarce, and their density certainly influences the search efficiency as well. Furthermore, the target could be fixed or mobile.

To analyze this complex problem, many ideas, models, and studies have been developed from different fields of science [Viswanathan et al. 2011]. Researches working in the area have often

improved the theoretical models by learning from nature, watching the evolution and extinction of species, observing and detecting movement patterns an so on. From the statistical physics perspective, the random search problem have been mostly approached as a stochastic diffusion-reaction process [Viswanathan et al. 2011]. Many mathematical tools at disposal, as well as statistical mechanics concepts and computing simulations have been used to try to reproduce the reality in the nearest way possible, including the analysis of the mechanisms that describe the search processes, which frequently involves the quest to find the more suitable distribution of step lengths along search paths subject to boundary conditions and external constraints.

The first works related to the random search problem were mostly empirical, dated from Ancient Greece with the investigations of Aristotle and Theophrastus about the relationship between the organisms and the environment [Goodenough, McGuire and Jakob 2009]. Later on, Darwin presented his thesis on the evolution of species [Darwin 1992]. Yet, no mathematical modeling was available until the formulation of Fick's law [Fick 1855] and Albert Einstein's work [Einstein 1905] about Brownian motion, observed by Robert Brown [Brown 1828] in pollen particles floating in a container with liquid. Was Karl Pearson in 1905, who introduced the model of random walk.

In the particular case of animal foraging, an important aspect is the search optimization, which leads to the highest possible efficiency given a specific context, achieved by employing specific search strategies to reach better results. The first step in this direction was taken around the 1960's by MacArthur [MacArthur and Pianka 1966] and Emlen [Emlen 1966], in an approach termed optimal foraging theory - OFT. However, until the 1990's all the attempts to describe animal foraging were related to agents generally displaying normal diffusion with step lengths much smaller than the path length and dynamics driven by the Central Limit Theorem (CLT), which we study in the next section. As the theory could not predict the existence of long steps observed in the movement patterns of some animal species, some of which eventually comparable to the path length itself, consequently many experimental data could not be suitably described by these first theoretical models. In this sense, the introduction in the 1990's of Lévy α-stable distributions of step lengths provided the possibility to adequately portray these types of animal movements in which large steps occurred with small but non-negligible probability [Viswanathan et al. 2011]. In the so-called stochastic optimal foraging theory - SOFT [Viswanathan et al. 2011], the predator is generally assumed not to have full information about the environment where it is seeking for food. Then randomness plays a fundamental role in the search optimization process. As we shall review in this work, in some situations the best efficiency is achieved by random

walkers with Lévy distributions of step lengths, whose statistics is described by the generalized CLT, to be presented below.

In this work, we address the random search problem in a one-dimensional search space using the Fock space formalism, to be detailed in Chapter 2. A random walk particle is left to move stochastically, starting from a given initial position and with the step lengths drawn from some PDF, and its movement stops only upon the finding of one of the two target sites placed at the borders of the one-dimensional interval. After finding a target, the searcher restarts the search from the same initial position and, thus, a search efficiency can be calculated as a function of the starting point and the PDF of step lengths.

1.2 CENTRAL LIMIT THEOREM (CLT)

The first works on the Central Limit Theorem (CLT) date to 1733. Abraham De Moivre discovered that the sum of all the results derived from the toss of a coin for a large number of events tended to a Gaussian distribution. This subject was published in his book *Doctrine of Chances* around 1736 [Moivre 1967]. Later on, Laplace extended the work of De Moivre to the sum of random variables with other distributions, for example an uniform distribution, and saw exactly the same result, a convergence to a Gaussian distribution as the number of variables increased considerably to a large number. He also developed the method of characteristic functions to study the convergence of sums of random variables published in his book *Analytical Theory of Probabilities*. Pólya finally coined out the name of CLT to the previous results of De Moivre and Laplace, due to the relevance of this subject to the theory of probabilities.

This theorem was known at the time as the “law of frequency errors”, because of its application to show that measurement errors can be approximately normally distributed. Yet, a rigorous demonstration of this theorem waited until 1901-1902 when the Russian mathematician and physicist Alexander Liapunov gave a proper proof, based on more general conditions and the work of Chevyshev and Markov.

Let us imagine the following experiment. We have 5 types of balls labeled from 1 to 5, and we associate to each type of ball a probability to be picked from a total of n balls contained in a box. The set of probabilities is the same each time a ball is going to be picked, and subsequent balls are picked independently one from the other. So we say that the picks of the balls are stochastic events described by random variables that are identically and independently distributed (i.i.d.), as we discuss below. For example, we associate to the balls of type 1 a probability $P_1 = 0.125$ to

be picked, to balls 2 a $P_2 = 0.125$, to balls 3 a $P_3 = 0.3$, to balls 4 a $P_4 = 0.4$, and to balls 5 a $P_5 = 0.05$, in a way that the sum of all probabilities is equal to 1. Then we have in this case a nonuniform set of probabilities to pick each type of ball from the box, as shown in Fig. 1.

Suppose now that N picks are independently taken from the box (each time a ball is picked, it returns to the box so that the set of probabilities remains unaltered at each pick). We call this a sample $\{X_1, X_2, ..., X_N\}$, where X_i is the label number of the ball drawn in the i-th pick ($X_i = 1, 2, ..., 5$), with $i = 1, 2, ..., N$. Let us define the random sum variable $S_N = X_1 + X_2 + \cdots + X_N$ associated with this sample. Now the idea is to pick various (L) samples. We prove next that, according to the CLT, the distribution of the L values of the variable S_N converges to a Gaussian for $N \gg 1$ and $L \gg 1$. Indeed, with the help of a program built in *Matlab* we show in Fig. 2 that the distribution of $L = 10^6$ values ($L = 10^6$ samples) of the sum variable S_N progressively converges to a Gaussian as larger N's are considered ($N = 5, 10, 100, 300$ in Fig. 2).

Figure 1 – PDF $P(x)$ for a set of 5 types of balls, each one with a given probability to be picked from a box. The continuous variable x assumes the values $x = 1, 2, 3, 4, 5$ related to the 5 types of balls, so that $P(x) \neq 0$ only for these values of x, whereas $P(x) = 0$ otherwise. Thus the PDF $P(x)$ can be written as a sum of five Dirac delta functions in the form $P(x) = \sum_{i=1}^{5} P_i \delta(x - i)$, where P_i is the probability to pick the ball of type i from the box. We notice that these probabilities are not uniformly distributed.

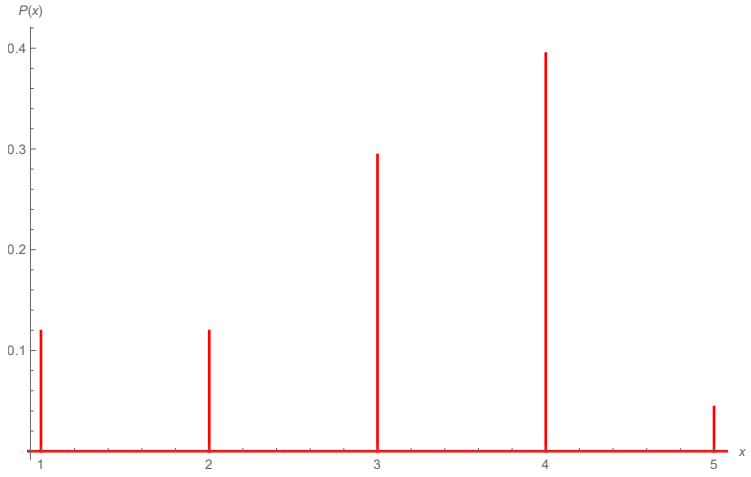

Figure 2 – PDF of the sum S_N of N random variables i.i.d. associated with the 5 types of balls picked from a box, see Fig. 1. The plots represent $L = 10^6$ values of the sum S_N with $N = 5, 10, 100, 300$ terms.

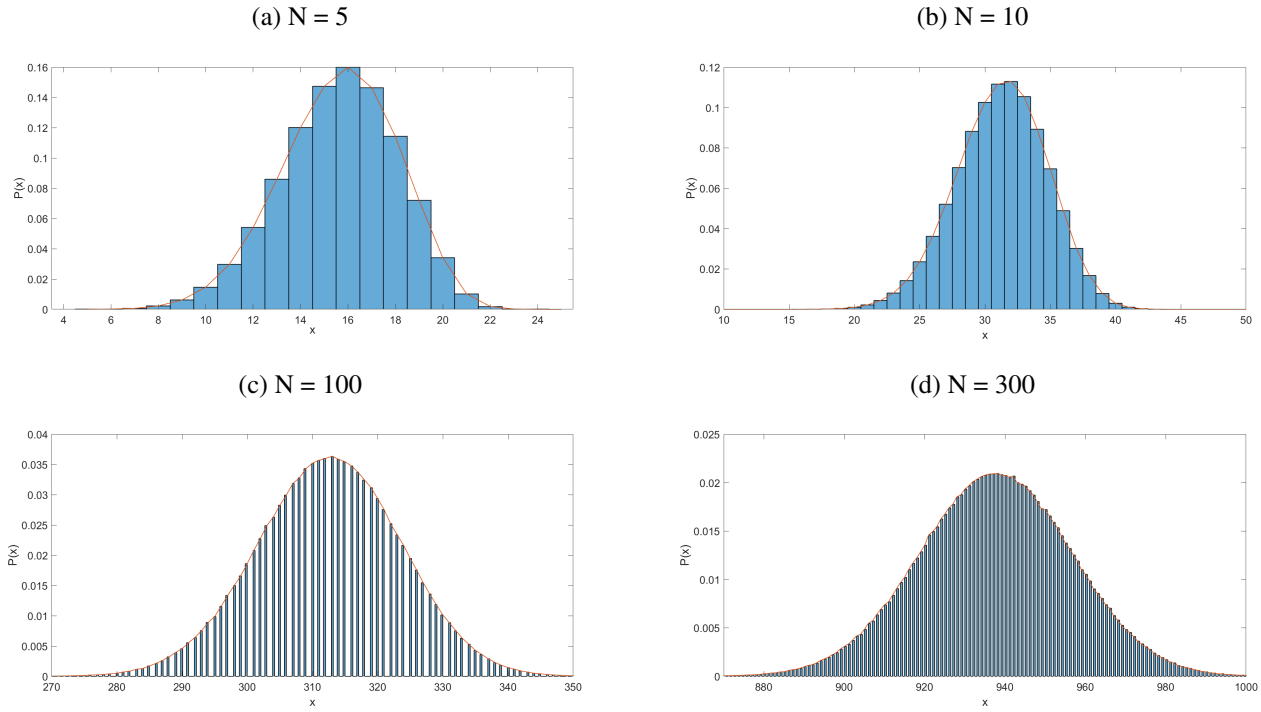

Based on [Ross 1997] we enunciate the CLT and prove it using moment generating functions.

Theorem 1 (Central Limit Theorem)**.** *Let* $S_N = \sum_{i=1}^{N} X_i = X_1 + X_2 + \cdots + X_N$ *be the sum of* N *i.i.d. random variables, each one having the same mean denoted by* μ *and finite variance* σ^2*. Then the distribution of the rescaled variable*

$$Z_N = \frac{S_N/N - \mu}{\frac{\sigma}{\sqrt{N}}} = \frac{S_N - N\mu}{\sigma\sqrt{N}} \tag{1.2}$$

tends to the standard normal distribution when $N \to \infty$*, i.e.,*

$$P\{Z_N \leqslant \varepsilon\} \overset{N\to\infty}{\longrightarrow} \frac{1}{\sqrt{2\pi}} \int_{-\infty}^{\varepsilon} e^{-x^2/2}\, dx, \tag{1.3}$$

for $-\infty < \varepsilon < \infty$*.*

Before proving this theorem we will define some concepts used in the demonstration, such as the n-th moment of the PDF $F_X(x)$ associated with the random variable x:

$$E(x^n) = M_X = \int_{-\infty}^{\infty} x^n F_X(x) dx \tag{1.4}$$

Equation (1.4) is known as the moment generating function. We can obtain from it the mean value or expectation value $(n = 1)$, the second moment $(n = 2)$, and then using these results to calculate the variance, and so on. Also, we consider the following lemma:

Lemma 1. *Let $Z_1, Z_2, \ldots$ be a succession of random variables with distribution function F_{Z_N} and moment generating functions $M_{Z_N}, N \geq 1$; and let Z be a random variable with distribution function F_Z and moment generating function M_Z. If $M_{Z_N}(t) \to M_Z(t)\ \forall t$, then $F_{Z_N}(t) \to F_Z(t)\ \forall t$ at which $F_Z(t)$ is continuous.*

Proof. If we let Z to be a random variable with normal distribution, i.e., $Z \sim N(\mu, \sigma^2)$, with $\mu = 0$ and $\sigma^2 = 1$, then we shall see below that $M_Z(t) = e^{\frac{t^2}{2}}$, and from the lemma 1 above $M_{Z_N}(t) \overset{N\to\infty}{\longrightarrow} e^{\frac{t^2}{2}}$ and $F_{Z_N}(t) \overset{N\to\infty}{\longrightarrow} F_Z(t)$.
According to Eq. (1.2), we write

$$\begin{aligned} M_{Z_N}(t) &= E(e^{tZ_N}) \\ &= E\left(e^{\frac{t}{\sqrt{N}}\sum_{i=1}^{N}\left(\frac{X_i-\mu}{\sigma}\right)}\right) \\ &= E\left(e^{\frac{t}{\sqrt{N}}\left(\frac{X_1-\mu}{\sigma}\right)+\cdots+\frac{t}{\sqrt{N}}\left(\frac{X_N-\mu}{\sigma}\right)}\right) \\ &= \left[M_{Z=\frac{X-\mu}{\sigma}}\left(\frac{t}{\sqrt{N}}\right)\right]^N \\ &= \left[1+\frac{t}{\sqrt{N}}E\left(\frac{X-\mu}{\sigma}\right)+\frac{t^2}{2N}E\left(\frac{X-\mu}{\sigma}\right)^2+\mathcal{O}\left(\frac{t^2}{N}\right)\right]^N, \end{aligned} \tag{1.5}$$

where

$$\begin{aligned} E\left(\frac{X-\mu}{\sigma}\right) &= \frac{1}{\sqrt{2\pi}\sigma}\int_{-\infty}^{\infty}\left(\frac{X-\mu}{\sigma}\right)e^{-\frac{(X-\mu)^2}{2\sigma^2}}dX \\ &= \frac{1}{\sqrt{2\pi}}\int_{-\infty}^{\infty} y\,e^{-\frac{y^2}{2}}dy \equiv 0. \end{aligned} \tag{1.6}$$

Similarly,

$$\begin{aligned} E\left(\frac{X-\mu}{\sigma}\right)^2 &= \frac{1}{\sqrt{2\pi}\sigma}\int_{-\infty}^{\infty}\left(\frac{X-\mu}{\sigma}\right)^2 e^{-\frac{(X-\mu)^2}{2\sigma^2}}dX \\ &= \frac{1}{\sqrt{2\pi}}\int_{-\infty}^{\infty} y^2\,e^{-\frac{y^2}{2}}dy \\ &= \frac{-2}{\sqrt{2\pi}}\frac{d}{d\beta}\int_{-\infty}^{\infty} e^{-\frac{\beta y^2}{2}}dy = \frac{-2}{\sqrt{2\pi}}\frac{d}{d\beta}\left(\frac{2\pi}{\beta}\right)^{\frac{1}{2}} = \left(\frac{1}{\beta}\right)^{\frac{3}{2}} \equiv 1, \qquad \beta = 1. \end{aligned} \tag{1.7}$$

Then, returning to Eq. (1.5) we find

$$\begin{aligned} M_{Z_N}(t) &= \left[1+\frac{t^2}{2N}+\mathcal{O}\left(\frac{t^3}{N}\right)\right]^N \\ &\overset{N\to\infty}{\longrightarrow} e^{\frac{t^2}{2}}. \end{aligned} \tag{1.8}$$

Sometimes the moment generating function is not defined, because the integral $E\left(\frac{X-\mu}{\sigma}\right)$ does not converge. In this case, making the variable t imaginary solves the problem and the

integral converges. The characteristic function is then obtained, $\varphi_Z(t) = E[e^{itZ}]$, and Eq. (1.8) takes the form

$$\varphi_{Z_N}(t) = \left[1 - \frac{\sigma^2 t^2}{2N} + \mathcal{O}\left(\frac{t^3}{N}\right)\right]^N \xrightarrow{N\to\infty} e^{\frac{-\sigma^2 t^2}{2}}. \tag{1.9}$$

□

We have proven, in a simple manner, that the sum of any succession of random variables i.i.d. with well-defined first and second moments converges to a normal distribution $\sim N(\mu, \sigma^2/N)$. The Gaussian distribution is then considered to be a statistical attractor for distributions that fulfill these criteria.

1.3 GENERALIZATION OF THE CENTRAL LIMIT THEOREM

So far we have seen that the CLT holds for any succession of random variables that are i.i.d. and with finite first and second moments. However, even if these conditions are relaxed the CLT might still work though in modified versions. For example, a Gaussian distribution can still be found in some specific circumstances in which short-range correlations occur between the random variables in the sum, or even if they are not i.i.d., in a weaker version of the CLT. Nevertheless, we will focus our attention here in what happens when the first moments of the random variables are not finite. In this context, before we formulate the generalized CLT (GCLT), we mention one important characteristic that concerns the stability of a PDF. Consider, e.g., a random variable X given by the linear combination of two other independent random variables, X_1 and X_2, with same distribution. A distribution is said to be stable if

$$aX_1 + bX_2 \overset{\mathrm{d}}{=} uX + v, \tag{1.10}$$

where the symbol $\overset{\mathrm{d}}{=}$ means that, up to location and scale parameters, X has the same distribution as X_1 and X_2 [Nolan 2018]. In more formal terms we can state the following.

Definition 1. *A random variable X is stable in the broad sense if for X_1 and X_2 independent copies of X and any positive constants a and b, the relation (1.10) holds for some positive u and some $v \in \mathbb{R}$. The random variable is strictly stable if (1.10) holds with $v = 0$ for all choices of a and b. A random variable is symmetric stable if it is stable and symmetrically distributed around 0, e.g., $X \overset{d}{=} -X$.*

The Gaussian distribution is a stable one, but there are other distributions that also fulfills this definition, with the difference that their first moments are not finite. The French mathematician and statistician Paul Lévy studied this type of special distributions in the 1930's. His work introduced the family of α-stable distributions, nowadays known as Lévy α-stable distributions, that are parametrized by a stability index $\alpha \in (0,2]$, with the Gaussian distribution as the limit case $\alpha = 2$. Lévy α-stable distributions generally lack closed forms for their probability densities in terms of elementary functions, except for three known cases. We dedicate a section to the Lévy α-stable distributions below.

We know enunciate the GCLT according to [Nolan 2018].

Theorem 2 (Generalized Central Limit Theorem)**.** *A nondegenerate random variable Z is α-stable for some $0 < \alpha \leq 2$ if and only if there is an i.i.d. sequence of random variables $X_1, X_2, X_3, \ldots$ and constants $a_n > 0$, $b_n \in \mathbb{R}$ with*

$$a_n(X_1 + \cdots + X_n) - b_n \xrightarrow{d} -Z. \tag{1.11}$$

Definition 2. *A random variable X is in the domain of attraction of Z if there exists constants $a_n > 0$, $b_n \in \mathbb{R}$ with $a_n(X_1 + \cdots + X_n) - b_n \xrightarrow{d} -Z$, where $X_1, X_2, X_3, \ldots$ are i.i.d. copies of X.*

The family of Lévy α-stable distributions that follows the GCLT thus extends the basin of statistical attractors, that is, the "attraction domain of stable laws" [Bercovici, Pata and Biane 1999], in which the Gaussian distribution is included as a particular case.

1.4 DIFFUSION. TYPES OF DIFFUSION.

The dynamics of the diffusion process of a random walk particle governed by the CLT can be generally described by a Fokker–Planck equation (FPE), which is a partial differential equation that determines the time evolution of the PDF of the particle. In this subsection we introduce and study the FPE and its associated normal diffusion dynamics, and in the next subsections we consider the cases of anomalous (subdiffusive and superdiffusive) dynamics.

First, let us assume for simplicity a one-dimensional stochastic process $\{x(t) : t \geq 0\}$. We consider the Chapman-Kolmogorov relation [Haag 2017],

$$P(x_1,t_1|x_3,t_3) = \int P(x_1,t_1|x_2,t_2)P(x_2,t_2|x_3,t_3)dx_2, \qquad t_1 < t_2 < t_3, \tag{1.12}$$

and

$$P(x_2,t_2) = \int P(x_2,t_2|x_1,t_1)P(x_1,t_1)dx_1, \tag{1.13}$$

Equation (1.13) shows that the probability distribution $P(x_1,t_1)$ is propagated in the time interval $t_2-t_1\geq 0$ by means of the conditional probability $P(x_2,t_2|x_1,t_1)$, also called the propagator to the distribution $P(x_2,t_2)$. The equivalent form of Eq. (1.12) represents a Markov homogeneous process, where we set $t_3=t+\tau$ and $t_2=t$, so to write

$$P_{t+\tau}(x_1|x_3)=\int P_\tau(x_3|x_2)P_t(x_2|x_1)dx_2 \tag{1.14}$$

Expanding $P_\tau(x_3|x_2)$ in Taylor series about $\tau\approx 0$ and following the standard procedure in [Kampen 2007], we find

$$P_\tau(x_3|x_2)=(1-a_0\tau)\delta(x_3-x_2)+\tau W(x_3|x_2)+\mathcal{O}(\tau^2), \tag{1.15}$$

with

$$a_0(x_3)=\int W(x_2|x_3)dx_2. \tag{1.16}$$

Then, Eq. (1.14) is expressed as

$$\begin{aligned} P_{t+\tau}(x_1|x_3) &= \int \left[(1-a_0\tau)\delta(x_3-x_2)+\tau W(x_3|x_2)\right]P_t(x_2|x_1)dx_2 \\ &= (1-a_0(x_3))\tau P_\tau(x_3|x_1)+\tau\int W(x_3|x_2)P_t(x_2|x_1)dx_2, \end{aligned} \tag{1.17}$$

and

$$\lim_{\tau\to 0}\frac{P_{t+\tau}(x_1|x_3)-P_\tau(x_3|x_1)}{\tau}=\frac{\partial P_\tau(x_3|x_1)}{\partial t}. \tag{1.18}$$

Finally, Eq. (1.17) takes the form

$$\frac{\partial P_\tau(x_3|x_1)}{\partial t}=\int\left\{W(x_3|x_2)P_t(x_2|x_1)-W(x_2|x_3)P_t(x_3|x_1)\right\}dx_2. \tag{1.19}$$

For a generic stochastic process $\{x(t):t\geq 0\}$, Eq. (1.19) can be generalize to

$$\frac{\partial P(x,t)}{\partial t}=\int\left\{T(x|x')P(x',t)-T(x'|x)P(x,t)\right\}dx'. \tag{1.20}$$

This equation will be actually very useful in the formulation of our Fock space approach of a random walk particle in a finite one-dimensional interval, as we shall see in the next chapters of this work. Equation (1.20) is the well-known master equation in the continuous case, where x and x' are continuous variables and $T(x|x')$ denotes the transition rate for the random walker to perform a jump from position x' to x with length $|x-x'|$. Then, redefining $T(x|x')=T(x',r)$ with $r=x-x'$, we rewrite Eq. (1.20) as

$$\frac{\partial P(x,t)}{\partial t}=\int T(x-r;r)P(x-r,t)dr-P(x,t)\int T(x;-r)dr. \tag{1.21}$$

Also, we consider

$$T(x',r) \simeq 0 \qquad \text{for} \quad |r| < \delta, \qquad \text{and} \qquad T(x'+\Delta x;r) \simeq T(x',r) \qquad \text{for} \quad |\Delta x| < \delta,$$

which, together with the assumption that $P(x,t)$ varies slowly, allows us to expand the product in the integrand above in Taylor series up to the second order, giving rise to

$$T(x-r;r)P(x-r,t) = T(x;r)P(x,t) - \frac{\partial}{\partial x}\left\{T(x;r)P(x,t)\right\} r + \frac{1}{2}\frac{\partial^2}{\partial x^2}\left\{T(x;r)P(x,t)\right\} r^2 + \mathcal{O}(r^3).$$

Substituting this result above, we write

$$\begin{aligned} \frac{\partial P(x,t)}{\partial t} = &\int T(x;r)P(x,t)dr - \int r\frac{\partial}{\partial x}\left\{T(x;r)P(x,t)\right\} dr \\ &+\frac{1}{2}\int r^2 \frac{\partial^2}{\partial x^2}\left\{T(x;r)P(x,t)\right\} dr - P(x,t)\int T(x;-r)dr, \end{aligned} \tag{1.22}$$

where

$$a_\nu(x) = \int_{-\infty}^{\infty} r^\nu T(x;r)dr \tag{1.23}$$

are the moments from the Kramer-Moyal expansion, Eq. (1.22). So we finally get

$$\frac{\partial P(x,t)}{\partial t} = -\frac{\partial}{\partial x}\left\{a_1(x)P(x,t)\right\} + \frac{1}{2}\frac{\partial^2}{\partial x^2}\left\{a_2(x)P(x,t)\right\}. \tag{1.24}$$

Equation (1.24) above is the renowned FPE.

For a random particle in Brownian motion we have that

$$a_1(x) = \frac{\langle \Delta x \rangle_x}{\Delta t} = 0 \tag{1.25}$$

$$a_2(x) = \frac{\langle (\Delta x)^2 \rangle_x}{\Delta t} = 2D \tag{1.26}$$

and Eq. (1.24) turns into the so-called diffusion equation,

$$\frac{\partial P(x,t)}{\partial t} = D\frac{\partial^2 P(x,t)}{\partial x^2}. \tag{1.27}$$

Equation (1.27) is the FPE for a normal diffusion process, and is quite similar to the heat conduction equation. Normal diffusion is very ubiquitous in nature. One of the main contributors to its study was the English mathematician and statistician Karl Pearson, who was originally interested in how mosquitoes spread malaria disease, which is in fact a diffusion process [Klafter and Sokolov 2005]. His work on the random walk problem as a generic way to describe transport phenomena was linked to previous relevant works, such as the observations by the Scottish botanist Robert Brown on the pollen movement, the Fick's law of conduction, and the seminal

theoretical studies by Albert Einstein and Marian Smoluchowski, ending with the experimental demonstrations of Jean Baptiste Perrin about the Brownian movement of particles.

One important characteristic of normal diffusion is that the second moment of the associated PDF is proportional to Dt, where D stands for the diffusion coefficient, as seen in Eq. (1.26). In other words, the root mean square (rms) deviation is proportional to the square root of time, $\sigma \propto t^{1/2}$. However, there are also other types of diffusion processes that behave differently. We now enter the kingdom of anomalous diffusion.

1.4.1 Subdiffusive case

This type of diffusion started to capture the interest of researchers in the early 2000's. For example, James Kirchner studied in 2000 the transport of pollutants in groundwater and discovered that, in this case, they take more time to move than expected if it were governed by a normal diffusion process [Kirchner, Feng and Neal 2000]. Marco Dentz and collaborators developed in 2004 a theory in which the normal diffusion FPE, Eq. (1.27), is modified to account for these slower processes. Specifically, in their work the time derivative is replaced by a fractional time derivative of order α, explaining in this way the time behavior of the solute transport [Dentz et al. 2004]. According to this work, the modified FPE has the form [Dentz et al. 2004]

$$\frac{\partial^{\alpha} P(x,t)}{\partial t^{\alpha}} = \frac{\partial}{\partial x}\left\{a_1(x)P(x,t)\right\} + \frac{1}{2}\frac{\partial^2}{\partial x^2}\left\{a_2(x)P(x,t)\right\}. \tag{1.28}$$

Other evidences of subdiffusion can be found in a number of biological processes, such as in the subdiffusive motion of proteins through membrane cells [Iino and Kusumi 2001].

1.4.2 Superdiffusive case

In this case the FPE is derived in a little bit different form, taking into account long range correlations proper of Lévy α-stable distributions in the transition rate quantities of a generalized master equation. The FPE derived in this way reads

$$\frac{\partial P(x,t)}{\partial t} = D_{\alpha}\frac{\partial^{\alpha} P(x,t)}{\partial x^{\alpha}} \tag{1.29}$$

The parameter α in Eq. (1.29) is the stability index of a Lévy α-stable distribution, with $\alpha \in (0,2]$ and $\alpha = 2$ corresponding to normal diffusion. To deal with Eq. (1.29) it is necessary to use tools of calculus with fractional derivatives, along with Fourier and Laplace transforms. As

mentioned before, the second moment of a Lévy distribution diverges, but one can define the finite average quantity $\sigma_L = \langle |x|^k \rangle^{1/k}$ for $k < \alpha$, which in the present case plays a role similar to that of the finite mean square deviation in normal diffusion processes. With this modification, it is possible to verify that $\sigma_L \propto t^{1/\alpha}$, which for $\alpha \neq 2$ is a sign of anomalous diffusion [Fogedby 1998]. Indeed, for $0 < \alpha < 2$ the transport process is faster than in the case of normal diffusion with $\alpha = 2$, and this is why this dynamics is called superdiffusive.

It is possible to classify types of diffusion processes according to the Hurst exponent H defined as [G.H. 1994]

$$\sigma \propto t^H. \tag{1.30}$$

So, if $H < 1/2$ in Eq. (1.30) one has subdiffusion, whereas normal diffusion corresponds to $H = 1/2$, and a superdiffusion process is characterized by $H > 1/2$. In particular when $H = 1$ the superdiffusion is in the ballistic regime.

There are several examples of superdiffusive phenomena taking place in diverse branches of science. For instance, the movement patterns of some animal species searching for food can be well described by Lévy random walks [Viswanathan et al. 1996, Viswanathan et al. 1999, Edwards et al. 2007, Ramos-Fernández et al. 2004]. In this work we study this type of diffusion in which the distribution of step lengths of a random particle is given by a Lévy α-stable distribution, and the particle is allowed to move in a one-dimensional discrete interval with absorbing borders, in a Fock space approach to the associated Schrödinger-like master equation.

1.5 LÉVY DISTRIBUTIONS

Lévy α-stable distributions are characterized by four parameters: $\alpha \in (0,2]$ is the stability index, also known as the characteristic exponent that describes the tail of the distribution, whereas $\beta \in [-1,1]$ represents the symmetry of the distribution, i.e., the skewness factor that tells how the distribution is turned to the right ($\beta > 0$) or to the left ($\beta < 0$). The other two parameters are the scale factor $b > 0$ and the location parameter $\mu \in (-\infty, \infty)$. So, the Lévy α-stable distribution can be generally denoted as $S(\alpha, \beta, b, \mu)$ [Nolan 2018].

We show in Fig. 3 the plot of the Lévy PDF for several values of $\alpha = 1/2, 1, 3/2, 2$.

Figure 3 – Lévy α-stable PDFs $P(x)$ as a function of the variable x for several values of α and skewness parameter $\beta = 0$. We depict in black line the distribution for $\alpha = 1/2$, in red the Cauchy distribution for $\alpha = 1$, in green the case with $\alpha = 3/2$, and in blue the Gaussian distribution with $\alpha = 2$.

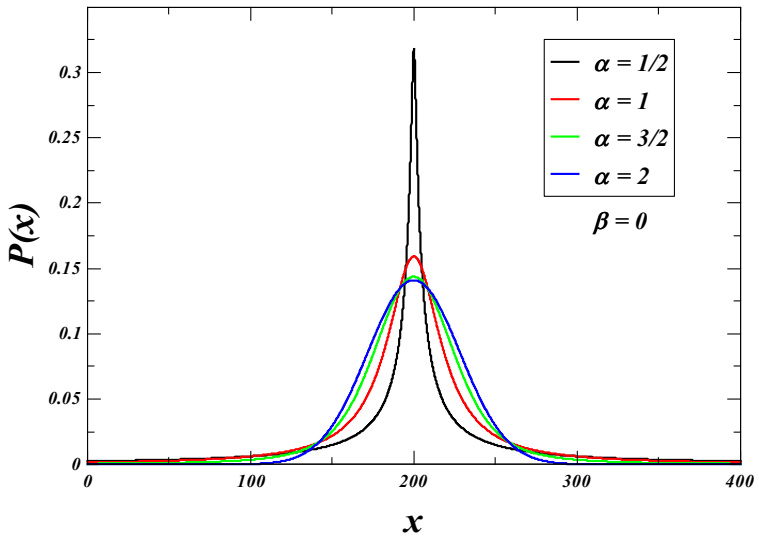

Lévy α-stable distributions generally lack closed analytical forms in terms of elementary functions, except for the following three cases.

1. Cauchy distribution for $\alpha = 1$ and $\beta = 0$:

$$P(x) = \frac{b}{\pi}\frac{1}{(b^2 + (x-\mu)^2)}. \tag{1.31}$$

2. Gaussian distribution for $\alpha = 2$ and $\beta = 0$:

$$P(x) = \frac{1}{2b\sqrt{\pi}} e^{-\frac{(x-\mu)^2}{4b^2}}. \tag{1.32}$$

3. Lévy distribution, a.k.a. inverse Gaussian or Pearson V distribution, for $\alpha = 1/2$ and $\beta = 1$:

$$P(x) = \sqrt{\frac{b}{2\pi}}\frac{e^{-\frac{b}{2(x-\mu)}}}{(x-\mu)^{3/2}}. \tag{1.33}$$

We show in Fig. 4 the plots of these closed-form cases.

Figure 4 – Lévy α-stable PDFs $P(x)$ as a function of the variable x for the known closed-form cases in terms of elementary functions. We depict in black line the Lévy distribution, also known as the inverse Gaussian or Pearson V, for $\alpha = 1/2$ and $\beta = 1$, in red the Cauchy distribution for $\alpha = 1$ and $\beta = 0$, and in blue the Gaussian distribution for $\alpha = 2$ and $\beta = 0$.

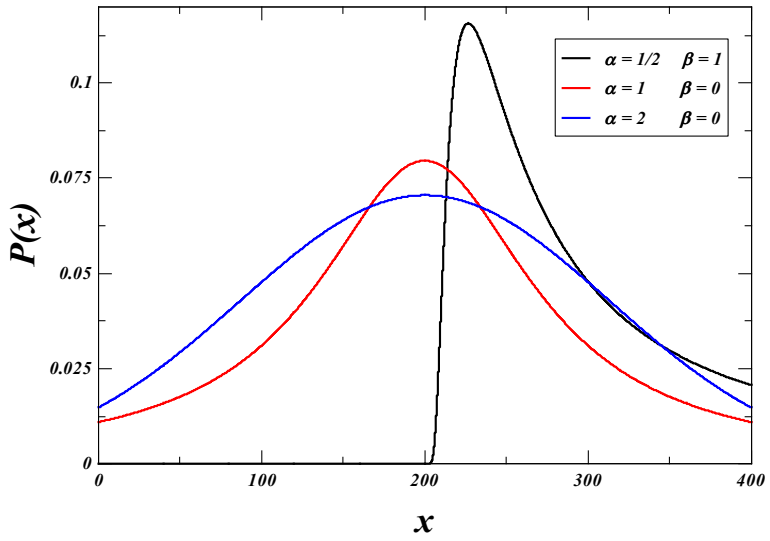

However, as mentioned above, the Lévy α-stable distributions can be also expressed through the characteristic function,

$$\hat{\phi}_\alpha(k) = \left\langle e^{ikx} \right\rangle = \begin{cases} \exp\{-b|k|^\alpha[1 - i\beta\tan(\pi\alpha/2)\text{sign}(k)] + ik\mu\}, & \text{for } \alpha \neq 1; \\ \exp\{-b|k|[1 + i\beta\frac{2}{\pi}\text{sign}(k)\ln|k|] + ik\mu\}, & \text{for } \alpha = 1, \end{cases} \tag{1.34}$$

Above all possibilities for the four parameters are considered, but we will work in this thesis only with symmetric distributions of step lengths x centered at $x = 0$, so that $\beta = 0$ and $\mu = 0$ in Eq. (1.34) (in the subsequent chapters we will denote the step length as ℓ). This means that the jump lengths to the right $(x > 0)$ or to the left $(x < 0)$ are equiprobable, that is, $p_\alpha(|x|) = p_\alpha(-|x|)$. In this case, Eq. (1.34) is expressed as

$$\hat{\phi}_\alpha(k) = e^{-b|k|^\alpha}. \tag{1.35}$$

Next we show in Fig. 5 the plots of the Lévy PDF for different values of the skewness parameter β and $\alpha = 3/2$, depicting a symmetric distribution $(\beta = 0)$, or asymmetric ones slightly turned to the left $(\beta = -1)$ or to the right $(\beta = 1)$.

Figure 5 – Lévy α-stable PDFs $P(x)$ as a function of the variable x for some values of the skewness parameter β and $\alpha = 3/2$. We depict in black line the symmetric distribution for $\beta = 0$, in red the asymmetric case with $\beta = 1$, and in blue the one with $\beta = -1$.

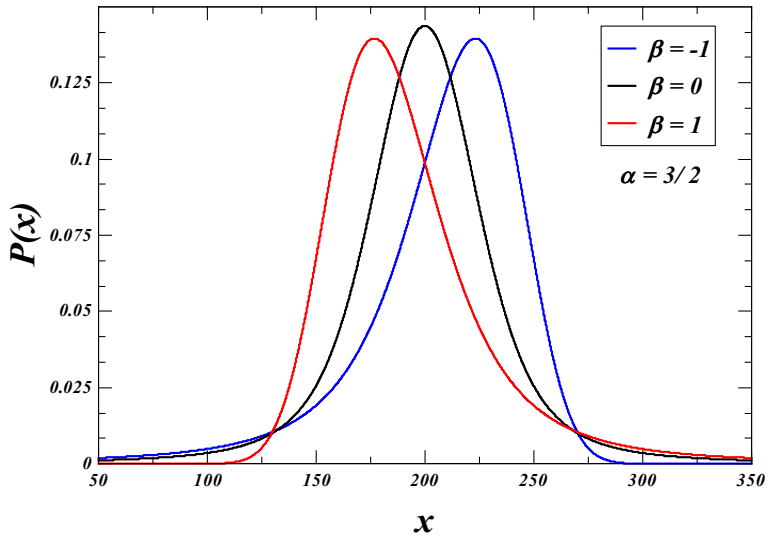

In addition, Lévy α-stable distributions also have an interesting asymptotic behavior, that is, they decay asymptotically in a power-law form, as we show in the following.

We first note that the general expression for the symmetric Lévy distributions of stability index α and scale factor b can be expressed as

$$P_L(x) = \frac{1}{\pi}\int_0^\infty e^{-b|k|^\alpha}\cos(kx)\,dk. \tag{1.36}$$

According to [Bergström 1952], we can write for $b = 1$ and $k > 0$,

$$e^{k^\alpha} = \int_0^\infty e^{-yk}F'_\alpha(k)dk, \tag{1.37}$$

where

$$F'_\alpha(k) = -\frac{1}{\pi}\sum_{j=1}^{\infty}\frac{(-1)^j}{j!}\sin(\pi\alpha j)\frac{\Gamma(\alpha j+1)}{x^{(\alpha j+1)}}. \tag{1.38}$$

By substituting Eq. (1.38) into Eq. (1.37), and then into Eq. (1.36), we obtain

$$P_L(x) = \frac{1}{\pi}\int_0^\infty\left[\int_0^\infty -\frac{1}{\pi}\sum_{j=1}^{\infty}\frac{(-1)^j}{j!}\sin(\pi\alpha j)\frac{\Gamma(\alpha j+1)}{y^{(\alpha j+1)}}e^{-yk}dy\right]\cos(kx)\,dk. \tag{1.39}$$

Then, noting that

$$\int_0^\infty e^{-yk}\cos(kx)\,dk = \mathcal{L}(\cos(kx)) = \frac{y}{y^2+x^2}, \tag{1.40}$$

and substituting Eq. (1.40) into Eq. (1.39), we get

$$P_L(x) = -\frac{1}{\pi^2}\sum_{j=1}^{\infty}\frac{(-1)^j}{j!}\sin(\pi\alpha j)\Gamma(\alpha j+1)\left[\int_0^{\infty}\frac{y^{-\alpha j}}{y^2+x^2}dy\right]. \tag{1.41}$$

Now, solving the integral in Eq. (1.41) as

$$\int_0^{\infty}\frac{y^{-\alpha j}}{y^2+x^2}dy = \frac{\pi}{2}\left(\frac{1}{x^2}\right)^{\frac{1}{2}(\alpha j+1)}\sec\left(\frac{\pi\alpha j}{2}\right), \tag{1.42}$$

we find

$$P_L(x) = -\frac{1}{\pi^2}\sum_{j=1}^{\infty}\frac{(-1)^j}{j!}\frac{2\sin(\frac{\pi\alpha j}{2})\cos(\frac{\pi\alpha j}{2})}{\cos(\frac{\pi\alpha j}{2})}\Gamma(\alpha j+1)\left[\frac{\pi}{2}\left(\frac{1}{x^2}\right)^{\frac{1}{2}(\alpha j+1)}\right]. \tag{1.43}$$

Doing the proper simplifications and subdividing the sum $\sum_{j=1}^{\infty}(\cdots) = \sum_{j=1}^{N}(\cdots) + \mathcal{O}(x^{-\alpha(N+1)-1})$, we finally obtain

$$P_L(x) = -\frac{1}{\pi}\sum_{j=1}^{N}\frac{(-1)^j}{j!}\frac{\Gamma(\alpha j+1)}{x^{(\alpha j+1)}}\sin\left[\frac{\pi\alpha j}{2}\right] + \mathcal{O}(x^{-\alpha(N+1)-1}). \tag{1.44}$$

From Eq. (1.44) we find the asymptotic approximation of a Lévy α-stable distribution for large values of x:

$$P_L(x) \sim \frac{\Gamma(\alpha+1)\sin(\pi\alpha/2)}{\pi x^{(\alpha+1)}} \sim x^{-(\alpha+1)}, \tag{1.45}$$

which, as indicated above, has the form of a power-law decay with exponent $\alpha+1$ for $\alpha \in (0,2)$. For $\alpha = 2$ the Lévy PDF is a Gaussian, as mentioned. Next we show this behavior graphically in Fig. 6 for different values of $\alpha = 1/2, 1, 3/2$ and $\beta = 0$.

Figure 6 – Log-log plot of the Lévy α-stable PDFs $P(x)$ as a function of the variable x for some values of α and $\beta = 0$ (solid lines). The large-x asymptotic power-law behavior, $P(x) \sim x^{-(\alpha+1)}$, is seen in dashed lines for the cases $\alpha = 1/2$ (black), $\alpha = 1$ (Cauchy distribution, red), and $\alpha = 3/2$ (blue).

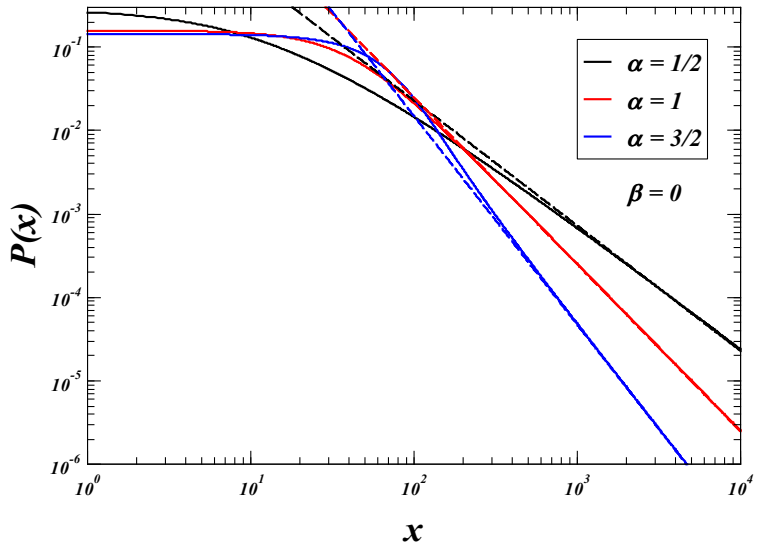

2 FOCK SPACE FORMALISM

« What we know is not much. What we don't know is enormous. »

Pierre Simon De Laplace

Resumo do capítulo.

Neste capítulo vamos desenvolver o formalismo do espaço de Fock que servirá de base para o nosso estudo de caminhadas aleatórias realizadas em um intervalo unidimensional com extremos absorventes. Partindo da equação mestra para uma distribuição de probabilidades, vamos demonstrar que é obtida uma equação que descreve um processo difusivo e que tem uma forma similar à equação de Schrödinger da mecânica quântica. A solução dessa equação permite determinar a distribuição de probabilidades de encontrar um caminhante aleatório numa determinada posição do espaço discreto em um dado instante. A partir desta distribuição outras grandezas importantes também podem ser obtidas, tais como o desvio padrão da caminhada e a taxa de sobrevivência do caminhante. O formalismo de Fock aplicado ao contexto das caminhadas aleatórias utiliza operadores de criação e destruição de forma semelhante à mecânica quântica no formalismo de segunda quantização. No presente caso tais operadores são aplicados para destruir uma partícula num determinado ponto do espaço discreto e criá-lo em outro ponto conectado com o primeiro através de um salto de comprimento igual à distância entre os pontos. Nesse sentido, como veremos, a distribuição de probabilidades dos tamanhos dos passos do caminhante aleatório tem um papel fundamental, similar ao das taxas de transição entre estados de um sistema quântico.

2.1 THEORETICAL FORMALISM OF THE FOCK SPACE

The Fock space formalism, related to the second quantization representation in quantum mechanics, is a suitable way to arrange the states of a quantum system of many particles in terms of occupation numbers. Interestingly, the second quantization formalism is not exclusive of quantum mechanics. It is also possible to apply it as well to classical systems of many particles, as Masao Doi introduced in his seminal article published in 1976 [Doi 1976].

Suppose that we have a system of many particles. Each particle is represented by a state according, e.g., to its position level in a spectrum of energy, if we are dealing with quantum

particles such us bosons or fermions. In the case of a stochastic process, for example, particles hopping in a lattice, each particle's state can be assigned to a lattice site position. So, to construct the Fock space we need to take the totality of basis states, $\{|n_0,n_1,n_2,...,n_N\rangle\}$, where $n_j = 0,1,2,...,N_j$ and $N_p = \sum_j n_j$, from the set $\{n_j\}$ of occupation numbers of particles. In this sense, the generic many-particle state can be represented by a linear superposition as

$$|\Psi\rangle = \sum_{n_0,n_1,...,n_N} c_{n_0,n_1,...,n_N}|n_0,n_1,n_2,...,n_N\rangle. \tag{2.1}$$

In particular, we are interested in a diffusion process of a random walk particle in a one-dimensional lattice with absorbing borders. As mentioned in the previous chapter, the presence of absorbing sites at the extremes of the interval makes this problem to establish a connection with the random search problem in one dimension. In this context, the random walker represents a random searcher and the absorbing sites are targets that, once found, makes the search to stop. After finding a target, the searcher restarts the search from the same initial position and, therefore, a search efficiency can be calculated as a function of the starting point.

Here the random particle is considered to step only in discrete positions $x_j = j\Delta x$, with two possibilities to occupy or not a lattice site, i.e., $n_j = 0,1$, and thus the particle's states have the simple form $\{|j\rangle\} = \{|0,0,...,0,n_j = 1,0,...0,0\rangle\}$. By denoting $P(x_j,t)\Delta x \equiv P(j,t)\Delta x$ as the probability to find the particle at the position $x_j = j\Delta x$ in time t, or equivalently the probability that the single-particle system occupies the state $|j\rangle$ in t, then its statistical description at this time can be expressed by rewriting Eq. (2.1) in the form of the superposition state (with $\Delta x \equiv 1$)

$$|\psi(t)\rangle = \sum_j P(j,t)|j\rangle. \tag{2.2}$$

We now introduce the ladder operators: the raising (creation) operator $a_j^\dagger$ and the lowering (annihilation) operator a_j are responsible to promote, respectively, the creation and destruction of a random particle at position x_j. For a general multiparticle system we have

$$\begin{aligned} a_j^\dagger|n_0,n_1,...,n_j,...,n_N\rangle &= |n_0,n_1,...,n_{j+1},...,n_N\rangle, \\ a_j|n_0,n_1,...,n_j,...,n_N\rangle &= n_j|n_0,n_1,...,n_{j-1},...,n_N\rangle, \\ a_j^\dagger a_j|n_0,n_1,...,n_j,...,n_N\rangle &= n_j|n_0,n_1,...,n_j,...,n_N\rangle. \end{aligned} \tag{2.3}$$

This means that, by applying the creation operator $a_j^\dagger$ to a state $|n_0,...,n_j,...,n_N\rangle$, there is only one way to add an extra particle at position j, and then the first line of Eq. (2.3) follows [Täuber, Howard and Vollmayr-Lee 2005]. But in the case of applying the annihilation operator a_j to the

same state, one has n_j ways to destroy one of the particles at position j, and so the n_j prefactor arises in the second line of Eq. (2.3) [Täuber, Howard and Vollmayr-Lee 2005]. The third line can be obtained after applying a_j to the state $|n_0,...,n_j,...,n_N\rangle$ and then $a_j^\dagger$ to the resulting state $|n_0,n_1,...,n_{j-1},...,n_N\rangle$. Moreover, we have also that

$$|n_0,n_1,...,n_j,...,n_N\rangle = a_1^{\dagger n_1} a_2^{\dagger n_2}...a_N^{\dagger n_N}|0\rangle = \prod_j a_j^{\dagger n_j}|0\rangle, \tag{2.4}$$

where the vacuum (no particles) state is represented by

$$|0\rangle = |0,0,0,...,0\rangle. \tag{2.5}$$

We have as well the following commutation relations of bosonic type, since in principle two random particles can occupy the same state (same position in the lattice): $[a_j, a_j^\dagger] = 1$ and $[a_j, a_j] = [a_j^\dagger, a_j^\dagger] \equiv 0$.

On the other hand, the master equation of a random particle in a one-dimensional discrete bounded space reads [Feller 1971]

$$\frac{\partial P(x,t)}{\partial t} = \sum_{x'} \Big[T(x,x')P(x',t) - T(x',x)P(x,t) \Big]. \tag{2.6}$$

We remark that in Chapter 1 we obtained the continuous analogous of this equation, Eq. (1.20). Following [Muzy et al. 2005], Eq. (2.6) can be expressed in terms of an evolution matrix $\mathbf{T}$ such that $T_{mn} = t_{mn}$ for $m \neq n$, and $T_{nn} = \sum_m t_{mn}$. Then, the master equation above takes the form

$$\frac{\partial P(n,t)}{\partial t} = \sum_{m=1}^{M} T_{mn} P(m,t). \tag{2.7}$$

Equation (2.7) represents the master equation of a stochastic process in terms of occupation numbers in a Fock space. Now, by combining the Fock space construction defined above with Eq. (2.7), the latter can be exactly represented [Doi 1976, Doi 1976, Mattis and Glasser 1998] in the form of a real-valued Schrödinger-like equation in terms of a Hamiltonian-like operator H,

$$\frac{\partial}{\partial t}|\psi(t)\rangle = -H(\{a_j^\dagger, a_j\})|\psi(t)\rangle. \tag{2.8}$$

We note that H does not have all the properties of a true Hamiltonian as in quantum mechanics, for example, Hermiticity [Sakurai 1994].

Now, let us check on the form of Eq. (2.8) in terms of the ladder operators $\{a_j^\dagger, a_j\}$ for the case of a simple diffusion process representing the jump of a random particle from site 1 to site 2, $\left(\boxed{1} \xrightarrow{\mathrm{D}} \boxed{2}\right)$. We can next generalize this particular process to a lattice with many sites.

Using Eqs. (2.4) and (2.6) we write

$$\begin{aligned}\frac{\partial|\psi(t)\rangle}{\partial t} &= \sum_{n_1,n_2}\Big[D(n_1+1)P(n_1+1,n_2-1,t)-D(n_1)P(n_1,n_2,t)\Big]a_1^{\dagger n_1}a_2^{\dagger n_2}|0\rangle \\ &= D\Big[P(n_1+1,n_2-1,t)\Big]a_2^\dagger a_1\left(a_1^\dagger\right)^{n_1+1}\left(a_2^\dagger\right)^{n_2-1}|0\rangle \\ &- D\Big[P(n_1,n_2,t)\Big]a_1^\dagger a_1\left(a_1^\dagger\right)^{n_1}\left(a_2^\dagger\right)^{n_2}|0\rangle \\ &= D\Big(a_2^\dagger a_1-a_1^\dagger a_1\Big)|\psi(t)\rangle \\ &= -H_{1\to 2}\Big(a_1^\dagger,a_2^\dagger,a_1\Big)|\psi(t)\rangle,\end{aligned} \tag{2.9}$$

where a Hamiltonian term associated with this jump process can be identified in the last line. We have used above the commutation relations, so that

$$a\left(a^\dagger\right)^{n+1} = aa^\dagger\left(a^\dagger\right)^n = \left(\mathbb{I}+a^\dagger a\right)\left(a^\dagger\right)^n = \Big(n+1\Big)\left(a^\dagger\right)^n. \tag{2.10}$$

In a similar manner, by using Eqs. (2.4) and (2.6) we obtain for a particle jumping from site 2 to site 1, $\left(\boxed{2}\xrightarrow{\mathrm{D}}\boxed{1}\right)$, the Hamiltonian term $H_{2\to 1}\Big(a_2^\dagger,a_1^\dagger,a_2\Big) = -D\Big(a_1^\dagger a_2-a_2^\dagger a_2\Big)$. So, the total diffusion process, $\left(\boxed{1}\overset{\mathrm{D}}{\leftrightarrows}\boxed{2}\right)$, is the sum of both terms, $H_{1\to 2}+H_{2\to 1}$, so that

$$H_{1\leftrightarrow 2}\Big(a_1^\dagger,a_2^\dagger,a_1,a_2\Big) = D\Big(a_2^\dagger-a_1^\dagger\Big)\Big(a_2-a_1\Big). \tag{2.11}$$

Equation (2.11) can be generalized to a diffusion process performed in a one-dimensional lattice with many sites in the form

$$H_{diff}\Big(a_i^\dagger,a_j^\dagger,a_i,a_j\Big) = D\sum_{i,j}\Big(a_i^\dagger-a_j^\dagger\Big)\Big(a_i-a_j\Big), \tag{2.12}$$

where in principle the random particle can make a jump linking any two sites i and j of the lattice (however, in our particular case of interest with absorbing borders, we must be careful since the particle can jump *to* a border site but cannot jump *from* a border site; see below). In Appendix A we provide an extension of the general construction of the Hamiltonian-like operator in the case of a set of random diffusing particles.

Once the Hamiltonian form H on the basis of Fock states is known, a time evolution operator can be defined in analogy to quantum mechanics, $U(0,t) = \exp[-tH(\{a_j^\dagger,a_j\})]$, so that the dynamics of the system governed by Eq. (2.8) implies

$$|\psi(t)\rangle = U(0,t)|\psi(0)\rangle, \tag{2.13}$$

where $|\psi(0)\rangle$ denotes the initial state, i.e., $|\psi(0)\rangle = |j_0\rangle$ if the particle departs from the position $x_0 = j_0\Delta x$. We thus find that

$$P(j,t) = \langle j|\psi(t)\rangle = \langle j|U(0,t)|\psi(0)\rangle. \tag{2.14}$$

Also, the time-dependence of the n-th moment of the distribution $P(j,t)$ can be obtained from

$$\langle j^n \rangle(t) = \sum_{j=0}^{N} j^n P(j,t). \tag{2.15}$$

In order to proceed with the calculations, it is convenient to express the Hamiltonian H in a Jordan normal form $J = Q^{-1}HQ$, so that $H = QJQ^{-1}$, where the matrices J and Q are built from the eigenvalues and eigenvectors of H [Dennery and Krzywicki 1996]. In this representation the time evolution operator can be written in a matrix form as

$$\begin{aligned} U(0,t) = \exp(-tH) &= \sum_{m=0}^{\infty} \frac{(-t)^m}{m!} \left(QJQ^{-1}\right)^m \\ &= Q \exp(-tJ) Q^{-1}, \end{aligned} \tag{2.16}$$

where Q^{-1} denotes the inverse of the matrix Q. Finally, once the time evolution operator U is known, one can conceivably calculate any relevant quantity of the problem.

2.2 THE SIMPLEST RANDOM WALK PROCESS AND THE FOCK SPACE APPROACH

To illustrate explicitly how the above Fock space formalism works in the case of diffusion processes involving random walk particles, we consider in this section the simplest example of a random walker in a boundless one-dimensional lattice that can take a step to the nearest site at its right with probability p and a step to the nearest site at its left with probability $q = 1 - p$.

Suppose the case of a discrete time variable, $t_n = t_0, t_1, t_2, \ldots$, that can mapped onto the number of steps n of the random walker. As indicated in the previous section, the state that describes this single-particle system is given by

$$|\psi(t)\rangle = \sum_i P(i,t)|i\rangle = e^{-Ht}|\psi(0)\rangle. \tag{2.17}$$

But the discrete time t can be written as an integer multiple of Δt, i.e., $t = m\Delta t$, implying

$$\begin{aligned} |\psi(t)\rangle = |\psi(m\Delta t)\rangle &= e^{-H\Delta t m}|\psi(0)\rangle \\ &= \left(e^{-H\Delta t}\right)^m |\psi(0)\rangle \\ &= \left(\mathbb{I} + \sum_{n=1}^{\infty} \frac{(-H\Delta t)^n}{n!}\right)^m |\psi(0)\rangle \\ |\psi(m\Delta t)\rangle &\cong (\mathbb{I} - H\Delta t)^m |\psi(0)\rangle. \end{aligned} \tag{2.18}$$

Making $\Delta t \equiv 1$, so that we count the time in terms of the index m of steps, we write

$$|\psi(m)\rangle \simeq (\mathbb{I} - H)^m |\psi(0)\rangle, \tag{2.19}$$

or, alternatively,

$$\begin{aligned} |\psi(t)\rangle = e^{-Ht}|\psi(0)\rangle &= \lim_{N\to\infty}\left(\mathbb{I} - \frac{Ht}{N}\right)^N |\psi(0)\rangle \\ &= \lim_{N\to\infty}\left(\mathbb{I} - H\Delta t\right)^N |\psi(0)\rangle. \end{aligned} \tag{2.20}$$

We now need to build the Hamiltonian H associated with this jump process. In the previous section, with a diffusion process of rate D involving only sites 1 and 2, we found that, e.g., $H_{1\to 2} = -D\left(a_2^\dagger a_1 - a_1^\dagger a_1\right)$, $(\boxed{1} \xrightarrow{\mathrm{D}} \boxed{2})$. In the present case, for a given lattice site i we have the nearest neighbor jump processes $(\boxed{i-1} \xleftarrow{\mathrm{q}} \boxed{i} \xrightarrow{\mathrm{p}} \boxed{i+1})$. Then

$$\begin{aligned} H_i &= -p\left(a_{i+1}^\dagger a_i - a_i^\dagger a_i\right) - q\left(a_{i-1}^\dagger a_i - a_i^\dagger a_i\right) \\ &= -p\left(a_{i+1}^\dagger a_i\right) - q\left(a_{i-1}^\dagger a_i\right) + a_i^\dagger a_i, \end{aligned} \tag{2.21}$$

and

$$H = \sum_i H_i = \sum_i -p\left(a_{i+1}^\dagger a_i\right) - q\left(a_{i-1}^\dagger a_i\right) + a_i^\dagger a_i. \tag{2.22}$$

Assuming that the particle is initially at site j at $t = 0$, that is, $|\psi(0)\rangle = |j\rangle$, then at $t = 1$, i.e., $m = 1$, we find

$$\begin{aligned} |\psi(1)\rangle &= (\mathbb{I} - H)|\psi(0)\rangle \\ &= \left[\mathbb{I} - \sum_i -p\left(a_{i+1}^\dagger a_i\right) - q\left(a_{i-1}^\dagger a_i\right) + a_i^\dagger a_i\right]|j\rangle \\ &= \mathbb{I}|j\rangle + \sum_i p\left(a_{i+1}^\dagger a_i\right)|j\rangle + q\left(a_{i-1}^\dagger a_i\right)|j\rangle - \sum_i a_i^\dagger a_i]\,|j\rangle. \end{aligned} \tag{2.23}$$

But $a_i|j\rangle = \delta_{ij}|0\rangle$, so that

$$\begin{aligned} |\psi(1)\rangle &= |j\rangle + p\sum_i a_{i+1}^\dagger \delta_{ij}|0\rangle + q\sum_i a_{i-1}^\dagger \delta_{ij}|0\rangle - \sum_i a_i^\dagger \delta_{ij}|0\rangle \\ &= |j\rangle + \left[p\sum_i a_{j+1}^\dagger + q\sum_i a_{j-1}^\dagger - \sum_i a_j^\dagger\right]|0\rangle \\ &= |j\rangle + p|j+1\rangle - q|j-1\rangle - |j\rangle \\ &= p|j+1\rangle - q|j-1\rangle. \end{aligned} \tag{2.24}$$

For $t=2$ and $m=2$,

$$\begin{aligned}
|\psi(2)\rangle &= (\mathbb{I}-H)^2|\psi(0)\rangle = (\mathbb{I}-H)|\psi(1)\rangle \\
&= \left[\mathbb{I}-\sum_i -p\left(a_{i+1}^\dagger a_i\right)-q\left(a_{i-1}^\dagger a_i\right)+a_i^\dagger a_i\right](p|j+1\rangle - q|j-1\rangle) \\
&= (p|j+1\rangle + q|j-1\rangle) - \sum_i (-pa_{i+1}^\dagger - qa_{i-1}^\dagger + a_i^\dagger)(p\,a_i|j+1\rangle + q\,a_i|j-1\rangle) \\
&= (p|j+1\rangle + q|j-1\rangle) - \sum_i (-pa_{i+1}^\dagger - qa_{i-1}^\dagger + a_i^\dagger)(p\,\delta_{i\,j+1} + q\,\delta_{i\,j-1})|0\rangle \\
&= (p|j+1\rangle + q|j-1\rangle) + p^2\sum_i a_{i+1}^\dagger \delta_{i\,j+1}|0\rangle + pq\sum_i a_{i+1}^\dagger \delta_{i\,j-1}|0\rangle \\
&+ pq\sum_i a_{i-1}^\dagger \delta_{i\,j+1}|0\rangle - p\sum_i a_i^\dagger \delta_{i\,j+1}|0\rangle - q\sum_i a_i^\dagger \delta_{i\,j-1}|0\rangle + q^2\sum_i a_{i-1}^\dagger \delta_{i\,j-1}|0\rangle \\
&= (p|j+1\rangle + q|j-1\rangle) + p^2 a_{j+2}^\dagger|0\rangle + pq\,a_j^\dagger|0\rangle \\
&+ pq\,a_j^\dagger|0\rangle + q^2 a_{j-2}^\dagger|0\rangle - p\,a_{j+1}^\dagger|0\rangle - q\,a_{j-1}^\dagger|0\rangle \\
&= p^2|j+2\rangle + 2pq|j\rangle + q^2|j-2\rangle.
\end{aligned} \tag{2.25}$$

For a general value of t (or m), we have

$$|\psi(m)\rangle = (\mathbb{I}-H)^m. \tag{2.26}$$

So we need to calculate the operator $(\mathbb{I}-H)^m$. Note that $[\mathbb{I},H]=0$ since

$$\begin{aligned}
\langle i|[\mathbb{I},H]|j\rangle &= \langle i|\mathbb{I}H - H\mathbb{I}|j\rangle = \langle i|\mathbb{I}H|j\rangle - \langle i|H\mathbb{I}|j\rangle \\
&= -\langle i|H|j\rangle + \langle i|\mathbb{I}\big(-p|j+1\rangle - q|j-1\rangle + |j\rangle\big) \\
&= -\langle i|\big(-p|j+1\rangle - q|j-1\rangle + |j\rangle\big) + \langle i|\big(-p|j+1\rangle - q|j-1\rangle + |j\rangle\big) \\
&= 0.
\end{aligned} \tag{2.27}$$

We can formally apply the binomial expansion,

$$(\mathbb{I}-H)^m = \sum_{k=0}^{m} \frac{m!}{k!(m-k)!}\mathbb{I}^k(-H)^{m-k}, \tag{2.28}$$

thus

$$\begin{aligned}
(\mathbb{I}-H)^m|j\rangle &= \sum_{k=0}^{m} \frac{m!}{k!(m-k)!}\mathbb{I}^k(-H)^{m-k}|j\rangle \\
&= \sum_{k=0}^{m} \frac{m!}{k!(m-k)!}\mathbb{I}^k(-1)^{m-k}(H)^{m-k}|j\rangle,
\end{aligned} \tag{2.29}$$

where

$$H^{m-k} = \left[\sum_i -p\left(a_{i+1}^\dagger a_i\right)-q\left(a_{i-1}^\dagger a_i\right)+a_i^\dagger a_i\right]^{m-k}. \tag{2.30}$$

Given the difficulty of calculating the power above, let us try to make an induction process. We already know the cases $m = 1, 2$. We now see what happens for $m = 3$:

$$\begin{aligned}
(\mathbb{I}-H)^3|j\rangle &= (\mathbb{I}-H)\left[p^2|j+2\rangle + 2pq|j\rangle + q^2|j-2\rangle\right] \\
&= \left(p\sum_i a^\dagger_{i+1}a_i + q\sum_i a^\dagger_{i-1}a_i\right)\left[p^2|j+2\rangle + 2pq|j\rangle + q^2|j-2\rangle\right] \\
&= \sum_i p^3\delta_{ij+2}|i+1\rangle + 2p^2q\delta_{ij}|i+1\rangle + pq^2\delta_{ij-2}|i+1\rangle \\
&+ p^2q\delta_{ij+2}|i-1\rangle + 2pq^2\delta_{ij}|i-1\rangle + q^3\delta_{ij-2}|i-1\rangle \\
&= p^3|j+3\rangle + 2p^2q|j+1\rangle + pq^2|j-1\rangle \\
&+ p^2q|j+1\rangle + 2pq^2|j-1\rangle + q^3|j-3\rangle.
\end{aligned} \tag{2.31}$$

Note, therefore, that

$$(\mathbb{I}-H)|j\rangle = p|j+1\rangle + q|j-1\rangle,$$

$$(\mathbb{I}-H)^2|j\rangle = p^2|j+2\rangle + 2pq|j\rangle + q^2|j-2\rangle,$$

$$\begin{aligned}
(\mathbb{I}-H)^3|j\rangle &= p^3|j+3\rangle + 3p^2q|j+1\rangle + 3pq^2|j-1\rangle + q^3|j-3\rangle, \\
&\vdots \\
(\mathbb{I}-H)^n|j\rangle &= \sum_{k=0}^{n}\frac{n!}{k!(n-k)!}p^{n-k}q^k|j+m\rangle,
\end{aligned} \tag{2.32}$$

$$m \equiv \underbrace{(n-k)}_{right} - \underbrace{k}_{left} \Rightarrow \textbf{walker displacement}.$$

Then we write

$$(\mathbb{I}-H)^n = \sum_{k=0}^{n}\frac{n!}{k!(n-k)!}p^{n-k}q^k a^\dagger_{j+n-2k}a_j. \tag{2.33}$$

On the other hand, we have that

$$|\Psi(n)\rangle = \sum_{k=0}^{n}\frac{n!}{k!(n-k)!}p^{n-k}q^k|j+n-2k\rangle, \tag{2.34}$$

where $|\Psi(0)\rangle = |j\rangle$.

We can calculate the moments $\langle\alpha^k\rangle$ of the probability distribution of the random the walker to be at the position α as a function of the time or number of steps. We can start with the zeroth

moment, $k=0$, that actually corresponds to the normalization condition to find the random particle anywhere in the boundless lattice:

$$\begin{aligned}\sum_{\alpha=-\infty}^{\infty}\langle\alpha|\Psi(n)\rangle &= \sum_{\alpha=-\infty}^{\infty}\sum_{k=0}^{n}\frac{n!}{k!(n-k)!}p^{n-k}q^{k}\underbrace{\langle\alpha|j+n-2k\rangle}_{\delta_{\alpha,j+n-2k}}\\ &= \sum_{k=0}^{n}\frac{n!}{k!(n-k)!}p^{n-k}q^{k} = (p+q)^{n} = 1^{n} = 1,\end{aligned} \tag{2.35}$$

which, as expected, does not depend on the time or number of steps.

Now, let us compute the mean value of the walker's position, $\langle\alpha\rangle$:

$$\begin{aligned}\langle\alpha\rangle &= \sum_{\alpha=-\infty}^{\infty}\alpha\underbrace{P(\alpha,n))}_{prob\,to\,be\,in\,\alpha\,in\,step\,n} = \sum_{\alpha=-\infty}^{\infty}\alpha\langle\alpha|\Psi(n)\rangle\\ &= \sum_{\alpha=-\infty}^{\infty}\alpha\,\langle\alpha|\sum_{k=0}^{n}\frac{n!}{k!(n-k)!}\,p^{n-k}q^{k}\,|j+n-2k\rangle\\ &= \sum_{\alpha=-\infty}^{\infty}\sum_{k=0}^{n}\frac{n!}{k!(n-k)!}\,p^{n-k}q^{k}\,\alpha\,\underbrace{\langle\alpha|j+n-2k\rangle}_{\delta_{\alpha,j+n-2k}}\\ &= \sum_{k=0}^{n}\frac{n!}{k!(n-k)!}\,p^{n-k}q^{k}\,(j+n-2k)\\ &= (j+n)\underbrace{\sum_{k=0}^{n}\frac{n!}{k!(n-k)!}\,p^{n-k}q^{k}}_{\equiv 1} - 2\sum_{k=0}^{n}\frac{n!}{k!(n-k)!}\,p^{n-k}q^{k}\,k.\end{aligned} \tag{2.36}$$

But it can be seen that

$$kq^{k} = q\frac{d}{dq}(q^{k}), \tag{2.37}$$

and so we can write

$$\begin{aligned}\sum_{k=0}^{n}\frac{n!}{k!(n-k)!}\,p^{n-k}q^{k}\,k &= \sum_{k=0}^{n}\frac{n!}{k!(n-k)!}\,p^{n-k}q\frac{d}{dq}(q^{k})\\ &= q\frac{d}{dq}\left(\sum_{k=0}^{n}\frac{n!}{k!(n-k)!}\,p^{n-k}q^{k}\right)\\ &= q\frac{d}{dq}\left[(p+q)^{n}\right] = qn(p+q)^{n-1} = qn(1)^{n-1} = qn.\end{aligned} \tag{2.38}$$

This result along with Eqs. (2.38) and (2.36) lead to

$$\langle\alpha\rangle = (j+n) - 2nq = j+n(p+q) - 2nq = j+np-nq = j+n(p-q). \tag{2.39}$$

The above result agrees with the average position after n steps of a random walker that started from the site j and has probability p ($q=1-p$) to step to its nearest right (left) neighbor.

We now compute the second moment $\langle\alpha^2\rangle$:

$$\begin{aligned}
\langle\alpha^2\rangle &= \sum_{\alpha=-\infty}^{\infty} \alpha^2 P(\alpha,n) = \sum_{\alpha=-\infty}^{\infty} \alpha^2 \langle\alpha|\Psi(n)\rangle \\
&= \sum_{\alpha=-\infty}^{\infty} \alpha^2 \langle\alpha| \sum_{k=0}^{n} \frac{n!}{k!(n-k)!}\, p^{n-k} q^k \,|j+n-2k\rangle \\
&= \sum_{\alpha=-\infty}^{\infty} \sum_{k=0}^{n} \frac{n!}{k!(n-k)!}\, p^{n-k} q^k\, \alpha^2 \underbrace{\langle\alpha|j+n-2k\rangle}_{\delta_{\alpha,j+n-2k}} \\
&= \sum_{k=0}^{n} \frac{n!}{k!(n-k)!}\, p^{n-k} q^k\, (j+n-2k)^2 \qquad (2.40)\\
&= \sum_{k=0}^{n} \frac{n!}{k!(n-k)!}\, p^{n-k} q^k \left((j+n)^2 + (2k)^2 - 4(j+n)k\right) \\
&= (j+n)^2 - 4(j+n) \underbrace{\sum_{k=0}^{n} \frac{n!}{k!(n-k)!}\, p^{n-k} q^k \cdot k}_{nq} + 4 \sum_{k=0}^{n} \frac{n!}{k!(n-k)!}\, p^{n-k} q^k \cdot k^2.
\end{aligned}$$

To proceed further, we use the following relation,

$$k^2 q^k = \left(q\frac{d}{dq}\right)^2 (q^k), \qquad (2.41)$$

that leads to

$$\begin{aligned}
&\sum_{k=0}^{n} \frac{n!}{k!(n-k)!}\, p^{n-k} q^k \cdot k^2 = \sum_{k=0}^{n} \frac{n!}{k!(n-k)!}\, p^{n-k} \left(q\frac{d}{dq}\right)^2 (q^k) \\
&= \left(q\frac{d}{dq}\right)^2 \sum_{k=0}^{n} \frac{n!}{k!(n-k)!}\, p^{n-k} q^k \\
&= \left(q\frac{d}{dq}\right)^2 (p+q)^n = \left(q\frac{d}{dq}\right) qn(p+q)^{n-1} \qquad (2.42)\\
&= q\left\{n(p+q)^{n-1} + qn(n-1)(p+q)^{n-2}\right\}; \qquad p+q=1 \\
&= q\left\{n + qn(n-1)\right\} = qn\left\{1 + q(n-1)\right\} \\
&= qn(p+nq) = (nq)^2 + npq,
\end{aligned}$$

so that

$$\begin{aligned}
\langle\alpha^2\rangle &= (j+n)^2 + 4\left[(nq)^2 + npq\right] - 4(j+n)nq \\
&= (j+n)^2 + 4nq\left[nq + p - (j+n)\right] = (j+n)^2 + 4nq\left[n(q-1) + p - j\right].
\end{aligned} \qquad (2.43)$$

Then we are able to compute the variance (mean square deviation),

$$\begin{aligned}\left\langle \alpha^2 \right\rangle - \langle \alpha \rangle^2 &= (j+n)^2 + 4nq\,[nq+p-(j+n)] - [j+n(p-q)]^2 \\ &= (j+n)^2 + 4nq\,[nq+p-(j+n)] - (j+n)^2 - 4(nq)^2 + 4nq(j+n) \\ &= (j+n)^2 + 4(nq)^2 + 4npq - 4nq(j+n) - (j+n)^2 - 4(nq)^2 + 4nq(j+n) \\ &\equiv 4npq.\end{aligned} \tag{2.44}$$

This result is also in perfect agreement with the variance of this random walk process calculated from standard statistical physics techniques (see, e.g., the next chapter).

Finally, we have everything set to address the problem of a random walker in a finite domain with absorbing boundaries using the Fock space formalism. As mentioned, the presence of absorbing sites at the extremes of the one-dimensional interval makes this problem to establish a connection with the random search problem in one dimension. In the next chapter, we consider a random walker with a fixed step length and equal probabilities to take a step to the left or to the right, that is, we return to the above problem with $p = q = 1/2$ and calculate several relevant quantities from the knowledge of the probability distribution to find the walker at a given position in a certain time. In the subsequent chapters, the random walker will be allowed to perform jumps of any length, particularly long jumps, drawn from power-law and Lévy α-stable distributions. Such cases are representative of highly efficient search strategies that have been applied in the last two decades to model animals looking for food sites in nature, in the so-called animal foraging problem.

3 RANDOM WALKER WITH FIXED STEP LENGTH IN A FOCK SPACE APPROACH

« Somewhere, something incredible is waiting to be known. »

Carl Sagan

Resumo do capítulo.

Neste capítulo vamos estudar o problema de um caminhante aleatório com tamanho do passo fixo, com igual probabilidade de ir para a direita e para a esquerda. Devido ao teorema central do limite (CLT), para um número grande de passos a distribuição da soma dos tamanhos dos passos converge para uma distribuição gaussiana $B(t) \sim N(\mu, \sigma^2(t))$, com média μ e variância dependente do tempo, $\langle r^2(t) \rangle \sim t$. Introduzimos o formalismo do espaço de Fock para tratar o caso em que o caminhante aleatório se move em um intervalo unidimensional com posições discretas e fronteiras absorventes. Nossos resultados são comparados com aqueles obtidos através de técnicas usuais da física estatística, mostrando uma boa concordância.

3.1 ANALYTICAL RESULTS FOR A RANDOM WALKER WITH FIXED STEP LENGTH

We start this section by introducing the classical problem of a random walker taking random steps in a given region of the space. As we shall see below, one of the main objectives in this problem is to calculate the probability to find the random walker at a certain position after a given number of successive random steps from the starting point.

A major advance on the random walk problem was due to Karl Pearson in 1905. However, we should also mention that Lord Rayleigh in earlier times also gave relevant contributions to its development. Today random walk models serve to describe many stochastic problems in diverse branches of science. Just to mention one, the foraging (search) strategy used by some animals to look for food can be described as a diffusive process modeled by a random walk. Under some specific conditions the random walk evolution describes a Brownian motion with normal diffusion. Actually, we can say that Brownian motion is the simplest transport mechanism characterized by a normal or Gaussian distribution representing a normal diffusion process. The problem studied in this chapter belongs to this class of stochastic processes. However, other (anomalous) types of diffusion can also arise in different types of random walks, such as, e.g., in the one performed by a random particle with step lengths drawn from a power-law or a Lévy

distribution. These random walk models with superdiffusive properties will be the subject of our study in the next two chapters.

Let us first consider the problem of a random walker moving in a boundless one-dimensional space. The random walker only takes steps of fixed length ℓ to the right ($\ell > 0$) with probability p or to the left ($\ell < 0$) with probability $q = 1 - p$. This means that its PDF of step lengths can be expressed in terms of Dirac delta functions in the form $P(x) = p\delta(x - |\ell|) + q\delta(x + |\ell|)$. It is clear that $P(x)$ presents finite first and second moments. The steps are taken independently and every step is drawn from the same PDF $P(\ell)$. In other words, the random variables associated with the length of each step are i.i.d. These features make the distribution of the sum of a large number of variables x (which actually corresponds to the position of the random walker) to converge to a Gaussian, according to the CLT. We will actually prove this result below. The developments detailed in the sequence follow the standard statistical physics approach by F. Reif in [Reif 1965].

Initially, we wish to calculate the probability $P_N(m)$ to find the random walker at the position $x = m\ell$, with m integer, after N steps. Here we denote by n_1 the number of steps taken to the right and by n_2 the number of steps taken to the left, so that

$$N = n_1 + n_2, \tag{3.1}$$

with

$$m = n_1 - n_2. \tag{3.2}$$

From the above equation we note that m represents the walker's net displacement (in ℓ units).

In a given sequence of N steps, the probability of the walker to take n_1 steps to the right and n_2 steps to the left is

$$\underbrace{pp\ldots p}_{n_1}\underbrace{qq\ldots q}_{n_2} = p^{n_1}q^{n_2}. \tag{3.3}$$

Eq. (3.3) actually refers to just one possible sequence of steps. In fact, the total number of such sequences is

$$\frac{N!}{n_1!n_2!}. \tag{3.4}$$

So, the probability $P_N(n_1)$ of taking n_1 steps to the right and n_2 steps to the left in a total of N steps is obtained by multiplying Eqs. (3.3) and (3.4), yielding

$$P_N(n_1) = \frac{N!}{n_1!n_2!}\, p^{n_1}q^{n_2}. \tag{3.5}$$

This result is known as the binomial distribution.

Here we consider a random walker with equal probabilities to take a step in any direction, that is, $p = q = 1/2$, so that Eq. (3.5) becomes

$$P_N(n_1) = \frac{N!}{n_1!\,n_2!}\left(\frac{1}{2}\right)^N. \tag{3.6}$$

We can also use Eqs. (3.1) and (3.2) to rewrite (3.6) as

$$P_N(m) = \frac{N!}{[\frac{1}{2}(N+m)]![\frac{1}{2}(N-m)]!}\left(\frac{1}{2}\right)^N. \tag{3.7}$$

Now we prove that, according to the CLT, for a large number N of steps the binomial distribution in Eq. (3.7) converges to a Gaussian. We use below the Stirling approximation for $N \gg 1$,

$$\ln(N)\,! \simeq N\ln N - N + \frac{1}{2}\ln(2\pi N). \tag{3.8}$$

Taking the log of Eq. (3.7),

$$\begin{aligned}
\ln P_N(m) \;=\;& -N\ln 2 + N\ln N - N + \frac{1}{2}\ln(2\pi N) \\
& -\frac{1}{2}(N+m)\ln\left[\frac{1}{2}(N+m)\right] + \frac{1}{2}(N+m) - \frac{1}{2}\ln\left[\pi(N+m)\right] \\
& -\frac{1}{2}(N-m)\ln\left[\frac{1}{2}(N-m)\right] + \frac{1}{2}(N-m) - \frac{1}{2}\ln\left[\pi(N-m)\right],
\end{aligned} \tag{3.9}$$

and simplifying it, we obtain

$$\begin{aligned}
\ln P_N(m) \;=\;& N\ln N - N + \frac{1}{2}\ln(2\pi N) \\
& -\frac{1}{2}(N+m)\ln(N+m) - \frac{1}{2}\ln\left[\pi(N+m)\right] \\
& -\frac{1}{2}(N-m)\ln(N-m) - \frac{1}{2}\ln\left[\pi(N-m)\right].
\end{aligned} \tag{3.10}$$

Now, using the approximation $\ln(1+x) \approx x - \frac{1}{2}x^2$ for $|x| \ll 1$ and considering $|m| \ll N$, we find

$$\begin{aligned}
\ln(N+m) &= \ln N\Big(1+\frac{m}{N}\Big) \\
&= \ln N + \ln\Big(1+\frac{m}{N}\Big) \\
&\cong \ln N + \frac{m}{N} - \frac{1}{2}\left(\frac{m}{N}\right)^2.
\end{aligned} \tag{3.11}$$

On the other hand, for the log terms in Eq. (3.10) that are not multiplied by $(N \pm n)$ it is sufficient to expand up to first order in m/N, that is,

$$\begin{aligned}
\ln\Big(\pi(N+m)\Big) &= \ln \pi N\Big(1+\frac{m}{N}\Big) \\
&\cong \ln \pi N + \frac{m}{N}.
\end{aligned} \tag{3.12}$$

By substituting Eqs. (3.11) and (3.12) into (3.10), we obtain

$$\begin{aligned}\ln P_N(m) \;\cong\; & N\ln N+\frac{1}{2}\ln(2\pi N)\\ & -\frac{N}{2}\left(1+\frac{m}{N}\right)\left[\ln N+\frac{m}{N}-\frac{1}{2}\left(\frac{m}{N}\right)^2\right]-\frac{1}{2}\left[\ln(\pi N)+\frac{m}{N}\right]\\ & -\frac{N}{2}\left(1-\frac{m}{N}\right)\left[\ln N-\frac{m}{N}-\frac{1}{2}\left(\frac{m}{N}\right)^2\right]-\frac{1}{2}\left[\ln(\pi N)-\frac{m}{N}\right],\end{aligned} \tag{3.13}$$

which after simplification and rearrangement leads to

$$\ln P_N(m) = -\frac{m^2}{2N}+\ln\left(\frac{2}{\sqrt{2\pi N}}\right). \tag{3.14}$$

Finally, by applying the exponential to Eq. (3.14) we get

$$P_N(m) \simeq \frac{2}{\sqrt{2\pi N}}\, e^{-\frac{m^2}{2N}}. \tag{3.15}$$

Equation (3.15) has obviously a Gaussian form, and so this completes the proof that the binomial distribution of the sum (corresponding to the walker's position) of i.i.d. random variables describing the step lengths converges to a Gaussian for a large number of steps, according to the CLT. The proof can be also readily extended to the more general case in which p and q are not necessarily equal (see below).

By recalling that $x = m\ell$ and setting a time variable proportional to the number of steps with fixed length, $t = N\tau$, we can also obtain the probability to find the random walker at a position x in time t after N steps,

$$P_N(x) \simeq \frac{2}{\sqrt{\frac{2\pi t}{\tau}}}\, e^{-\frac{x^2}{t}\left(\frac{\tau}{2\ell^2}\right)}. \tag{3.16}$$

Where $\sigma \propto t^{1/2}$ and $\mu = 0$.

Getting back to Eq. (3.5), we now focus our attention on how to calculate the moments of the binomial distribution in the general case in which p and q can be different. We can rewrite Eq. (3.5) as

$$P_N(n_1) = \frac{N!}{(n_1)!\,(N-n_1)!}\, p^{n_1} q^{(N-n_1)} \tag{3.17}$$

First, we should verify the normalization to unit of this probability distribution, i.e., the condition

$$\sum_{i=1}^{N} P_N(n_1) = 1. \tag{3.18}$$

Substituting Eq. (3.18) into Eq. (3.17), and using the binomial theorem, we have

$$\begin{aligned}\sum_{i=1}^{N}\frac{N!}{(n_1)!\,(N-n_1)!}\,p^{n_1}q^{(N-n_1)} &= (p+q)^N \\ &= 1^N \\ &= 1,\end{aligned} \tag{3.19}$$

as expected. So, we are now ready to calculate the statistical moments of order n,

$$\langle n_1^n\rangle = \sum_{i=1}^{N} n_1^n\,\frac{N!}{(n_1)!\,(N-n_1)!}\,p^{n_1}q^{(N-n_1)}. \tag{3.20}$$

By using Eq. (3.20), the mean value of the number of steps to the right is obtained for $n=1$:

$$\begin{aligned}\langle n_1\rangle &= \sum_{i=1}^{N} n_1\,\frac{N!}{(n_1)!\,(N-n_1)!}\,p^{n_1}q^{(N-n_1)} \\ &= \sum_{i=1}^{N}\frac{N!}{(n_1)!\,(N-n_1)!}\left[p\frac{\partial}{\partial p}(p)^{n_1}\right]q^{(N-n_1)} \\ &= p\frac{\partial}{\partial p}\sum_{i=1}^{N}\frac{N!}{(n_1)!\,(N-n_1)!}\,p^{n_1}q^{(N-n_1)} \\ &= p\frac{\partial}{\partial p}\,(p+q)^N \\ &= p(p+q)^{N-1} \\ &= pN.\end{aligned} \tag{3.21}$$

We now turn to the calculation of the mean square deviation,

$$\langle(\Delta n_1)^2\rangle = \langle n_1^2\rangle - \langle n_1\rangle^2. \tag{3.22}$$

First, we determine the second cumulant $\langle n_1^2\rangle$,

$$\begin{aligned}\langle n_1^2\rangle &= \sum_{i=1}^{N} n_1^2\,\frac{N!}{(n_1)!\,(N-n_1)!}\,p^{n_1}q^{(N-n_1)} \\ &= \sum_{i=1}^{N}\frac{N!}{(n_1)!\,(N-n_1)!}\left[\left(p\frac{\partial}{\partial p}\right)^2 p^{n_1}\right]q^{(N-n_1)} \\ &= \left(p\frac{\partial}{\partial p}\right)^2\sum_{i=1}^{N}\frac{N!}{(n_1)!\,(N-n_1)!}\,p^{n_1}q^{(N-n_1)} \\ &= \left(p\frac{\partial}{\partial p}\right)pN(p+q)^{N-1} \\ &= p\left[N(p+q)^{N-1}pN(N-1)(p+q)^{N-2}\right] \\ &= p\left[N+pN(N-1)\right] = pN(1+pN-p) \\ &= (pN)^2+Npq \\ &= \langle n_1\rangle^2+Npq.\end{aligned} \tag{3.23}$$

So, using Eqs. (3.22) and (3.23) we obtain

$$\begin{aligned}\langle(\Delta n_1)^2\rangle &= \langle n_1\rangle^2 + Npq - \langle n_1\rangle^2 \\ &= Npq.\end{aligned} \tag{3.24}$$

We end this section by mentioning the general results when the probabilities to step to the right or to the left are not necessarily the same. By returning to Eq. (3.15), it can be generally expressed for any non-negative p and q with $p+q=1$ as

$$P_N(m) = \frac{1}{\sqrt{2\pi Npq}}\, e^{-\frac{[m-N(p-q)]^2}{8Npq}}. \tag{3.25}$$

In the continuous limit of the variable $x = m\ell$ we can obtain its associated PDF $P(x)$ in the form

$$\mathcal{P}(x)dx = \frac{P_N(m)}{2\ell}dx. \tag{3.26}$$

Then, making use of Eq. (3.25) we find

$$\begin{aligned}\mathcal{P}(x)dx &= \frac{1}{2\ell\sqrt{2\pi Npq}}\, e^{-\frac{[x/\ell-N(p-q)]^2}{8Npq}}\, dx \\ &= \frac{1}{\sqrt{2\pi\sigma^2}}\, e^{-\frac{(x-\mu)^2}{2\sigma^2}}\, dx,\end{aligned} \tag{3.27}$$

where

- $\mu \equiv (p-q)N\ell$ (mean),
- $\sigma^2 \equiv 4\ell^2 Npq$ (variance).

Equation (3.27) is the standard form of a Gaussian probability distribution, in agreement with the CLT. We also note that $\sigma \sim N^{1/2} \sim t^{1/2}$, which, as commented in the last chapter, is a signature of normal (Brownian-like) diffusion.

3.2 NUMERICAL RESULTS FOR THE RW WITH FIXED STEP LENGTH USING THE FOCK SPACE FORMALISM

We now apply the Fock space approach introduced in the previous chapter to study the statistical properties of a random walker with fixed step length moving in a one-dimensional lattice with absorbing boundaries. We remark that the case with reflective boundaries will also be indicated below, although it does not correspond to the main focus of this thesis, since we are mostly interested in situations in which the walker stops to diffuse when a boundary site is found, in similarity to the finding of a target by a random searcher in the random search problem.

To illustrate the procedure in the Fock space we start with a small system with only $N = 4$ sites and fixed step length $|\ell| = 1$. First, by following the rules presented in Chapter 2 we write the Hamiltonian operator in the form

$$H = \sum_{i=0}^{4} -p(a_{i+1}^{\dagger} a_i) - q(a_{i-1}^{\dagger} a_i) + (a_i^{\dagger} a_i), \tag{3.28}$$

from which we obtain the following matrix in the basis $\{|\mathbf{1}\rangle = |\mathbf{1000}\rangle, |\mathbf{2}\rangle = |\mathbf{0100}\rangle, |\mathbf{3}\rangle = |\mathbf{0010}\rangle, |\mathbf{4}\rangle = |\mathbf{0001}\rangle\}$ of occupation number states, that is for example, a particle occupies the site 2 after left the site 3 with probability p_{32}

$$H_{N=4} = \begin{pmatrix} p_{11} & -p_{21} & 0 & 0 \\ -p_{12} & p_{22} & -p_{32} & 0 \\ 0 & -p_{23} & p_{33} & -p_{43} \\ 0 & 0 & -p_{34} & p_{44} \end{pmatrix}, \tag{3.29}$$

where the $p_{11}, p_{12}, p_{43}, p_{44}$ are the probabilities at the borders represented by the symbol λ, also the diagonal elements $p_{22} = p_{33} = 1$ and the other probabilities are equal to $p = q = 1 - p$, as the following

$$H_{N=4} = \begin{pmatrix} \lambda & -1+p & 0 & 0 \\ -\lambda & 1 & -1+p & 0 \\ 0 & -p & 1 & -\lambda \\ 0 & 0 & -p & \lambda \end{pmatrix}, \tag{3.30}$$

then $\lambda = 0$ ($\lambda = 1$) represents the case with absorbing (reflective) boundaries. Also, as in the previous section, p stands for the probability of taking a step to the right, and $q = 1 - p$ otherwise. We set here $p = q = 1/2$. Then, for $\lambda = 0$ and $p = q = 1/2$ we have

$$H_{N=4} = \begin{pmatrix} 0 & -1/2 & 0 & 0 \\ 0 & 1 & -1/2 & 0 \\ 0 & -1/2 & 1 & 0 \\ 0 & 0 & -1/2 & 0 \end{pmatrix}. \tag{3.31}$$

We notice that the sum of the elements in each column is zero.

Next, we proceed to diagonalize the above Hamiltonian using the Jordan decomposition method, with the help of the software *Mathematica*. After that we determine the time evolution operator, from which the state vectors of the system can be obtained. In particular, we are interested in computing the probability of the random walker to be at a position a in a time t,

having started from position j,

$$P(a,t;j) = \langle a|e^{-Ht}|j\rangle. \tag{3.32}$$

The knowledge of $P(a,t;j)$ allows to determine diverse relevant statistical properties of the system, such as the mean square deviation and the survival probability according to the following expressions.

$$X_{rms}{}^2(t) = \sigma(t)^2 = \langle X^2\rangle - \langle X\rangle^2 \tag{3.33}$$

where

$$\langle X\rangle = \sum_{a=0}^{N} a\cdot P(a,t,j_0) \tag{3.34}$$

and

$$\langle X^2\rangle = \sum_{a=0}^{N} a^2\cdot P(a,t,j_0) \tag{3.35}$$

and the survival probability,

$$\begin{aligned} S(t) &= \sum_{a=2}^{N-1} P(a,t) \\ &= 1 - P(j=1,t) - P(j=N,t). \end{aligned} \tag{3.36}$$

3.2.1 One-dimensional system with N = 301 sites

We consider here a system domain with $N = 301$ sites. The step length is chosen as $|\ell| = 1$. By following the steps outlined above, we first plot in Fig. 7 the probability distribution $P(j,t)$ as a function of the position $j(= 1,2,...,N)$, with starting point at $j_0 = 150$. Also, in this plot we display the comparison with the associated Gaussian distribution for three values of time $t(= 5,10,15)$. We remark that for these values of t the walker have not yet reached the boundaries, and this explains the nice agreement observed in Fig. 7. Deviations from the Gaussian behavior are actually expected to occur when the boundaries are reached for larger times, see below.

Figure 7 – Probability $P(j,t)$ for a random walker with fixed step length as a function of the position j in a finite domain from $j = 1$ to $j = 301$, with the starting point at $j_0 = 150$, for different elapsed times, $t = 5, 10, 15$. Symbols depict the results using the Fock space approach and lines are the corresponding adjust to Gaussian distributions.

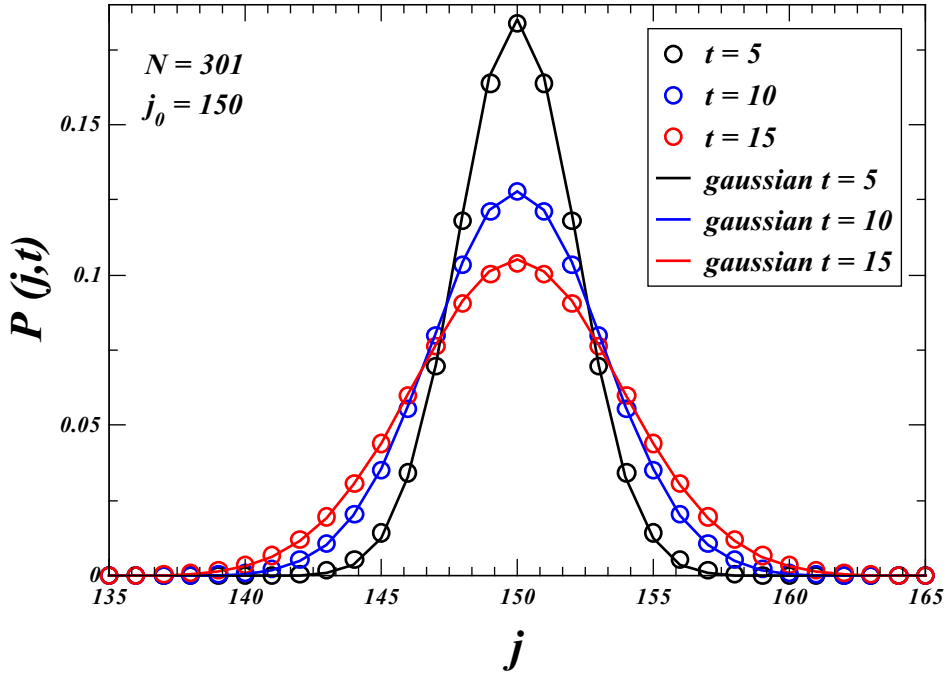

We next show in Fig. 8 the probability $P(j,t)$ for a random walker starting at $j_0 = 4$, close to the left boundary. We notice in this case that the probability of being absorbed by this boundary is non-null and increases with t. As a consequence, the symmetry observed in Fig. 7 in the numerical and Gaussian distributions around the starting position can no longer be seen in this case.

Figure 8 – Probability $P(j,t)$ for a random walker with fixed step length as a function of the position j in a finite domain from $j = 1$ to $j = 301$, with the starting point near the left boundary, $j_0 = 4$, and for different elapsed times, $t = 5, 10, 15$. Symbols depict the results using the Fock space approach. Lines are guides to the eye.

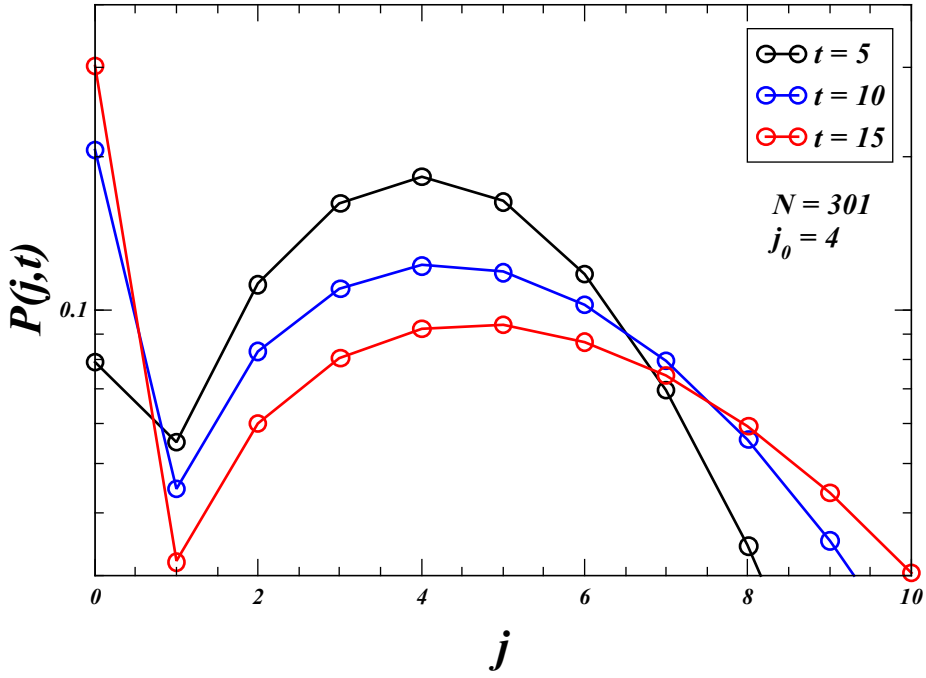

The behavior of the survival probability $S(t)$ as a function of time t is shown in Fig. 9. As the name indicates, the survival probability represents the probability of the random walker to remain alive (i.e., unabsorbed) after some given time. We notice that, after a short transient period, a good agreement is found with the power-law behavior $S(t) \sim t^{-\gamma}$ with $\gamma = 0.51$. This result agrees nicely with the Sparre-Andersen theorem [Andersen 1953, Andersen 1954] with $\gamma = 1/2$ for random walks in a one-dimensional space with a single absorbing site. In the present case, since the faraway boundary at $j = 301$ has not been reached up to the times shown in Fig. 9, then the statistical behavior of $S(t)$ is actually equivalent to that of a random walker in a semi-infinite domain described by the Sparre-Andersen theorem. On the other hand, when the faraway boundary starts to be reached this power-law behavior shifts to an exponential decay. Although we do not observe this change in Fig. 9, since it takes much longer to reach the position $j = 301$ for a random walker with fixed unit step length, in the next chapters this shift will be seen as we consider power-law and Lévy distributions of step lengths that can eventually lead to quite large jumps.

Figure 9 – Log-log plot of the survival probability $S(t)$ as a function of time t for a random walker with fixed step length in a finite domain from $j = 1$ to $j = 301$, with the starting point near the left absorbing site, $j_0 = 4$. Solid line depicts the results using the Fock space approach. Dashed line shows the best fit to the power-law behavior $S(t) \sim t^{-\gamma}$ with exponent $\gamma = 0.51$ in nice agreement with the prediction $\gamma = 1/2$ of the Sparre-Andersen theorem.

(a) Power-law behavior

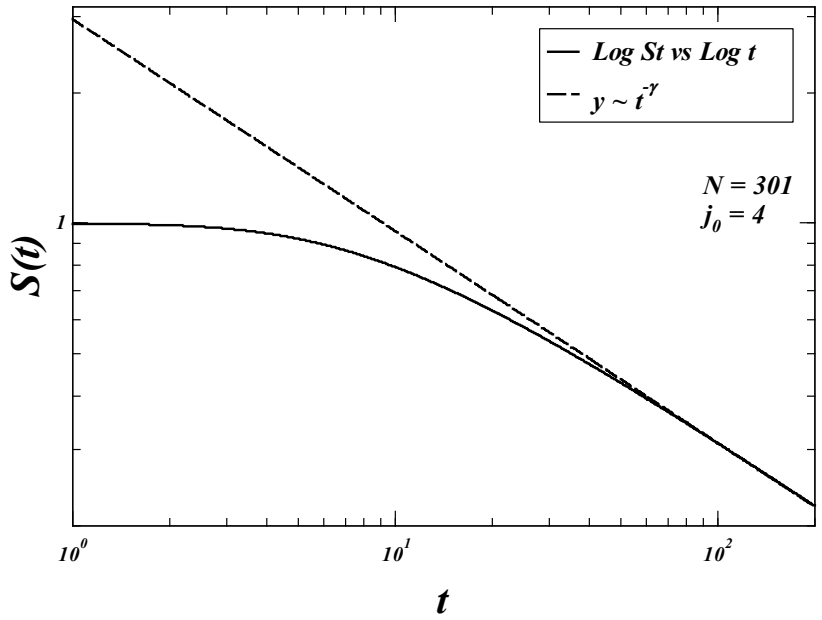

Figure 10 – Mean square deviation $X^2_{rms}(t)$ for a random walker with fixed step length as a function of time t in a finite domain from $j = 1$ to $j = 301$, with the starting point (a) near the left boundary, $j_0 = 4$, and (b) at $j_0 = 150$. The normal diffusion behavior $X^2_{rms}(t) \sim t$ of a random walker in boundless space is shown in dashed line for comparison. The influence of the absorbing borders on the random walk dynamics starts to be reached when the solid and dashed lines begin to depart.

(a) $j_0 = 4$ (b) $j_0 = 150$

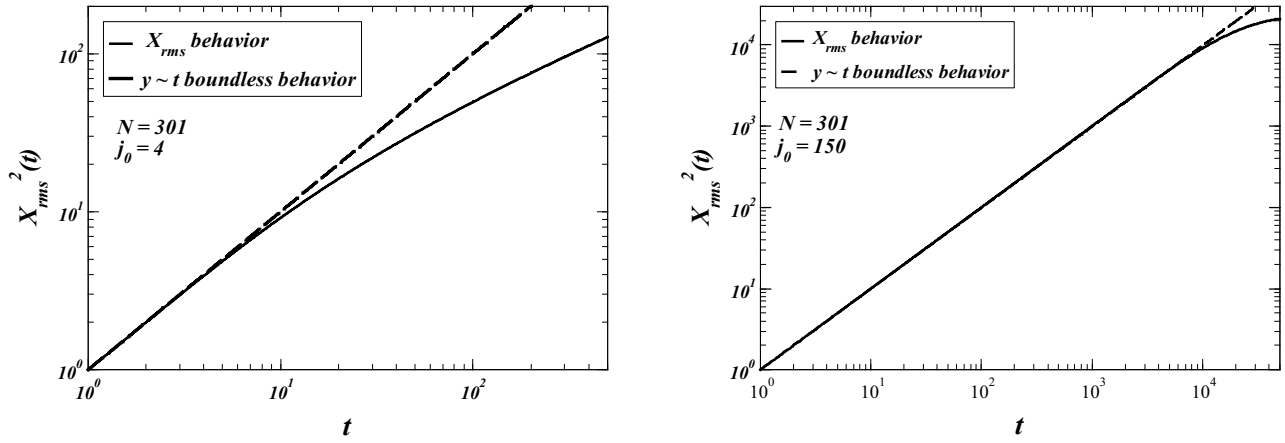

We finally show in Fig. 10 the behavior with t of the mean square deviation $X^2_{rms}(t)$ for the walker starting at $j_0 = 4$ [Fig. 10(a)] and $j_0 = 150$ [Fig. 10(b)]. In the former case, it takes to the random walker only a few steps to find the left boundary, and so deviations from the expected behavior $X^2_{rms}(t) \sim t$ in the boundless space are soon observed. In the latter, as expected, this Brownian-like signature of normal diffusion extends for much longer, near one thousand times longer than in the former case.

4 RANDOM WALKER WITH POWER-LAW DISTRIBUTION OF STEP LENGTHS IN A FOCK SPACE APPROACH

« Present what is true, write it down for clarity, defend it to the last breath! »

Edward Boltzmann

Resumo do capítulo.

Neste capítulo inicialmente estudaremos a distribuição de lei de potência, suas características principais e como ela representa o limite assintótico de uma distribuição α-estável de Lévy. Em seguida vamos considerar um caminhante aleatório em um espaço unidimensional com extremos absorventes, com tamanhos de passos distribuídos de acordo com uma lei de potência. Discutiremos nossos resultados obtidos a partir do formalismo do espaço de Fock para diferentes valores do exponente da lei de potência μ.

4.1 CHARACTERISTICS OF THE POWER-LAW DISTRIBUTION AND THE ASYMPTOTIC LIMIT OF THE LÉVY ALFA-STABLE DISTRIBUTION

Power-law distributions are generally expressed as $P(x) \propto x^{-\mu}$, with the exponent μ characterizing one of their main features, namely the existence of a heavy (long) tail which contrasts with many PDFs with exponential (or faster) decay [Chen 2003, Pinto, Lopes and Machado 2012]. Examples of the power-law distribution can be found in economics, biology, and astronomy [Chen 2003, Pinto, Lopes and Machado 2012]. Moreover, they are much common in other areas as well, such as computer science, information theory, language, and city-sizes distribution in demography studies. Depending on the context, power-law distributions can be also termed as the Pareto distribution [Pareto 1896/97] or the Zipf's law [G.K. 1949].

In a more rigorous way, the PDF of the power-law distribution has the form [Newman 2005]

$$P(x) = Cx^{-\mu} = \frac{(\mu-1)}{x_{min}}\left(\frac{x}{x_{min}}\right)^{-\mu}, \tag{4.1}$$

where $\mu > 1$ and x_{min} is the minimum value of x to allow for the normalization of $P(x)$ to unit, and the normalization constant reads $C = (\mu-1)x_{min}^{\mu-1}$.

We can compute the first moment of the power-law distribution from Eq. (4.1):

$$\langle x \rangle = \int_{x_{min}}^{\infty} xP(x)dx = C\int_{x_{min}}^{\infty} x^{-\mu+1}dx = \frac{C}{2-\mu}\left[x^{-\mu+2}\right]_{x_{min}}^{\infty}, \tag{4.2}$$

where for $\mu < 2$ the mean value is not defined. For $\mu > 2$, instead, the mean value is given by

$$\langle x \rangle = \frac{\mu - 1}{\mu - 2} x_{min}. \tag{4.3}$$

In a similar manner we can compute the second moment,

$$\langle x^2 \rangle = \int_{x_{min}}^{\infty} x^2 P(x) dx = C \int_{x_{min}}^{\infty} x^{-\mu+2} dx = \frac{C}{3-\mu} \left[x^{-\mu+3} \right]_{x_{min}}^{\infty}. \tag{4.4}$$

Only for $\mu > 3$ Eq. (4.4) is defined, so that

$$\langle x^2 \rangle = \frac{\mu - 1}{\mu - 3} (x_{min})^2. \tag{4.5}$$

This result implies that the distribution of a sum of i.i.d. variables with power-law PDF converges to a Gaussian according to the CLT (finite variance) if $\mu > 3$, and to a Lévy α-stable distribution according to the GCLT (infinite variance) if $1 < \mu < 3$, with $\alpha = \mu - 1$ (see below). It can be also shown [Mantegna and Stanley 2000, Bouchaud and Potters 2000] that the limit case $\mu = 3$ is still attracked by the Gaussian PDF, which, as mentioned in Chapter 1, corresponds to the particular case of Lévy α-stable distributions with $\alpha = 2$.

It is also worth recalling that in Chapter 1 we obtained that the Lévy α-stable distributions decay asymptotically in the form of a power law with exponent $\mu = \alpha + 1$ for $\alpha \in (0, 2)$ [Mantegna and Stanley 2000, Bouchaud and Potters 2000]:

$$P_L(\ell) \sim \frac{\Gamma(\alpha + 1) \sin(\pi\alpha/2)}{\pi \ell^{(\alpha+1)}} \sim \ell^{-(\alpha+1)}. \tag{4.6}$$

For $\alpha = 2$ the Lévy PDF is a Gaussian, as already mentioned.

4.2 NUMERICAL RESULTS FOR A RANDOM WALKER WITH POWER-LAW DISTRIBUTION OF STEP LENGTHS IN THE FOCK SPACE APPROACH

In this section we present and discuss the results obtained using the Fock space approach for a random walker moving in a finite domain with absorbing boundaries, in which the steps lengths are drawn from a power-law distribution in the form

$$p(\ell) = \frac{A}{|\ell|^{\mu}}, \tag{4.7}$$

for $|\ell| \geq \ell_0$, and $p(\ell) = 0$ otherwise, where $\mu > 1$ and the normalization constant $A = \frac{(\mu-1)\ell_0^{\mu-1}}{2}$.

Differently from the case studied in the last chapter, where the random walker had fixed step length, in the present situation of power-law distribution rather large steps can occur so that,

for example, any boundary can be in principle reached in only one step. This implies that every site in the one-dimensional lattice can be accessed in a step from anywhere in the interval and, therefore, more complicated transition rates should take this fact into account. Indeed, in this case we can calculate the transition probability from a site j to a site k in a finite domain of N sites and discrete positions $x = n\Delta x$, with n integer, as follows:

$$P_{kj} = \begin{cases} 0, & k = j; \\ \displaystyle\int_{(|k-j|)\Delta x}^{(|k-j|+1)\Delta x} p(\ell)d\ell, & 1 \leq k, j \leq N; \\ \displaystyle\int_{\ell_0}^{\infty} p(\ell)d\ell, & 1 \leq j \leq N, \quad k = 1; \\ \displaystyle\int_{(|k-j|)\Delta x}^{\infty} p(\ell)d\ell, & 1 \leq j \leq N, \quad k = N. \end{cases} \tag{4.8}$$

The first line above indicates that the walker cannot stay at the same site in a move step. In the third and fourth lines the walker is absorbed by the left and right boundaries, respectively, and in the second line the walker remains unabsorbed after the step.

For example, the transition probability matrix with absorbing boundaries for a random walker in the case of $N = 6$ sites is

$$P_{kj} = \begin{pmatrix} 0 & p_{21} & p_{31} & p_{41} & p_{51} & 0 \\ 0 & 0 & p_{32} & p_{42} & p_{52} & 0 \\ 0 & p_{23} & 0 & p_{43} & p_{53} & 0 \\ 0 & p_{24} & p_{34} & 0 & p_{54} & 0 \\ 0 & p_{25} & p_{35} & p_{45} & 0 & 0 \\ 0 & p_{26} & p_{36} & p_{46} & p_{56} & 0 \end{pmatrix}. \tag{4.9}$$

Using Eq. (4.7) with $\ell_0 = \Delta x = 1$, we have, e.g., for the case $\mu = 2$,

$$P_{kj} = \begin{pmatrix} 0 & 1/2 & 1/4 & 1/6 & 1/8 & 0 \\ 0 & 0 & 1/4 & 1/12 & 1/24 & 0 \\ 0 & 1/4 & 0 & 1/4 & 1/12 & 0 \\ 0 & 1/12 & 1/4 & 0 & 1/4 & 0 \\ 0 & 1/24 & 1/12 & 1/4 & 0 & 0 \\ 0 & 1/8 & 1/6 & 1/4 & 1/2 & 0 \end{pmatrix}. \tag{4.10}$$

In a lattice with N sites the elements of the Hamiltonian in the basis of occupation number states read

$$\begin{aligned}\langle m|H|n\rangle &= -\sum_{i=2}^{L-1}\sum_{\substack{k=1\\ i\neq k}}^{L} P_{ik}\,\langle m \mid (a_k^\dagger a_i - a_i^\dagger a_i) \mid n\rangle \\ &= -\sum_{j=1}^{N}\sum_{\substack{k=2\\ k\neq j}}^{N-1} P_{kj}\left(\delta_{kn}\delta_{mj} - \delta_{kn}\delta_{mk}\right),\end{aligned} \tag{4.11}$$

so that in the example above we write

$$H_{kj} = \begin{pmatrix} 0 & -1/2 & -1/4 & -1/6 & -1/8 & 0 \\ 0 & 1 & -1/4 & -1/12 & -1/24 & 0 \\ 0 & -1/4 & 1 & -1/4 & -1/12 & 0 \\ 0 & -1/12 & -1/4 & 1 & -1/4 & 0 \\ 0 & -1/24 & -1/12 & -1/4 & 1 & 0 \\ 0 & -1/8 & -1/6 & -1/4 & -1/2 & 0 \end{pmatrix}. \tag{4.12}$$

As we did in the last chapter, once the Hamiltonian matrix is built for a given value of the power-law exponent μ, we next diagonalize it using the Jordan decomposition with the help of *Mathematica*, then obtain the time evolution operator, the probability distribution and, from it, all the relevant quantities of interest.

4.2.1 Case $\mu = 3$

We start our numerical analysis in the Fock space approach with the case of $\mu = 3$, which corresponds to the normal diffusive regime, as mentioned.

We show in symbols in Fig. 11 the probability distribution $P(j,t)$ as a function of the position j for some values of time t, for a walker starting at $j_0 = 50$, with $N = 101$ and $\ell_0 = \Delta x = 1$. In the case of a Brownian-like dynamics, it is expected that this distribution approaches a Gaussian as long as the the borders are still not reached. This can be seen in Fig. 11 through the good fit of the numerical data to the Gaussian function (lines)

$$P_0(j,t) = \frac{1}{\sqrt{2\pi\sigma^2 t}} e^{-j^2/(2\sigma^2 t)}. \tag{4.13}$$

Figure 11 – Probability $P(j,t)$ for $\mu = 3$ (Gaussian regime) as a function of the position j in a finite domain from $j = 1$ to $j = 101$, with the starting point at $j_0 = 50$, for different elapsed times, $t = 5, 10, 20$. Symbols correspond to the results using the Fock space approach. Lines are fits to the Gaussian distribution.

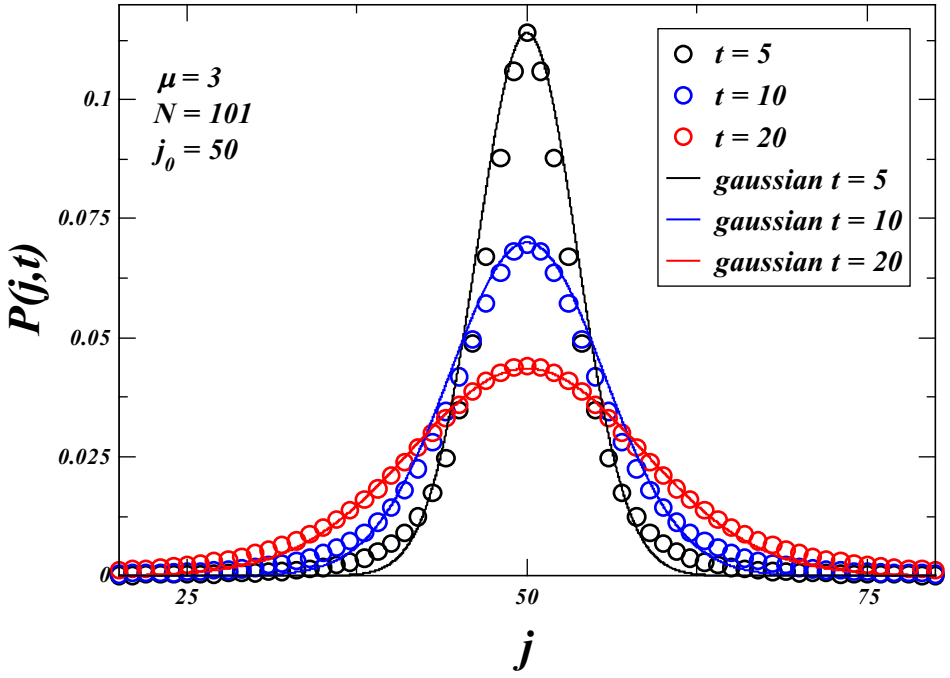

The probability distribution $P(j,t)$ for a walker starting from a point near the left boundary, $j_0 = 4$, is shown in Fig. 12. As in the case worked in the last chapter with fixed step length, the probability to be absorbed by the close boundary increases with t, breaking the symmetry of $P(j,t)$ around $j = j_0$.

Figure 12 – Probability $P(j,t)$ for $\mu = 3$ (Gaussian regime) as a function of the position j in a finite domain from $j = 1$ to $j = 101$, with the starting point near the left boundary, $j_0 = 4$, for different elapsed times, $t = 5, 10, 20$. Symbols correspond to the results using the Fock space approach. Lines are guides to the eye.

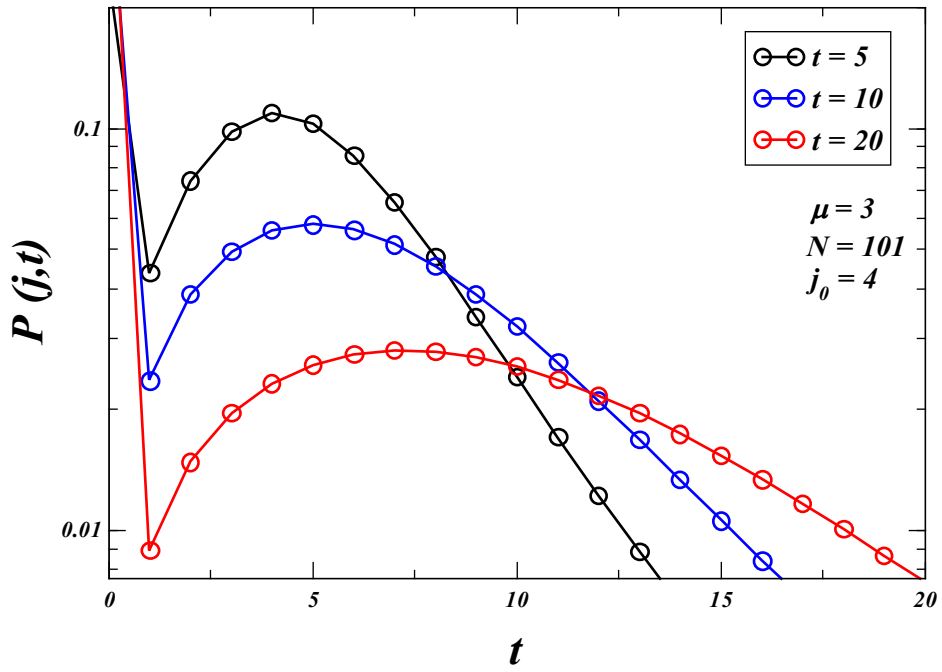

It is also interesting to calculate the mean square (3.33) deviation and the survival probability (3.36) previously defined in chapter 3. The expression for $S(t)$ is justified since the walker remains alive (unabsorbed) as long as it has not reached the boundary sites at $j = 1$ and $j = N$.

In Fig. 13 we show the mean square deviation $X^2_{rms}(t)$ versus time t in log-log scale for the walker starting near the left boundary [Fig. 13(a)] and from the middle of the interval [Fig. 13(b)]. In both cases, as long as the border are not reached we find then expected normal diffusion behavior $X^2_{rms}(t) \sim t$ typical of a random walker in a boundless space. As the borders start to be accessed, what naturally happens earlier in Fig. 13(a), deviations from this behavior become evident.

Figure 13 – Mean square deviation $X^2_{rms}(t)$ for $\mu = 3$ (Gaussian regime) as a function of time t in a finite domain from $j = 1$ to $j = 101$, with the starting point (a) near the left boundary, $j_0 = 4$, and (b) at $j_0 = 50$. Solid lines depict the results using the Fock space approach. Dashed lines represent the normal diffusion behavior $X^2_{rms}(t) \sim t$ typical of a random walker in a boundless space. When the solid and dashed lines depart the influence of the borders start to show up.

(a) $j_0 = 4$ (b) $j_0 = 50$

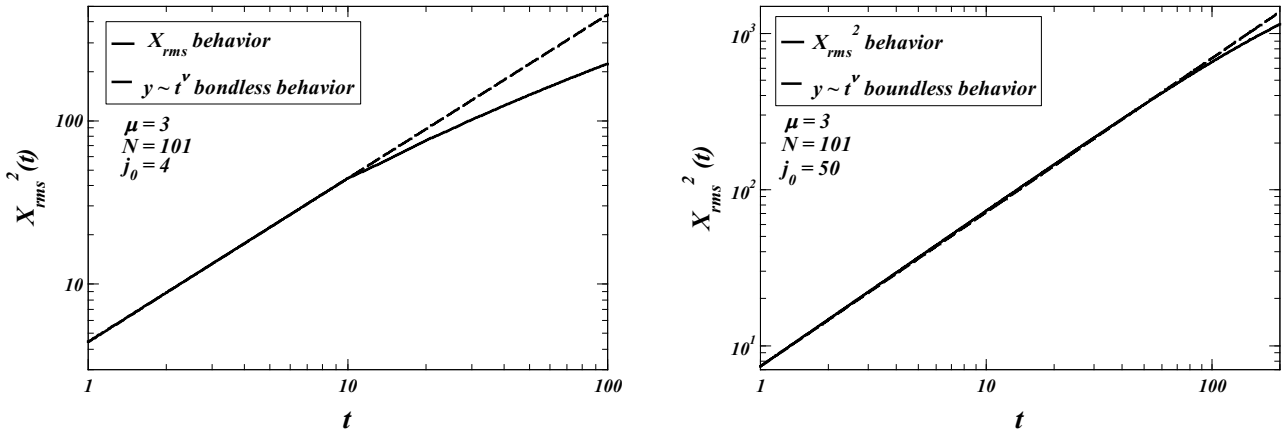

We can also compare the behavior of the survival probability with result of the Sparre-Andersen theorem. The Sparre-Andersen theorem [Andersen 1953, Andersen 1954] states that, for a Markovian stochastic process governed by a symmetrical and continuous step lengths distribution, the survival probability $S(t)$ for a random walk in a semi-infinite one-dimensional space scales asymptotically with the time t as $t^{-1/2}$, or with the number of steps n as $n^{-1/2}$. Here this theorem does not apply in a rigorous manner because we consider the random walker in a finite domain between two boundaries. However, just as argued in the previous chapter, as long as only one border is reached we expect the Sparre-Andersen power-law behavior of $S(t)$ to hold. As the time increases and both borders start to be accessed, a shift takes place to an exponential decay, $S(t) \sim e^{-\lambda t}$ [Araújo 2017]. Indeed, this is exactly what is shown in Fig. 14.

Figure 14 – (a) Log-log plot of the survival probability $S(t)$ as a function of time t for $\mu = 3$ in a finite domain from $j = 1$ to $j = 101$, with the starting point near the left boundary, $j_0 = 4$. The solid line depicts the results using the Fock space approach. The dashed line is the fit to $S(t) \sim t^{-\gamma}$, with $\gamma = 0.50$ in nice agreement with the Sparre-Andersen theorem, which works fine up to $t \sim 100$ when both borders start to be reached. (b) Log-linear plot of the survival probability $S(t)$ with parameters as in (a), showing in dashed line the exponential decay typical of the regime in which both borders can be accessed.

(a) Power-law behavior

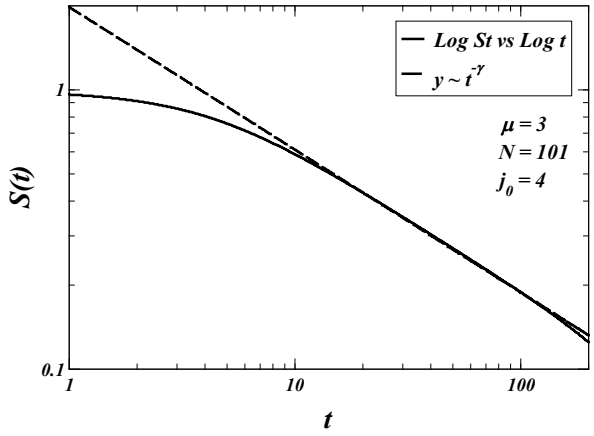

(b) Exponential decay behavior

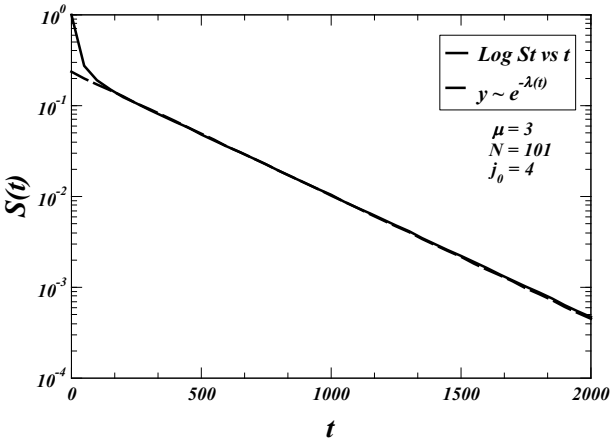

4.2.2 Case $\mu = 2$

The case of a power-law distribution of step lengths with exponent $\mu = 2$ corresponds to the asymptotic limit of the Cauchy distribution, i.e., the Lévy distribution with $\alpha = \mu - 1 = 1$. In the context of the random search problem with low density of target sites (scarce regime), this distribution of step lengths is important because it provides the highest efficiency when the searcher has no information about the search space and starts the search very close to the last target found (the so-called asymmetric nondestructive search) [Viswanathan et al. 2011].

We focus below on the discussion about the differences with respect to the case $\mu = 3$. For example, the probability distribution $P(j,t)$ for an interval with $N = 101$ sites, shown in Figs. 15 and 16, is suitably compared with the Cauchy distribution (instead of a Gaussian as in the case $\mu = 3$) when the walker starts from $j_0 = 50$.

Figure 15 – $P(j,t)$ for $\mu = 2$ as a function of the position j in a finite domain from $j = 1$ to $j = 101$, with the starting point at $j_0 = 50$, for different elapsed times, $t = 5, 10, 20$. Symbols correspond to the results using the Fock space approach. Lines are fits to the Cauchy distribution.

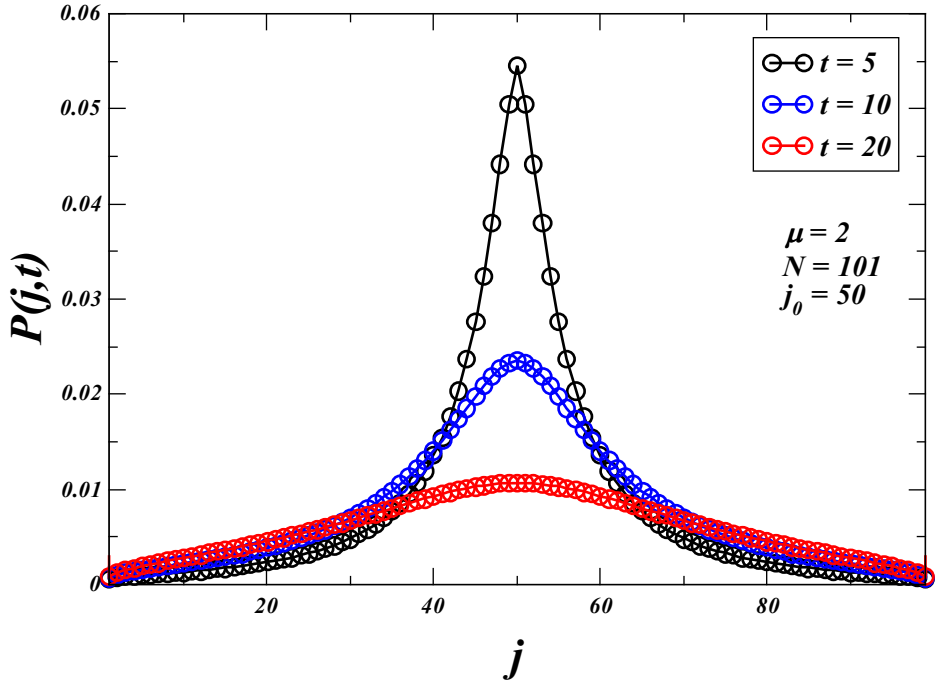

Figure 16 – Probability $P(j,t)$ for $\mu = 2$ as a function of the position j in a finite domain from $j = 1$ to $j = 101$, with the starting point near the left boundary, $j_0 = 4$, for different elapsed times, $t = 5, 10, 20$. Symbols correspond to the results using the Fock space approach. Lines are guides to the eye.

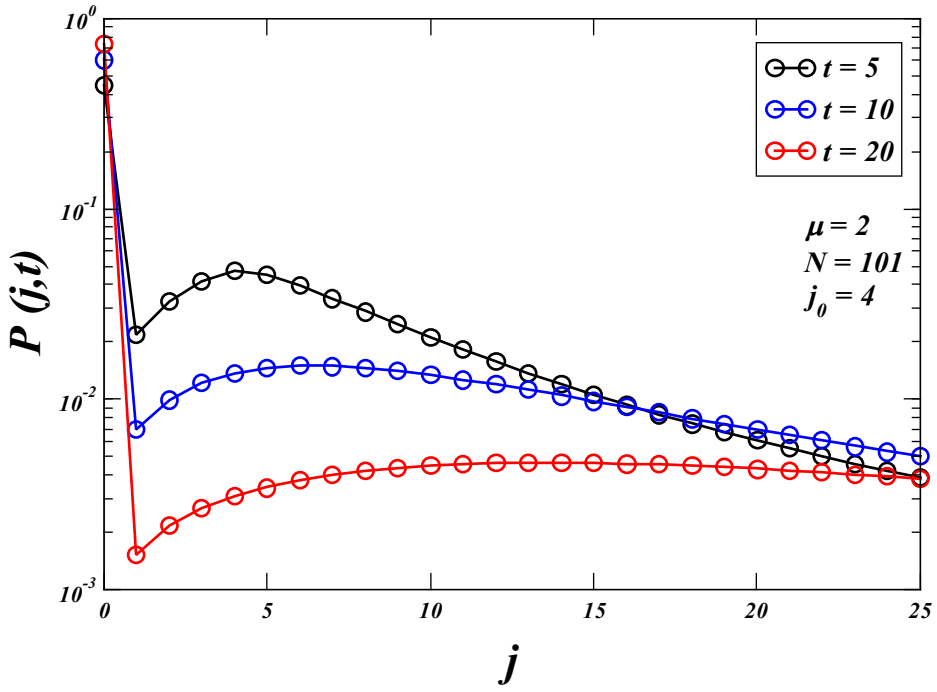

Also, the survival probability $S(t)$ does not show in Fig. 17 the power-law behavior typical of the Sparre-Andersen theorem in the semi-infinite space because for $\mu = 2$ both boundaries are rapidly reached when $N = 101$, due to the diverging second moment of the PDF $P(x)$ of step lengths. In this case, $S(t)$ presents exponential decay.

Another effect of this fast reaching of the borders for $\mu = 2$ is that it somewhat precludes the signature of the superdiffusive dynamics obtained from the mean square deviation in a system with $N = 101$ sites. Indeed, in order to clearly see superdiffusion before accessing the boundaries a larger value of N should be considered.

Figure 17 – (a) Log-log plot of the survival probability $S(t)$ as a function of time t for $\mu = 2$ in a finite domain from $j = 1$ to $j = 101$, with the starting point near the left boundary, $j_0 = 4$. No good fit to a power-law Sparre-Andersen-like behavior can be obtained. Instead, $S(t)$ presents exponential decay.

(a) Power-law behavior (b) Exponential decay behavior

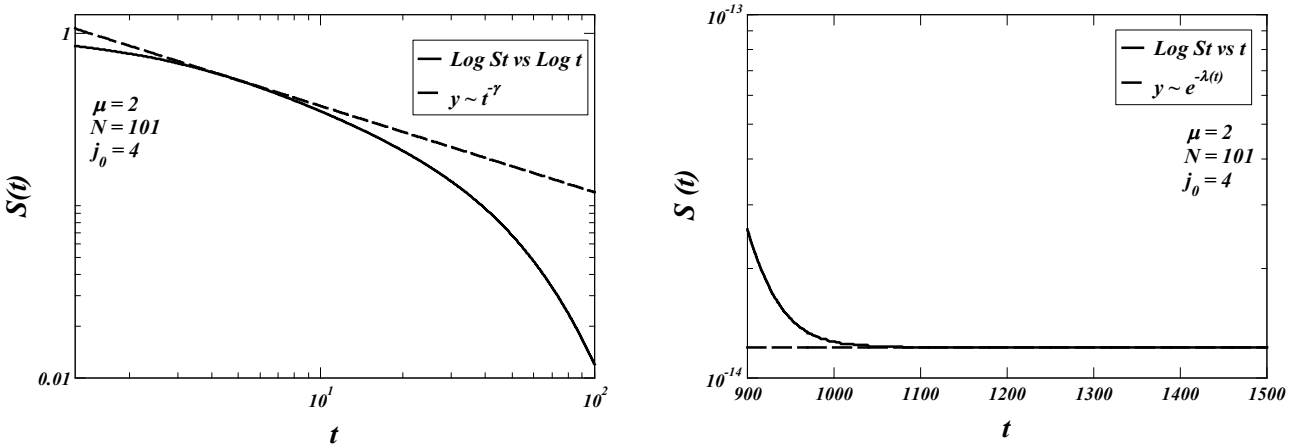

4.2.3 Case $\mu = 1.01$

This value of μ is very close to its lower boundary since $\mu \in (1,3]$. In this case, steps are very long and the random walker moves nearly ballistically. In the context of random searches in the scarce regime, a power-law distribution of step lengths with $\mu \to 1$ arises as the optimal strategy when the searcher starts as distant as possible from the target sites, e.g., from the middle of the one-dimensional interval (symmetric destructive search) [Viswanathan et al. 2011].

We show in Figs. 18 and 19 the behavior of the probability distribution $P(j,t)$ as a function of the position j. It is interesting to notice that $P(j,t)$ for $\mu = 1.01$ assumes values much lower than those for $\mu = 2$ and $\mu = 3$ for the same t, because of that to enhance this behavior we use a log-linear scale. The minimum value shown for $P(j,t)$ is around 10^{-11} and the fluctuations error according to the computing software Mathematica precision is around 10^{-16}. This is an indication of how fast the walker moves away from the starting point in the nearly ballistic regime.

Figure 18 – Probability $P(j,t)$ for $\mu = 1.01$ as a function of the position j in a finite domain from $j = 1$ to $j = 101$, with the starting point at $j_0 = 50$, for different elapsed times, $t = 5, 10, 20$.

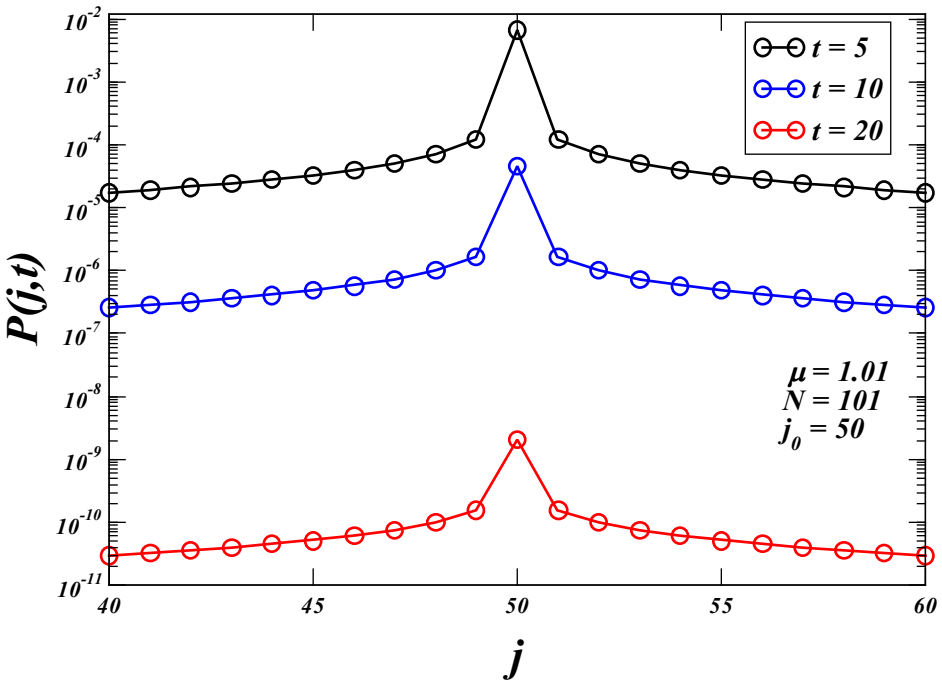

Figure 19 – Probability $P(j,t)$ for $\mu = 1.01$ as a function of the position j in a finite domain from $j = 1$ to $j = 101$, with the starting point near the left boundary, $j_0 = 4$, for different elapsed times, $t = 5, 10, 20$.

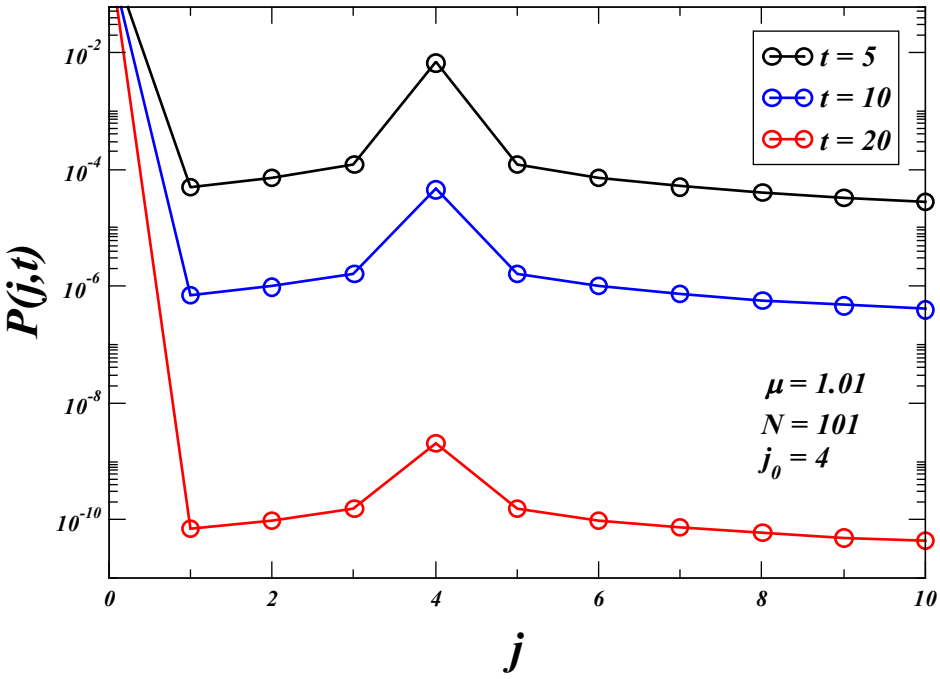

The survival probability $S(t)$ for $\mu = 1.01$ decays really fast to zero and it is not possible to characterize neither a power-law behavior nor an exponential decay as a function of time for $N = 101$.

We finally comment that we have also studied other values of the exponent μ, such as $\mu = 1.5$ and $\mu = 2.5$. However, since the results with these values did not show any significant qualitative difference with respect to the case $\mu = 2$ detailed above, then we have opted not to show them in this thesis.

5 RANDOM WALKER WITH LÉVY DISTRIBUTION OF STEP LENGTHS IN A FOCK SPACE APPROACH

« A philosopher once said, 'It is necessary for the very existence of science that the same conditions always produce the same results'. Well, they don't! »

Richard Feynman

Resumo do capítulo.

Neste capítulo vamos inicialmente revisar os processos de difusão anômala superdifusiva típicos de caminhantes aleatórios com distribuições de passos de Lévy, os quais foram apresentados e discutidos no Capítulo 1. Tais caminhadas são importantes no contexto das buscas aleatórias porque fornecem as eficiências de busca mais altas na situação em que o agente que procura não possui qualquer informação sobre o espaço de busca no regime de baixas densidades de sítios. Em seguida, estudaremos estes processos de Lévy no contexto da abordagem do espaço de Fock para um sistema unidimensional finito com extremos absorventes, tal como fizemos anteriormente para os casos em que o caminhante tinha tamanho de passo fixo ou distribuído segundo uma lei de potência. A maior parte dos resultados desse capítulo encontra-se publicada no artigo [Araújo et al. 2020].

5.1 IMPORTANCE OF LÉVY PROCESSES IN RANDOM SEARCHES

Diffusion phenomena occur in many branches of science. Historically, the study of diffusion processes dates at least from the late 18th and early 19th centuries with the observation of Brownian motion of coal dust and pollen particles in liquids, respectively by Jan Ingenhousz and Robert Brown [Brown 1828]. This discovery was rapidly extended to other areas, such as in the work by A. Fick in the mid 19th century on the flux of salt diffusing between two reservoirs of water [Fick 1855]

These first examples of diffusion processes display normal diffusion behavior, in which the variance scales linearly with the time or number of moves of the diffusing particles. However, not all diffusion dynamics behave this way. As discussed in Chapter 1, in some specific circumstances the dynamical process can display a dynamics which evolves slower or faster than normal diffusion, as respectively happens in subdiffusive or superdiffusive phenomena.

From the point of view of diffusing random walk particles in a boundless space, normal diffusion generally occurs when the distribution of step lengths has finite variance, being therefore governed by the CLT. On the other hand, superdiffusive motion is typical of distributions of step lengths with infinite variance driven by the GCLT, such as the power-law ones with $1 < \mu < 3$ and the Lévy α-stable themselves, with $0 < \alpha < 2$ [Nolan 2014, Shlesinger 1993, Mandelbrot 1960].

An important application of the Lévy distribution takes place in animal foraging theory in biology and ecology [Viswanathan et al. 2011, Buchanan 2008, Clauset, Shalizi and Newman 2009, Viswanathan, Raposo and Luz 2008, Humphries et al. 2012, Humphries, Weimerskirch and Sims 2013]. In a certain way, the movement of animals resembles that of random walks of dust particles in a fluid, but the first theories to explain the animal movement patterns, built on the basis of correlated random walk models with dynamics driven by the CLT, could not describe the existence of long steps observed in the empirical data of some species. In such cases, only the introduction in the late 1990's of power-law and Lévy distributions of step lengths, with presence of long jumps and governed by the GCLT, could provide the suitable description of these data [Viswanathan et al. 2002]. Since then, the Lévy flight approach to random searches and animal foraging have became paradigmatic [Clauset, Shalizi and Newman 2009, Viswanathan, Raposo and Luz 2008, Humphries et al. 2012, Humphries, Weimerskirch and Sims 2013]. In this chapter we study such Lévy processes through a different view, based on the formulation of the problem in terms of the Fock space of occupation numbers usually employed to treat quantum mechanical systems.

5.2 LÉVY FLIGHTS IN FOCK SPACE

In this section we discuss the problem of a random particle with Lévy α-stable distribution of step lengths moving in a finite domain with absorbing boundaries. Our analysis is based on the Fock space approach introduced in Chapter 2.

We have briefly presented the Lévy α-stable distributions in Chapter 1. They are defined as

$$\begin{aligned} p_\alpha(\ell) &= \frac{1}{2\pi}\int_{-\infty}^{\infty} dk\, e^{-b|k|^\alpha\left[1-\beta\,\mathrm{sgn}(k)\Phi(k)\right]-ik(\ell-\nu)} \\ &= \frac{1}{2\pi}\int_{-\infty}^{\infty} dk\, e^{-|k|^\alpha - ik\ell}, \end{aligned} \tag{5.1}$$

in which in the last line above we have considered symmetric distributions around $\ell = 0$ related to step lengths to the right or to the left with equal probabilities, $p_\alpha(|\ell|) = p_\alpha(-|\ell|)$ (skewness

parameter $\beta = 0$ and location parameter $\nu = 0$, see Chapter 1). The most important parameter above is the stability Lévy index $\alpha \in (0,2]$, which governs the asymptotic power-law behavior of (5.1) in the form $P(\ell) \sim 1/|\ell|^{\alpha+1}$ for $\alpha \in (0,2)$. As mentioned in Chapter 1, the variance of the Lévy distribution for $\alpha \in (0,2)$ is infinite and they represent the attractor family of distributions driven by the GCLT. On the other hand, the limit case $\alpha = 2$ corresponds to the Gaussian distribution and CLT.

Interestingly, although Lévy distributions can be generally cast [Zolotarev and Uchaikin 1999, Metzler and Klafter 2000, Metzler and Klafter 2004] in terms of Fox-H functions, whose calculation relies on complex integrals of the Mellin-Barnes type, they lack closed-form expressions based on elementary functions [Penson and Górska 2010, Górska and Penson 2011], with exceptions for $\beta = 0$ of the Cauchy $(\alpha = 1)$ and Gaussian $(\alpha = 2)$ cases. This fact contributes to enhance the difficulty to find analytical expressions for the probability distribution $P(x,t)$ of a Lévy random particle on a bounded interval.

Moreover, due to the non-negligible probability of long steps for $0 < \alpha < 2$, occasionally the Lévy particle can take a jump that surpasses one of the boundaries, effectively resulting in the absorption by the corresponding extreme site. In such a case, the method of images usually employed to treat normal diffusion processes breaks down [Chechkin et al. 2003]. In this context, the application of the Fock space approach to Lévy processes can be seen as a welcome contribution to this area that also proved to be quite efficient, as seen below.

5.2.1 Methodology

The general methodology of the Fock space approach applied to classical statistical physics systems was explained in detail in Chapter 2. In the particular case of a random particle with Lévy distribution of step lengths, we note that any discrete site in the lattice can be reached from anywhere due to the possibility of large steps. Thus, the Hamiltonian-like operator for a bounded Lévy flier with discrete positions $j(1,2,...,N)$ and absorbing boundaries at $j = 1$ and $j = N$ reads

$$H = -\sum_{j=1}^{N} \sum_{\substack{k=2 \\ k \neq j}}^{N-1} P_{kj} \, (a_j^{\dagger} a_k - a_k^{\dagger} a_k), \tag{5.2}$$

where P_{kj} is the probability of jumping from site j to k (transition probability), calculated from

$$P_{kj} = \begin{cases} 0, & k = j; \\ \int_{(|k-j|-1)\Delta x}^{|k-j|\Delta x} p_\alpha(\ell)d\ell, & 1 \leq k, j \leq N; \\ \int_{(j-1)\Delta x}^{\infty} p_\alpha(\ell)d\ell, & 1 \leq j \leq N, \quad k = 1; \\ \int_{(N-j-1)\Delta x}^{\infty} p_\alpha(\ell)d\ell, & 1 \leq j \leq N, \quad k = N. \end{cases} \tag{5.3}$$

The third and fourth lines in Eq. (5.3) refer, respectively, to jumps starting at site j whose length is equal to or larger than the respective distances to the left and right boundaries. These flights are thus absorbed by the sites at $k = 1$ and $k = N$, respectively. Notice that, since we are working with symmetric Lévy distributions, then $p_\alpha(|\ell|) = p_\alpha(-|\ell|)$ and the integral in the third line above, which is in principle taken over a negative argument, from $-\infty$ to $-(j-1)\Delta x$, is in fact equivalent to the corresponding integral calculated over the positive range, from $(j-1)\Delta x$ to ∞.

The integrals in Eq. (5.3) can be expressed for any $\alpha \in (0,2]$ in terms of the following double integral with $a > 0$:

$$\begin{aligned} I_\alpha(a) &= \frac{1}{2\pi}\int_{-\infty}^{\infty} d\ell \int_0^{\infty} e^{-|k|^\alpha - ik\ell}\, dk, \\ &= \frac{1}{\pi}\int_0^{\infty} \frac{e^{-ika-k^\alpha}}{ik}\, dk, \\ &= \frac{1}{\pi}\int_0^{\infty} \frac{\sin(ka)}{k} e^{-k^\alpha} dk. \end{aligned} \tag{5.4}$$

Then, in the symmetric case with absorbing boundary conditions, where $P_{kj} = P_{jk}$, we have $P_{kj} = 0$ if $j = 1$ and $j = N$, since the flier cannot leave an extreme site when absorbed. For all other $j \neq 1, N$, one has $\sum_k P_{kj} = 1$ to give the correct normalization. Although our main focus in this work is on absorbing boundary conditions, we also notice that, under reflecting boundary conditions, one might have $P_{kj} \neq 0$ even for $j = 1$ and $j = N$ (see last section of this chapter).

The matrix elements of H with absorbing boundaries can be obtained for any Lévy index $\alpha \in (0,2]$ on the basis of Fock states, using the algebra for the raising and lowering operators, respectively $\{a_j^\dagger\}$ and $\{a_j\}$, which promote the creation and destruction of a random particle at

position x_j (see Chapter 2). By applying this algebra to Eq. (5.2) we find

$$\begin{aligned}\langle m|H|n\rangle &= -\sum_{i=2}^{L-1}\sum_{\substack{k=1\\ i\neq k}}^{L} P_{ik}\,\langle m \mid (a_k^{\dagger}a_i - a_i^{\dagger}a_i) \mid n\rangle \\ &= -\sum_{j=0}^{N}\sum_{\substack{k=1\\ k\neq j}}^{N-1} P_{kj}\left(\delta_{kn}\delta_{mj} - \delta_{kn}\delta_{mk}\right),\end{aligned} \tag{5.5}$$

where $m,n = 1,...,N$, which implies $\langle m|H|n\rangle = -P_{mn}$ if $m \neq n$ and $\langle m|H|m\rangle = 1$, but with $\langle m|H|n\rangle = 0$ if $n = 1$ or $n = N$ due to the absorbing condition at the boundary sites $j = 1$ and $j = N$. For large N the eigenvalues and eigenvectors of H are obtained with a symbolic computing software (*Mathematica*).

At this point, in order to make a summary of the Fock space procedure applied to a Lévy flier in a unidimensional lattice with absorbing boundaries, we consider in the next sections the following three steps:

1. Compute the matrix P_{kj} of probabilities of jumping from site j to site k.
2. Write the Hamiltonian matrix H.
3. Perform the Jordan decomposition to obtain the time evolution operator U.

Once the time evolution operator U is obtained, one can conceivably calculate any relevant quantity of the system, as presented in the next sections.

5.2.2 Lévy flights in a Fock space approach with different alfa values

5.2.2.1 Case $\alpha = 2$

As mentioned above, this is the limit Gaussian case of Lévy processes. We choose in Eq. (5.1) the scale factor $b = 1/2$, which corresponds to a Gaussian distribution of step lengths with unit variance, $\sigma^2 = 2b = 1$ [Metzler and Klafter 2004]. In this case Eq. (5.4) yields

(5.6)

where $\operatorname{erf} z = \dfrac{2}{\sqrt{\pi}}\displaystyle\int_0^z e^{-t^2}\,dt$ denotes the error function. If, e.g., $m \neq n$, with $m \neq 1$, $n \neq 1$, $m \neq N$ and $n \neq N$, the elements of the Hamiltonian-like matrix read

$$\langle m|H|n\rangle = \frac{1}{2}\left[\operatorname{erf}((|m-n|-1)/2) - \operatorname{erf}(|m-n|/2)\right]. \tag{5.7}$$

The other matrix elements are similarly calculated from the first, third and fourth lines of Eq. (5.3) combined with Eqs. (5.4) and (5.7).

As described in the previous chapters, we calculate the probability distribution $P(j,t)$ to find the Lévy particle at discrete position j in time t, and plot it as a function of j in a domain of length $N = 100$, shown in Fig. 20, with the starting point at the middle of the interval, $j_0 = N/2$. Results using the Fock space approach are depicted in circles for times $t = 5$ (black), 15 (blue), and 100 (red). The curves are symmetrical with respect to the center of the interval, as expected.

Figure 20 – Probability $P(j,t)$ for $\alpha = 2$ (Gaussian limit) as a function of the position j in a finite domain of length $N = 100$, with the starting point at the middle of the interval, $j_0 = N/2$, and for different elapsed times, $t = 5, 15, 100$.

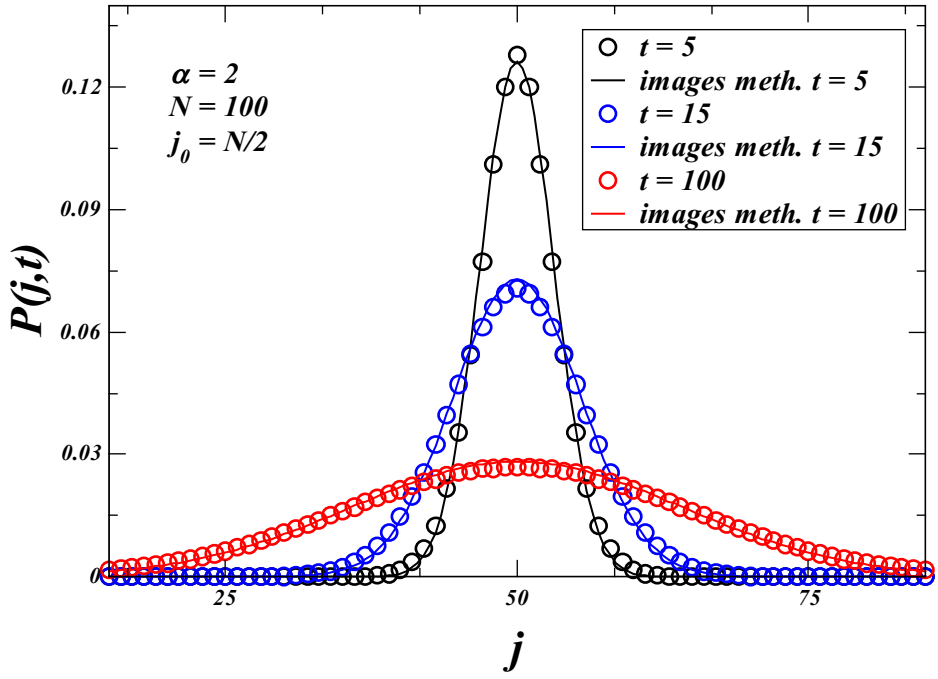

In all cases in Fig. 20 we observe a nice agreement with the solid lines representing the exact solution from the method of images [Metzler and Klafter 2004, Chechkin et al. 2006], which, as mentioned, holds in the $\alpha = 2$ diffusive regime:

$$P(j,t) = \sum_{n=-\infty}^{\infty} \Big[P_0(|j - j_0| + 2Nn, t) - P_0(j + j_0 + 2Nn, t) \Big], \tag{5.8}$$

where the Gaussian function

$$P_0(j,t) = \frac{1}{\sqrt{2\pi\sigma^2 t}} e^{-j^2/(2\sigma^2 t)} \tag{5.9}$$

is the solution of the Brownian diffusion equation in the one-dimensional unbounded space (i.e., without absorbing boundary sites). We also display in Fig. 21 the distribution $P(j,t)$ with starting point $j_0 = 10$ near the left border for different elapsed times. As expected, the close proximity of the border makes with that the particle is absorbed even for small times with probability increasing with t.

Figure 21 – Probability $P(j,t)$ for $\alpha = 2$ (Gaussian limit) as a function of the position j in a finite domain of length $N = 100$, with the starting point near the left boundary, $j_0 = 10$, and for different elapsed times, $t = 5, 10, 50$.

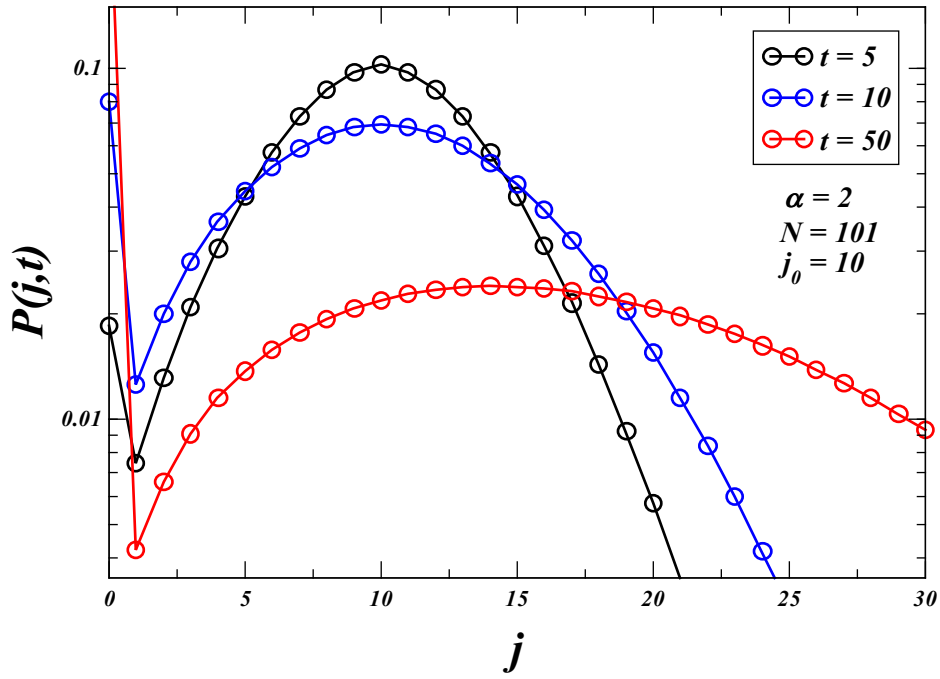

Another important quantity to calculate is the survival probability [Cox 2017, Blumenthal, Getoor and Ray 1961, Chechkin et al. 2006]. In Fig. 22 we show in circles the Fock space results of $S(t)$ in log-log scale as a function of t for the $\alpha = 2$ Gaussian case with $b = 1/2$, in a larger domain with $N = 300$ and starting from the position $j_0 = 9$ close to the left boundary. Moreover, results from numerical simulations are also depicted in solid line. In this case, since long jumps are quite rare when $\alpha = 2$ the faraway right boundary at $j = 300$ is not effectively reached. In practice, this situation resembles that of a random walker in a semi-infinite domain, in which, as discussed in the previous chapter, the Sparre-Andersen theorem predicts [Andersen

1953, Andersen 1954] the asymptotic power-law form,

$$S(t) \sim \frac{1}{\sqrt{t}}. \tag{5.10}$$

Although in the present case the Lévy flier actually evolves in a finite domain, so that the conditions for the Sparre-Andersen theorem are not strictly observed, the long-term regime of the survival probability in Fig. 22 (dashed line) is given by $S(t) \sim t^{-\gamma}$, with the best-fit value $\gamma = 0.49$. Consistently, the probability of being absorbed by the faraway boundary at $j = 300$ is rather low, 8.3×10^{-6} for $t = 2000$ and 5.4×10^{-10} for $t = 1000$.

Figure 22 – Log-log plot of the survival probability $S(t)$ as a function of time t for the $\alpha = 2$ Gaussian case in a large extension domain with $N = 300$ and starting point $j_0 = 9$ close to the left boundary. Circles and solid line depict, respectively, the results from the Fock space approach and numerical simulations. In this case, only the left boundary is effectively reached by the flier for the values of t shown. The long-term behavior is given by the power law $S(t) \sim t^{-\gamma}$ (dashed line), with the best-fit value $\gamma = 0.49$.

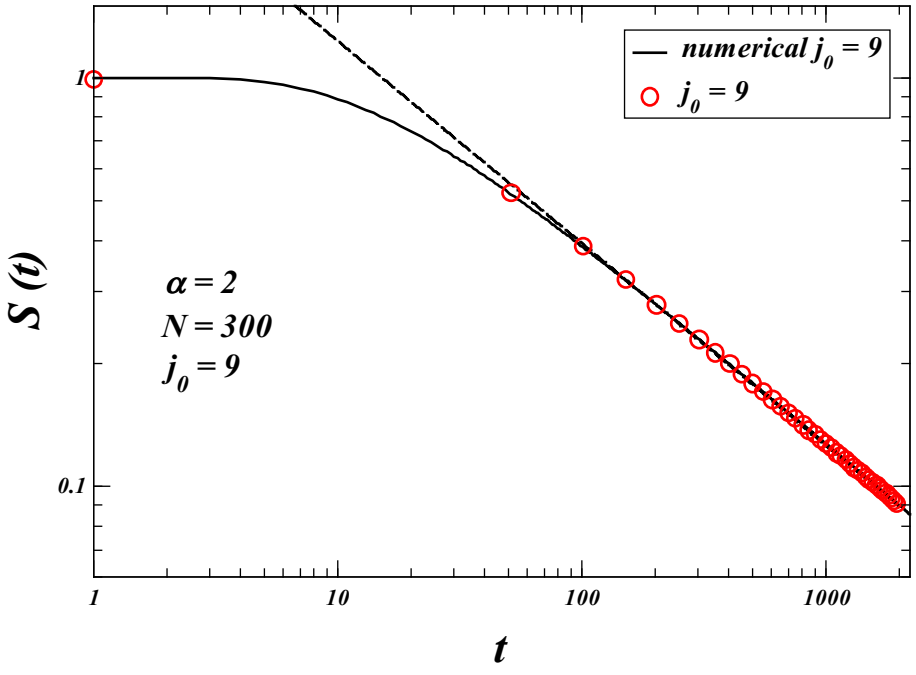

A quite interesting dynamical crossover takes place when the other boundary site also becomes progressively reached. In this case, the power-law behavior observed in Fig. 22 is smoothly replaced by an exponentially decaying survival probability [Araújo and Raposo 2016, Dybiec, Gudowska-Nowak and Chechkin 2016],

$$S(t) \sim e^{-\lambda t}. \tag{5.11}$$

In order to capture this change with the $\alpha = 2$ Gaussian case ($b = 1/2$), we consider in Fig. 23 a narrower interval (in comparison with Fig. 22), so that the right boundary site could also be possibly reached in feasible computational times. Indeed, Fig. 23 displays the Fock space (circles) and numerical simulation (solid lines) results in the linear-log plot of $S(t)$ as a function of t, with $N = 100$ and starting points $j_0 = 9$ (black) and $j_0 = N/2$ (red). We observe in this case that the power-law decay becomes restricted to the low-t regime, with the exponential decay of $S(t)$ emerging for larger times (dashed lines). We also notice that our best-fit value $\lambda = 0.001085$ compares nicely with the results obtained from the discretized Riesz fractional differential operator, $\lambda = 0.000990$ [Zoia, Rosso and Kardar 2007], and Wiener-Hopf decomposition, $\lambda = 0.000955$ [Araújo and Raposo 2016], techniques.

Figure 23 – Linear-log plot of the survival probability $S(t)$ as a function of time t for the $\alpha = 2$ Gaussian case in a narrower domain with $N = 100$ (in comparison with $N = 300$ in Fig. 22). Starting points are $j_0 = 9$ (black) and $j_0 = N/2$ (red). Circles and solid lines depict, respectively, the results from the Fock space approach and numerical simulations. Dashed lines are fits to the asymptotic exponential decay behavior, $S(t) \sim e^{-\lambda t}$, observed when absorption takes place in both boundary sites. This contrasts with the asymptotic power-law behavior in Fig. 22 when only a single absorbing site (the initially closer one) is reached.

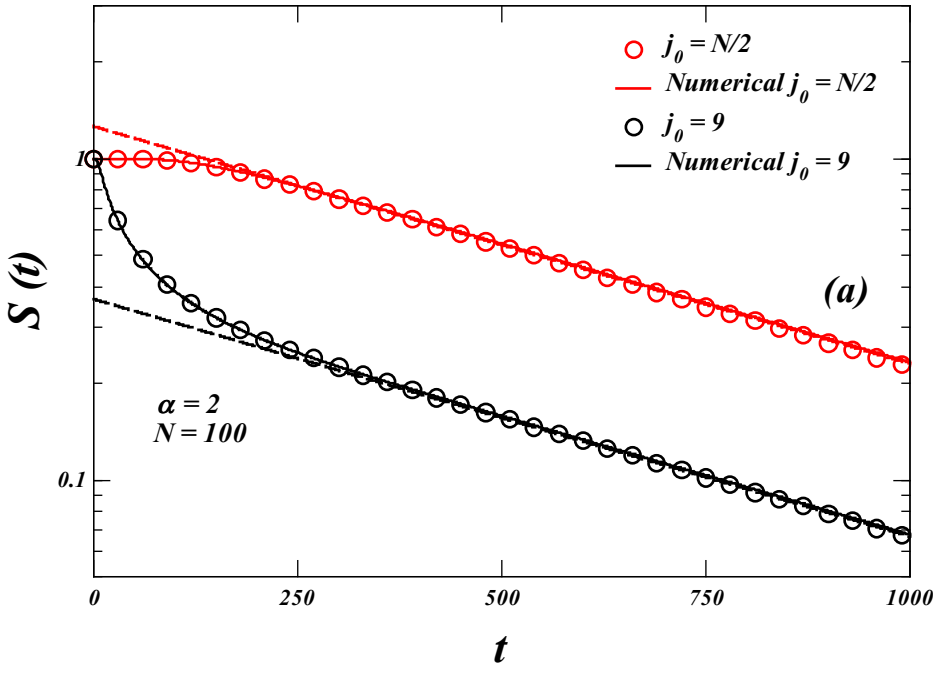

5.2.2.2 Case $\alpha = 3/2$

In this regime with $\alpha \neq 2$, due to the failure of the method of images and further difficulties related to other analytical techniques mentioned earlier, no exact expression for $P(x,t)$ is available. Thus, our results using the Fock space formalism are compared below with direct numerical simulations, in which a random particle is allowed to evolve in a bounded space with jump lengths drawn from the Lévy distribution $p_\alpha(\ell)$, with averages taken over a large number of runs. At this point, we comment that some careful must be taken when trying to compare the continuous time results of the Fock space approach with the discrete time results from numerical simulations. Indeed, in numerical simulations jumps take place in discrete time units δt, so that $t = n\,\delta t$ with n denoting the number of jumps. Hence, in order to establish a proper comparison with the results from numerical simulations for very short times, typically $t \lesssim 10$, we have employed in the Fock space formalism the discretization scheme for small times t that is usually considered for the discrete time propagator in quantum mechanics [Sakurai 1994], namely, $U(0,t) = [U(\delta t)]^n$, with identity matrix (operator). However, we point out that, as the discreteness of t in the numerical simulations loses relevance for larger times, $t \gtrsim 10$, then the results using both the continuous exponential and discretized forms of U become indistinguishable for such values of t, as expected.

We now present the results for the value $\alpha = 3/2$ with the scale factor set to unit in the Lévy distribution, $b = 1$. In this case Eq. (5.4) implies

$$\begin{aligned} I_{\alpha=3/2}(a) &= \frac{1}{\pi}\big[a\Gamma(5/3)\,{}_3F_4(\mathbf{a}_1;\mathbf{b}_1;c) \\ &\quad -\frac{a^3}{9}\,{}_4F_5(\mathbf{a}_2;\mathbf{b}_2;c) \\ &\quad +\frac{7a^5}{405}\Gamma(4/3)\,{}_3F_4(\mathbf{a}_3;\mathbf{b}_3;c)\big], \end{aligned} \tag{5.12}$$

where Γ and ${}_pF_q$ denote the gamma and generalized hypergeometric functions, respectively, with parameters $\mathbf{a}_1 = (1/6,5/12,11/12)$, $\mathbf{a}_2 = (1/2,3/4,1,5/4)$, $\mathbf{a}_3 = (5/6,13/12,19/12)$, $\mathbf{b}_1 = (1/3,1/2,5/6,7/6)$, $\mathbf{b}_2 = (2/3,5/6,7/6,4/3,3/2)$, $\mathbf{b}_3 = (7/6,3/2,5/3,11/6)$, $c = -4a^6/729$. The off-diagonal Hamiltonian matrix elements are

$$\langle m|H|n\rangle = I_{\alpha=3/2}(|m-n|-1) - I_{\alpha=3/2}(|m-n|), \tag{5.13}$$

if $m \neq n$, with $m \neq 1$, $n \neq 1$, $m \neq N$ and $n \neq N$. The first, third and fourth lines of Eq. (5.3) combined with Eqs. (5.5) and (5.12) provide the other matrix elements.

In Figs. 24 and 25 we depict in circles the results using the Fock space approach with $N = 100$ and $t = 5, 10, 50$, for the Lévy particle starting, respectively, from the middle of the interval, $j_0 = N/2$, and near the left boundary, $j_0 = 9$. For comparison, results from direct numerical simulations averaged over 5×10^4 random walk runs are depicted in solid lines. Compared to the Gaussian case $\alpha = 2$, jump lengths are considerably larger when $0 < \alpha < 2$ (in fact, the mean jump length is infinite for $\alpha \leq 1$ in unbounded space). As a consequence, in this superdiffusive regime the boundary absorbing sites are reached by the flier in much fewer jumps.

Figure 24 – $P(j,t)$ for $\alpha = 3/2$ as a function of the position j in a finite domain of length $N = 100$, with the starting point at the middle of the interval, $j_0 = N/2$. Results using the Fock space approach are depicted in circles for times $t = 5$ (black), 15 (blue), and 50 (red). No exact solution for $P(j,t)$ is available for comparison when $\alpha \neq 2$. Nice agreement is noted with direct numerical simulations (solid lines).

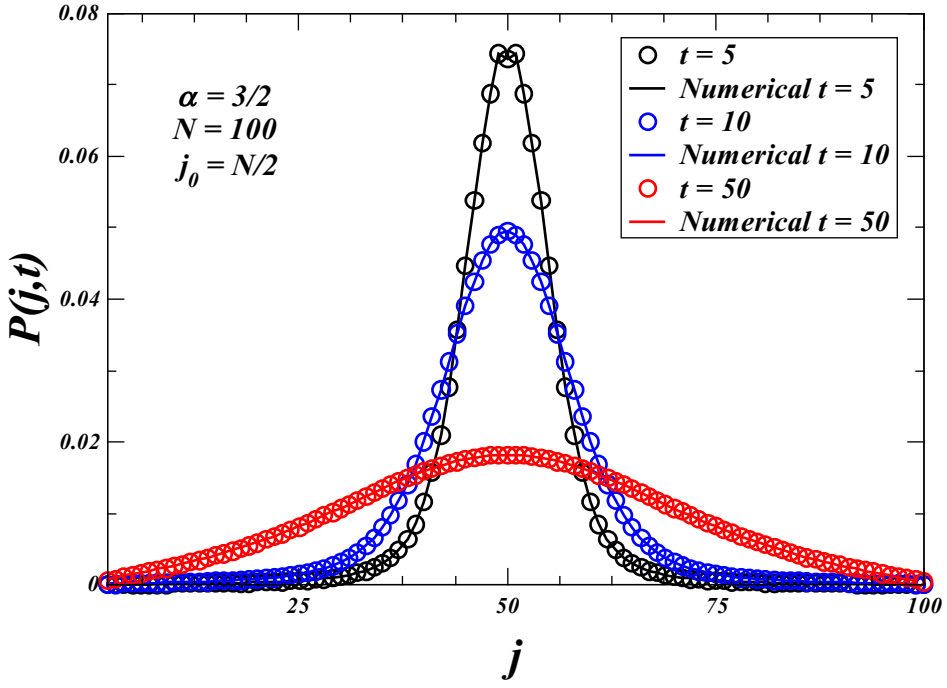

Figure 25 – $P(j,t)$ for $\alpha = 3/2$ as a function of the position j in a finite domain of length $N = 100$, with the starting point near the left boundary, $j_0 = 9$. Results using the Fock space approach are depicted in circles for times $t = 5$ (black), 15 (blue), and 50 (red). No exact solution for $P(j,t)$ is available for comparison when $\alpha \neq 2$. Nice agreement is noted with direct numerical simulations (solid lines).

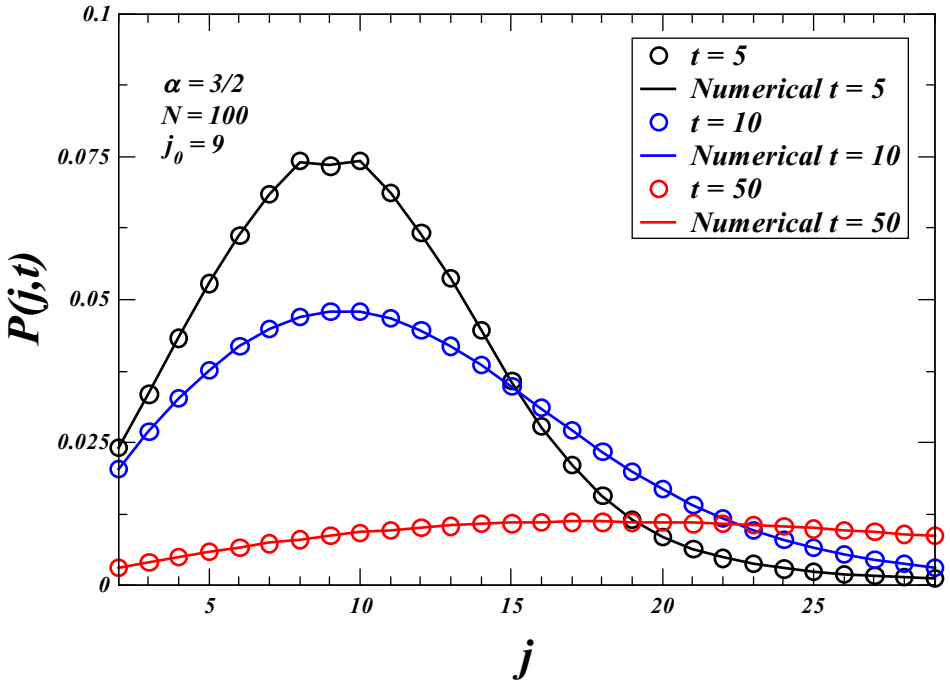

By denoting now as $Q_0(t)$ and $Q_N(t)$ the respective probabilities of being absorbed by the boundary sites at $j = 1$ or $j = N$, we show in Fig. 26 the time evolution of $Q_0(t)$ and $Q_N(t)$ for the initial position $j_0 = 9$ close to the left boundary, in good agreement with the numerical simulations. As expected, $Q_0(t)$ is higher than $Q_N(t)$ for this value of j_0, with both quantities increasing with time and displaying a slow tendency to saturation.

Figure 26 – Probabilities $Q_0(t)$ and $Q_N(t)$ of being absorbed respectively by the boundary sites at $j = 0$ and $j = N$ as a function of time t for $\alpha = 3/2$ in a finite domain of length $N = 100$, with the starting point next to the left boundary, $j_0 = 9$. Nice agreement is noted between the Fock space results (circles) and numerical simulations (stars).

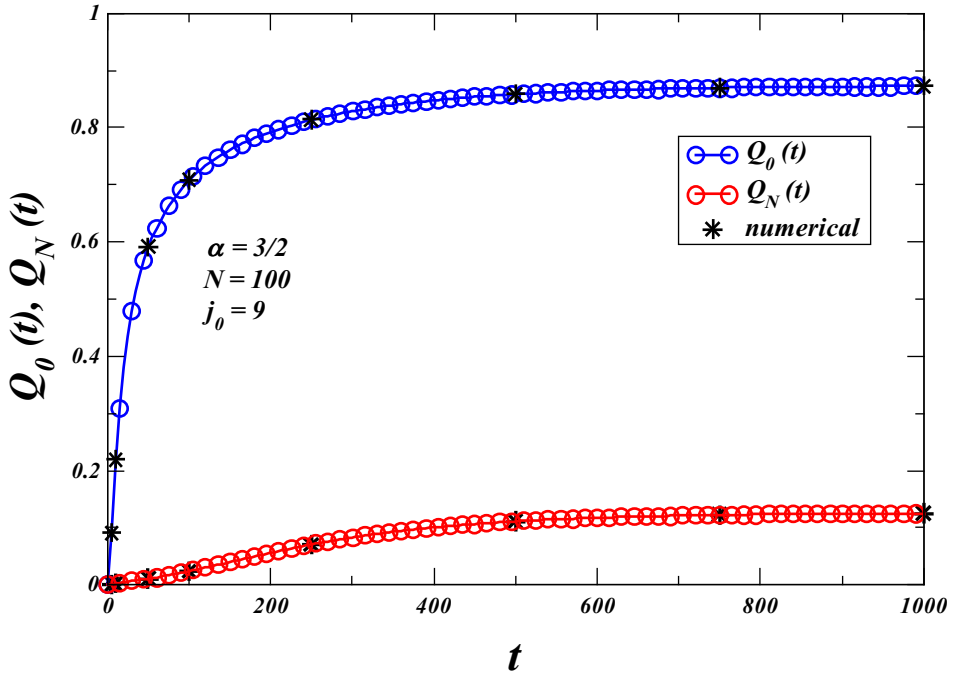

Next we show in Fig 27 the survival probability $S(t)$ as a function of t, in log-log scale for short times and in log-linear scale for long times.

Figure 27 – (a) Log-log plot of the survival probability $S(t)$ as a function of time t for $\alpha = 3/2$ in a finite domain of length $N = 101$, with the starting point near the left boundary, $j_0 = 10$ (solid line). Dashed line is the fit to the Sparre-Andersen-like power-law behavior, $S(t) \sim t^{-1/2}$, observed for short times while the faraway boundary has not been reached yet. (b) Log-linear plot of $S(t)$ with parameters as in (a) (solid line) and the fit to the exponential decay behavior (dashed line) for long times, $S(t) \sim \exp(-\lambda t)$, when both boundaries are reached.

(a) Power-law behavior

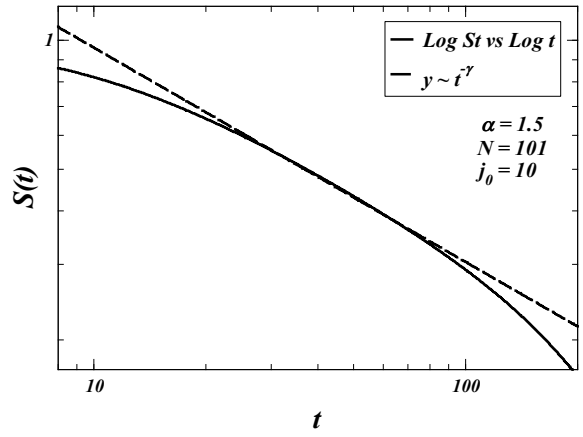

(b) Exponential decay behavior

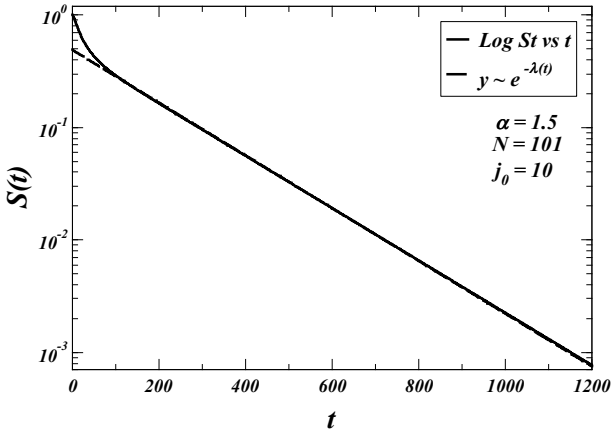

5.2.2.3 Case $\alpha = 1$

We consider now the case of a Cauchy flier with $\alpha = 1$. The integral (5.4) for $\alpha = 1$ reads

$$I_{\alpha=1}(a) = \frac{\arctan(a)}{\pi}, \tag{5.14}$$

from which the off-diagonal elements of the Hamiltonian matrix can be obtained as

$$\langle m|H|n\rangle = [\arctan(|m-n|-1) - \arctan(|m-n|)]/\pi, \tag{5.15}$$

if $m \neq n$, $m \neq 1$, $n \neq 1$, $m \neq N$ and $n \neq N$. The other matrix elements are calculated from the first, third and fourth lines of Eq. (5.3) combined with Eqs. (5.5) and (5.15).

We first show in Figs. 28 and 29 the probability distribution $P(j,t)$ as a function of j for $N = 101$ and different elapsed times, $t = 5, 10, 50$, with the Lévy particle starting, respectively, from $j_0 = 50$, and near the left boundary, $j_0 = 10$.

Figure 28 – Probability $P(j,t)$ for $\alpha = 1$ as a function of the position j in a finite domain of length $N = 101$, with the starting point at $j_0 = 50$, and for different elapsed times, $t = 5, 10, 50$.

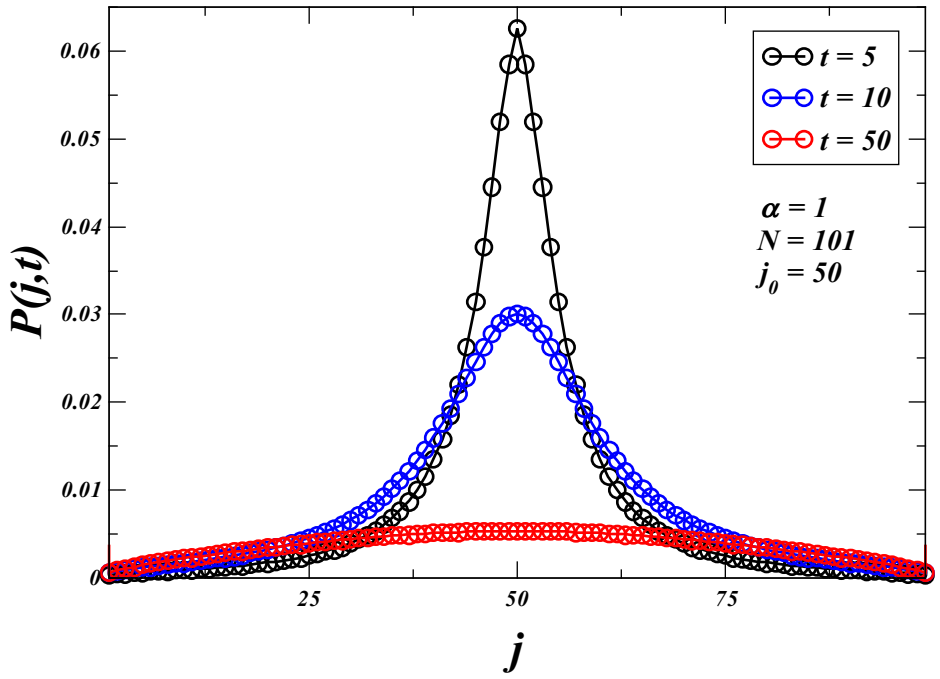

Figure 29 – Probability $P(j,t)$ for $\alpha = 1$ as a function of the position j in a finite domain of length $N = 101$, with the starting point near the left boundary, $j_0 = 10$, and for different elapsed times, $t = 5, 10, 50$.

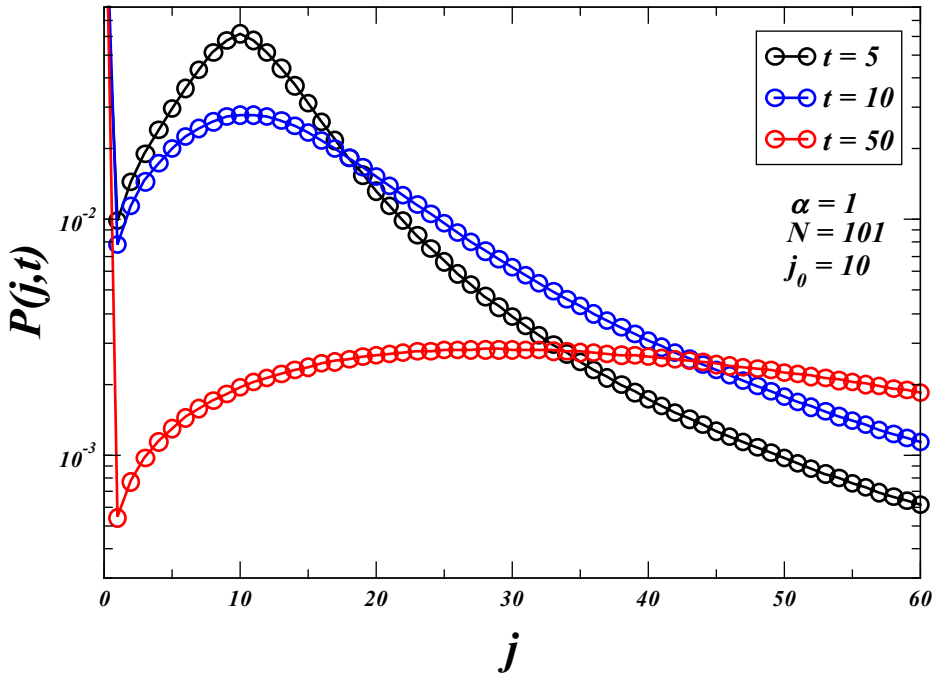

A similar behavior of the survival probability also occurs for the Cauchy flier with $\alpha = 1$, as shown in Fig. 30 with the same parameters as in Fig. 23 for the Gaussian flier with $\alpha = 2$. Here we see the exponential decay of $S(t)$ for long times according to Eq. (5.11). In this case, however, since jumps are much larger than when $\alpha = 2$, the crossover from the power-law to the exponential behavior of $S(t)$ takes place much earlier. In particular, our best-fit decay rate in Eq. (5.11), $\lambda = 0.0239$ for $\alpha = 1$, $b = 1$ and $N = 100$, was found to be in nice agreement with the results for the same parameters from both discretized Riesz fractional differential operator [Zoia, Rosso and Kardar 2007] ($\lambda = 0.0236$) and Wiener-Hopf decomposition [Araújo and Raposo 2016] ($\lambda = 0.0231$) techniques.

Figure 30 – Linear-log plot of the survival probability $S(t)$ as a function of time t for $\alpha = 1$ in a narrower domain with $N = 100$. Starting points are $j_0 = 9$ (black) and $j_0 = N/2$ (red). Circles and solid lines depict, respectively, the results from the Fock space approach and numerical simulations. Dashed lines are fits to the asymptotic exponential decay behavior, $S(t) \sim e^{-\lambda t}$, observed when absorption takes place in both boundary sites.

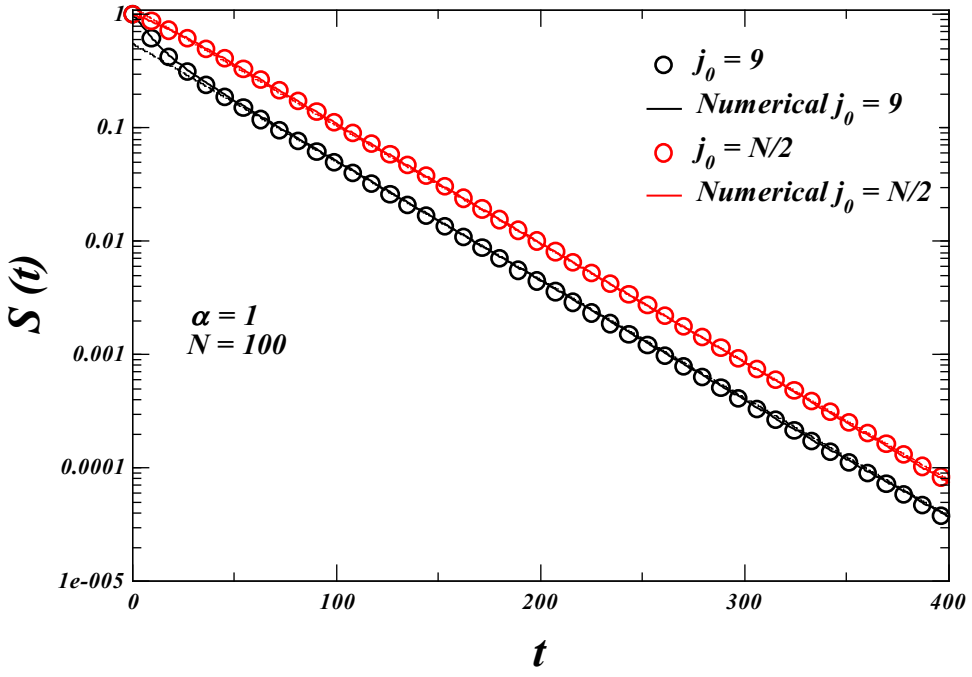

At this point, we remark that this similarity of results for λ obtained through different methods might indicate the existence of some interesting connection between the Fock space formalism and the spectrum of eigenvalues λ_k of the fractional Laplacian operator [Zoia, Rosso and Kardar 2007, Kwasnicki 2012, Garbaczewski and Stephanovich 2019]. Indeed, as stated in [Zoia, Rosso and Kardar 2007], the exact values of λ_k are not known and their calculation still remains an open question. As a consequence, the investigation of several associated quantities is hindered by this fact. For instance, the survival probability can be cast [Zoia, Rosso and Kardar 2007] in the form $S(t) = \sum_k a_k e^{-|\lambda_k| t}$, so that the smallest eigenvalue $|\lambda_{k=1}|$ (in absolute value) essentially determines the long-term behavior of $S(t)$, i.e., $\lambda = |\lambda_{k=1}|$.

Analogously, we generally find in the Fock space approach that $S(t) = \sum_i c_i e^{-\mu_i t}$, with c_i and $\mu_i > 0$ determined from the calculation of the eigenvalues and eigenvectors of the matrix $\exp(-tH)$. Moreover, we also stress that the discretized Riesz fractional differential operator [Zoia, Rosso and Kardar 2007] and the Wiener-Hopf decomposition [Araújo and Raposo 2016] methods were not able to provide the short-term behavior of $S(t)$, which is

possible in our approach due to the calculation of $P(x,t)$ for all t.

5.2.2.4 Case $\alpha = 1/2$

We now consider the last case with $\alpha = 1/2$. As in the case $\alpha = 3/2$, no analytical expression in terms of elementary functions is known for the Lévy distribution with $\alpha = 1/2$ and $\beta = 0$. The integral (5.4) for $\alpha = 1/2$ reads

$$\begin{aligned} I_{\alpha=1/2}(a) &= \frac{1}{2} - \mathit{Fresnel}\ C\left[\frac{1}{\sqrt{2a\pi}}\right] + \mathit{Fresnel}\ C\left[\frac{1}{\sqrt{2a\pi}}\right]^2 \\ &\quad - \mathit{Fresnel}\ S\left[\frac{1}{\sqrt{2a\pi}}\right] + \mathit{Fresnel}\ S\left[\frac{1}{\sqrt{2a\pi}}\right]^2, \end{aligned} \tag{5.16}$$

where *Fresnel C* and *Fresnel S* represent the Fresnel cosine and sine integral functions, respectively. The off-diagonal Hamiltonian matrix elements are

$$\langle m|H|n\rangle = I_{\alpha=1/2}(|m-n|-1) - I_{\alpha=1/2}(|m-n|), \tag{5.17}$$

As in the preceding cases, we show in Figs. 31 and 32 the probability distribution $P(j,t)$ as a function of j for $\alpha = 1/2$, $N = 101$, and different elapsed times, $t = 5, 10, 50$, with the Lévy particle starting, respectively, from $j_0 = 50$, and near the left boundary, $j_0 = 10$.

Figure 31 – Probability $P(j,t)$ for $\alpha = 1/2$ as a function of the position j in a finite domain of length $N = 101$, with the starting point at $j_0 = 50$, and for different elapsed times, $t = 5, 10, 50$.

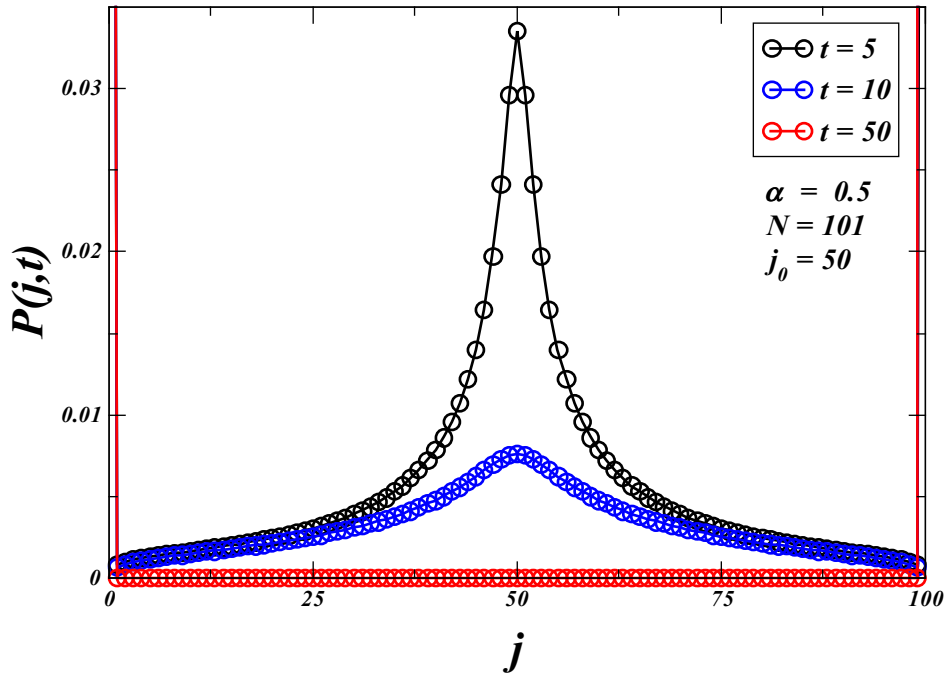

Figure 32 – Probability $P(j,t)$ for $\alpha = 1/2$ as a function of the position j in a finite interval of length $N = 101$, with the starting point near the left boundary, $j_0 = 10$, and for different times elapsed, $t = 5, 10, 50$.

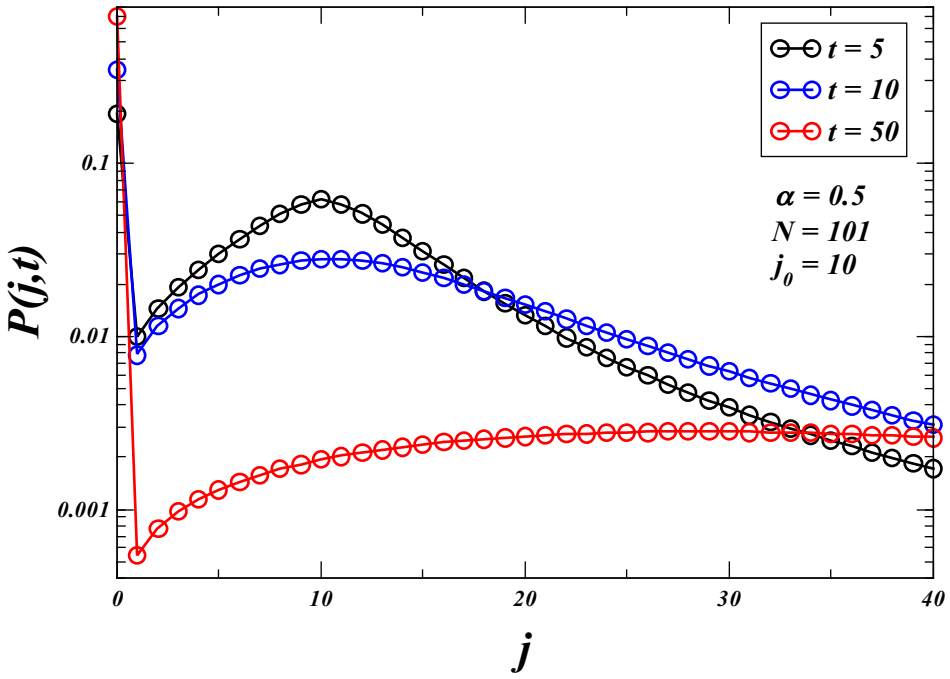

We also display in Fig. 33 the plot of the survival probability as a function of time, with the short-time power-law and long-time exponential behaviors.

Figure 33 – (a) Log-log plot of the survival probability $S(t)$ as a function of time t for $\alpha = 1/2$ in a finite domain of length $N = 101$, with the starting point near the left boundary, $j_0 = 10$ (solid line). Dashed line is the fit to the Sparre-Andersen-like power-law behavior. (b) Log-linear plot of $S(t)$ (solid line) and the fit (dashed line) to the exponential behavior.

(a) Power law behavior

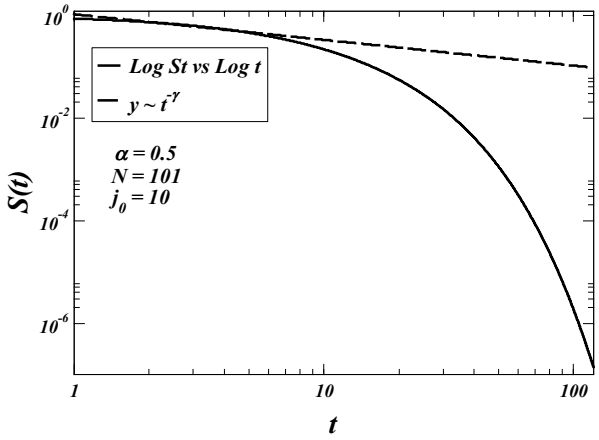

(b) Exponential decay behavior

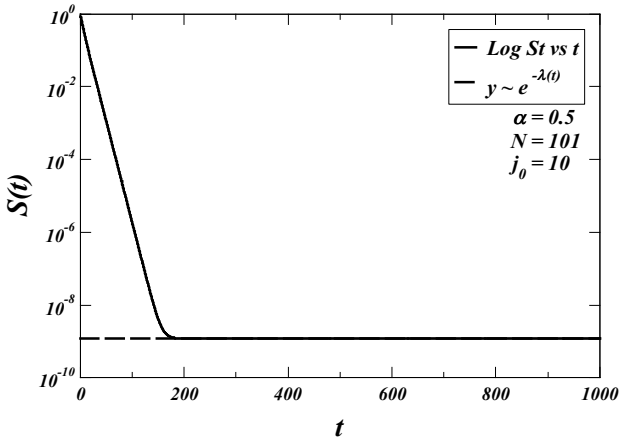

5.2.3 Some miscellaneous results and further comparisons with direct numerical simulations

In this section we present some further results that could not fit in any of the previous sections because they are displayed in the same plot for different values of α.

For example, Fig. 34 shows the probability distribution $P(j,t)$ of the Lévy particle with $\alpha = 1/2, 1, 3/2$, for $N = 100$ and $t = 5$, starting, respectively, from the middle of the interval, $j_0 = N/2$, and near the left boundary, $j_0 = 9$. We notice in both plots a nice agreement of the Fock space results with the ones obtained by direct numerical simulations.

Figure 34 – Probability $P(j,t)$ for $\alpha = 1/2$ (red), 1 (blue), and 3/2 (black), as a function of the position j for $t = 5$, in a finite domain of length $N = 100$, with the starting point (a) at the middle of the interval, $j_0 = N/2$, and (b) near the left boundary, $j_0 = 9$.

(a) $j_0 = N/2$

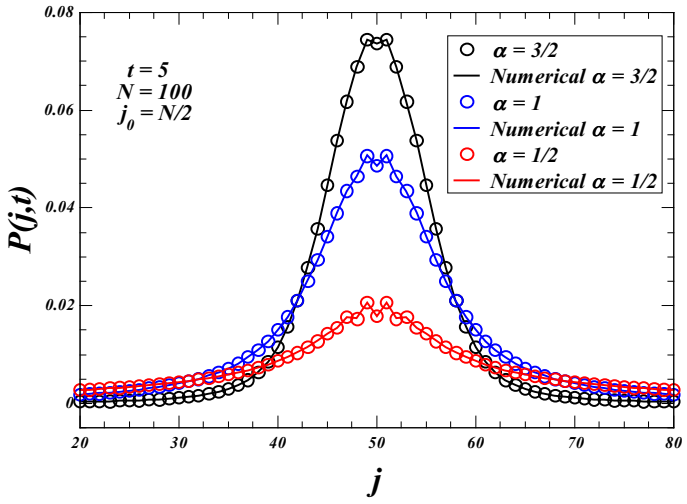

(b) $j_0 = 9$

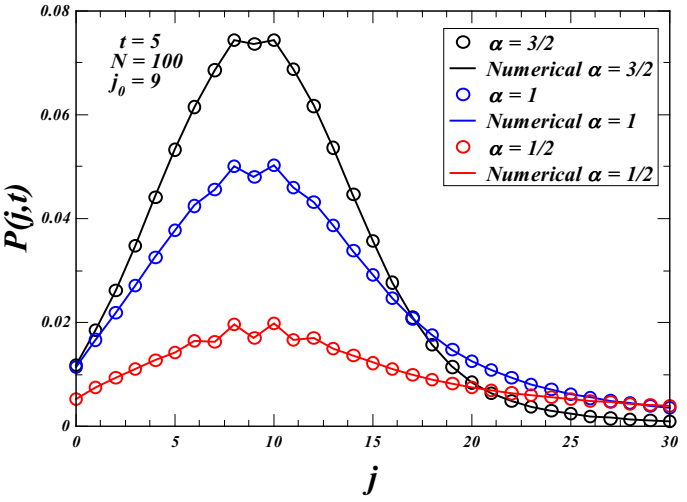

5.2.4 Approach to the continuous space limit and the case of reflective boundaries

Two last subjects are addressed in this final section of this chapter. In the first, we approach the continuous space limit by considering $\Delta x/L \to 0$ in Eq. (5.3) of the present discrete Fock space formalism. In the second we study the case with reflective boundaries, which allows to compare our Fock space results with the exact stationary distribution $P_{st}(x)$.

We start with the calculation of the mean first passage time for any of the boundaries in the continuous space limit. The exact result for a Lévy flier with stability index α, starting from the position x_0 in a bounded continuous space of length L reads [Buldyrev et al. 2001, Buldyrev et al. 2001, Getoor 1961]

$$\langle t \rangle (x_0) = \frac{1}{\Gamma(1+\alpha)} [x_0(L-x_0)]^{\alpha/2}. \tag{5.18}$$

We first noticed that the convergence rate of the discrete-space Fock space results to Eq. (5.18) depends on both α and $\Delta x/L$ in Eq. (5.3). For example, the maximum relative error with respect to the exact expression above (i.e., the relative error with the starting point in the middle of the interval, $x_0 = L/2$) decreases when $\alpha = 1$ from 0.032 for $\Delta x/L = 0.01$ to 0.011 for $\Delta x/L = 0.002$, while when $\alpha = 1/2$ it decreases from 0.062 for $\Delta x/L = 0.01$ to 0.032 for $\Delta x/L = 0.002$. Smaller $\Delta x/L$ progressively approach the exact result in continuous space, as expected. We also observe that the convergence takes place much faster (maximum relative error of 0.004 for $\Delta x/L = 0.01$ with $\alpha = 1/2$) when P_{kj} in Eq. (5.3) is given by the continuous space approximation [Zoia, Rosso and Kardar 2007] $P_{kj} = -A(|k-j|)/A(0)$ with

$$A(n) = \frac{\Gamma(-\alpha/2+n)\Gamma(\alpha+1)}{\pi\Gamma(1+\alpha/2+n)} \sin(\pi\alpha/2), \tag{5.19}$$

for $1 \leq k, j \leq N-1$; P_{kj} for the jumps absorbed by the boundaries at $k = 0$ and $k = N$ is calculated by summing (5.19) over the jump lengths that exceed the distance to the respective extreme sites. We note, however, that Eq. (5.3) in the limit $\Delta x/L \to 0$ is quite general and applies to any distribution $p(\ell)$ of step lengths, while Eq. (5.19) is specific of Lévy flights. The results shown in Fig. 35 display a nice agreement between Eq. (5.18) (solid lines) and the Fock space approach (circles).

Figure 35 – Comparison between the Fock space results (circles) and the exact mean first passage time, Eq. (5.19) (solid lines), of Lévy flights with $\alpha = 1, 1/2, 3/2$, in a continuous bounded domain of length $L = 100$ as a function of the initial position j_0.

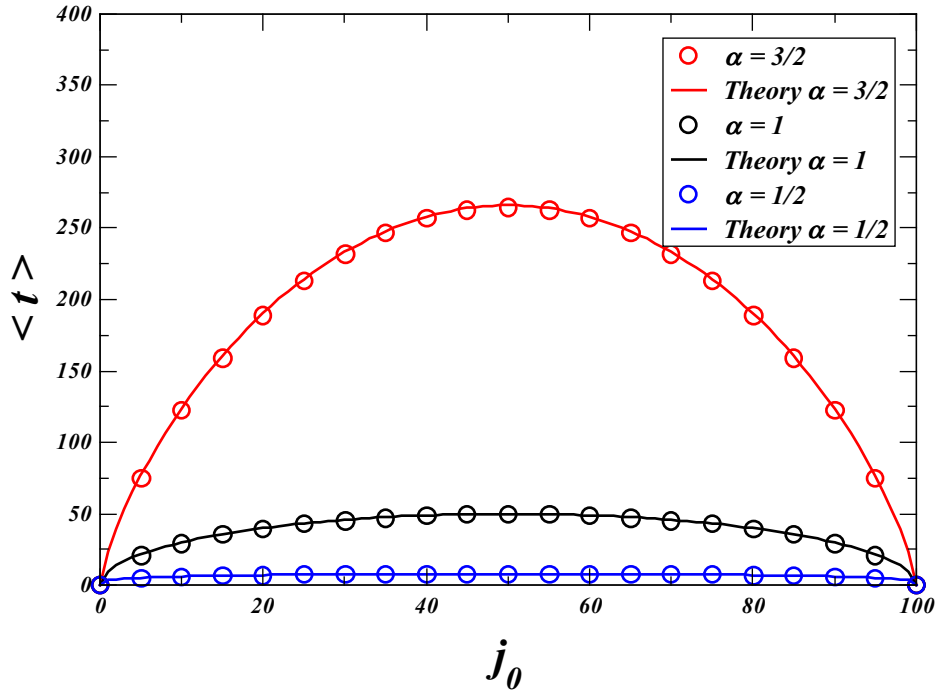

Additionally, we can also apply the Fock space formalism to treat the case with reflecting boundaries in Eq. (5.3), in which one might have $P_{kj} \neq 0$ even for $j = 1$ and $j = N$. In this context, the stationary regime of the probability distribution $P(x,t)$ in the continuous space domain $x \in [0,L]$ and initial position $x_0 = L/2$ is exactly given by [Denisov, Horsthemke and Hänggi 2008]

$$P_{st}(x) = \frac{L^{1-\alpha}[x(L-x)]^{\alpha/2-1}\Gamma(\alpha)}{[\Gamma(\alpha/2)]^2}. \tag{5.20}$$

We observe in Fig. 36 that Eq. (5.20) (solid lines) and the Fock space results (circles) agree well for a number of values of α. Eventually we note that our Fock space results cannot reach the singularities of $P_{st}(x)$ at the boundaries, even though the agreement apart from the extremes is good.

Figure 36 – Comparison between the Fock space results (circles) and the exact stationary limit of $P(x,t)$, Eq. (5.20) (solid lines), of Lévy flights with $\alpha = 1, 1/2, 3/2, 2$, as a function of the position j in a bounded domain of length $L = 100$, with $j_0 = L/2$ and reflecting boundaries.

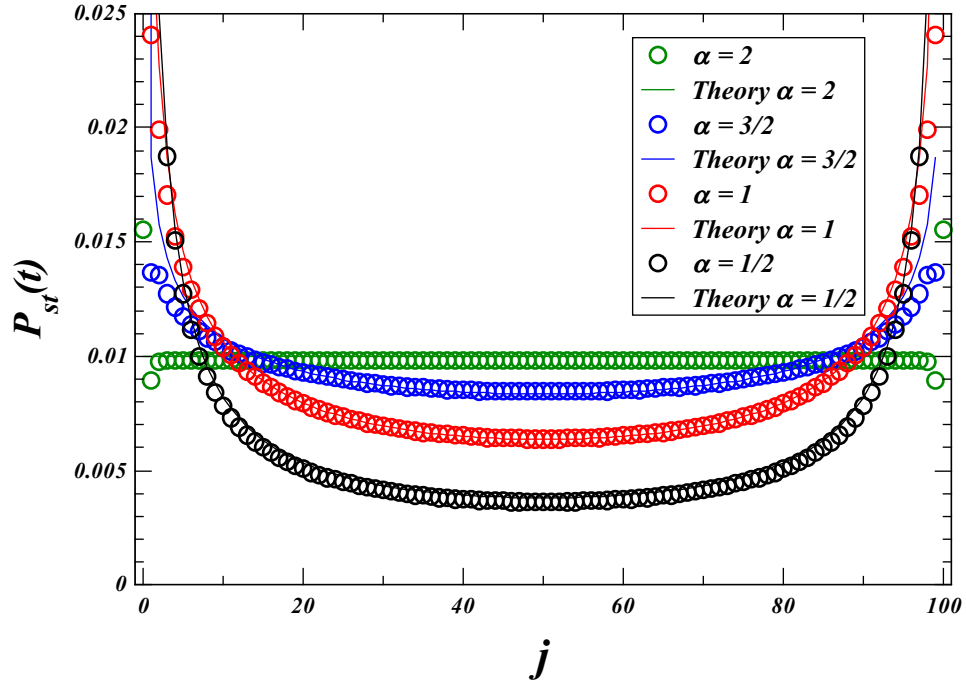

6 CONCLUSIONS AND PERSPECTIVES

« Mathematics is the language in which God has written the universe. »

Galileo Galilei

In this thesis we have applied the Fock space formalism to the study of a random walker in a one-dimensional lattice of discrete sites with absorbing borders in different scenarios. We have studied three distinct distributions of step lengths: fixed step length (Dirac delta), power-law, and Lévy α-stable distribution. In particular, this problem has an important connection with the random search problem and applications such as the context of animals looking for food sites in nature (animal foraging problem). In this case, the absorbing boundary sites are equivalent to the target sites, whereas the random particle plays the role of the the searcher agent. In general our results were shown to be in good agreement with direct numerical simulations.

For the random particle with fixed step length we verified the Gaussian behavior of the probability distribution as a function of the position in the lattice and time. The mean square deviation with time showed the influence of the borders and a clear separation from the normal diffusion behavior in boundless space as time passes and the walker starts to find the borders.

In a second study, the random particle takes its steps from a power-law distribution. We have analyzed its behavior from the superdiffusive regime with $1 < \mu < 3$ up to the normal diffusion regime with $\mu = 3$. We show the expected behavior in the plot of probability distribution $P(j,t)$ as a function of the position j in a finite domain for some values of time. We have also studied quantities such as the mean square deviation and survival probability. For the latter we have found out that after a few steps the observed power-law behavior obeys the Sparre-Andersen theorem for the semi-infinite interval, even though in our case with finite interval it is not strictly applicable. On the other hand, the long-term asymptotic behavior shows an exponential decay.

Finally, we have also studied the behavior of a random particle with a Lévy α-stable distribution of step lengths. Due to the lack of closed forms of the Lévy PDF and absence of exact results for the distribution $P(j,t)$ in the superdiffusive regime, the Fock space formalism emerges as an important mathematical tool to compute several quantities of statistical relevance to this problem, in agreement with numerical simulations. In particular, the survival probability also showed a shift from a Sparre-Andersen-like power-law behavior for short times to an exponential behavior for long times. In this latter case, the exponential decay rates were found in nice agreements

with the results obtained from the discretized Riesz fractional differential operator and the Wiener-Hopf decomposition techniques.

We have also applied the Fock space approach to a finite domain with reflective barriers and computed quantities like the mean first passage time in the continuous space, with good agreement with previously reported results.

Overall, we believe that the Fock space formalism has a great potential to suitably deal with random particles diffusing in a finite domain in diverse contexts. Among the future perspectives, we remark that the Fock space formalism is general enough to be readily extended to other types of random particles with arbitrary distributions of step lengths, including biased and/or asymmetric ones, different boundary conditions, and even ensembles of several particles diffusing simultaneously on a bounded domain. Indeed, we emphasize that while some methods are particularly associated with specific forms of step length distributions (e.g., the discretization of the fractional Laplacian operator related to the Lévy step lengths distribution), the Fock space approach can be promptly applied to any distribution. In particular, in recent years there has been a growing interest, in contexts such as random search foraging, related to less conventional forms of distributions of step lengths, e.g., hyper-exponentials, attenuated power laws, and multiple-scale expressions.

REFERENCES

ANDERSEN, E. S. On the fluctuations of sums of random variables. *MATHEMATICA SCANDINAVICA*, v. 1, p. 263–285, Dec. 1953. Available at: <https://www.mscand.dk/article/view/10385>.

ANDERSEN, E. S. On the fluctuations of sums of random variables. *Mathematica Scandinavica*, Mathematica Scandinavica, v. 1, n. 2, p. 263–285, 1954. ISSN 00255521, 19031807. Available at: <http://www.jstor.org/stable/24488934>.

ARAÚJO, H. A.; LUKIN, M. O.; LUZ, M. G. E. da; VISWANATHAN, G. M.; SANTOS, F. A. N.; RAPOSO, E. P. Revisiting lévy flights on bounded domains: a fock space approach. *Journal of Statistical Mechanics: Theory and Experiment*, IOP Publishing, v. 2020, n. 8, p. 083202, aug 2020. Available at: <https://doi.org/10.1088%2F1742-5468%2Faba593>.

ARAÚJO, H. A.; RAPOSO, E. P. Lévy flights between absorbing boundaries: Revisiting the survival probability and the shift from the exponential to the sparre-andersen limit behavior. *Phys. Rev. E*, American Physical Society, v. 94, p. 032113, Sep 2016. Available at: <https://link.aps.org/doi/10.1103/PhysRevE.94.032113>.

ARAúJO, H. de A. *Superdifusão em espaços finitos e derivadas fraccionárias*. Phd Thesis (PhD Thesis) — Ufpe, 2017.

BAEZ, J.; BIAMONTE, J. *Quantum techniques in stochastic mechanics*. Singapore: World Scientific Publishing Co. Pte Ltd, 2018. ISBN 9789813226937.

BERCOVICI, H.; PATA, V.; BIANE, P. Stable laws and domains of attraction in free probability theory. *Annals of Mathematics*, John Hopkins University Press, v. 149, p. 1023–1060, 1999. ISSN 0003-486X. Available at: <http://doi.org/10.2307/121080>.

BERGSTRöM, H. On some expansions of stable distribution functions. *Arkiv för Matematik*, Springer Netherlands, v. 2, p. 375–378, 1952. ISSN 0004-2080,1871-2487. Available at: <http://doi.org/10.1007/bf02591503>.

BLUMENTHAL, R. M.; GETOOR, R. K.; RAY, D. B. On the distribution of first hits for the symmetric stable processes. *Transactions of the American Mathematical Society*, American Mathematical Society, v. 99, p. 540–540, 1961. ISSN 0002-9947,1088-6850. Available at: <http://doi.org/10.1090/S0002-9947-1961-0126885-4>.

BOUCHAUD, J.-P.; POTTERS, M. *Theory of financial risks: from statistical physics to risk management*. 1. ed. Cambridge University Press, 2000. ISBN 0521782325,9780521782326,9780511010286. Available at: <http://gen.lib.rus.ec/book/index.php?md5=7d71e5879869c21e0f50909250392688>.

BROWN, R. Xxvii. a brief account of microscopical observations made in the months of june, july and august 1827, on the particles contained in the pollen of plants; and on the general existence of active molecules in organic and inorganic bodies. *Philosophical Magazine Series 2*, v. 4, p. 161–173, 1828. ISSN 1941-5850,1941-5869. Available at: <http://doi.org/10.1080/14786442808674769>.

BUCHANAN, M. Ecological modelling: The mathematical mirror to animal nature. *Nature*, Nature Publishing Group, v. 453, p. 714–716, 2008. ISSN 0028-0836,1476-4679. Available at: <http://doi.org/10.1038/453714a>.

BULDYREV, S.; GITTERMAN, M.; HAVLIN, S.; KAZAKOV, A.; LUZ], M. [da; RAPOSO, E.; STANLEY, H.; VISWANATHAN, G. Properties of lévy flights on an interval with absorbing boundaries. *Physica A: Statistical Mechanics and its Applications*, v. 302, n. 1, p. 148 – 161, 2001. ISSN 0378-4371. Proc. Int. Workshop on Frontiers in the Physics of Complex Systems. Available at: <http://www.sciencedirect.com/science/article/pii/S0378437101004617>.

BULDYREV, S. V.; HAVLIN, S.; KAZAKOV, A. Y.; LUZ, M. G. E. da; RAPOSO, E. P.; STANLEY, H. E.; VISWANATHAN, G. M. Average time spent by lévy flights and walks on an interval with absorbing boundaries. *Physical Review E*, American Physical Society (APS), v. 64, n. 4, Sep 2001. ISSN 1095-3787. Available at: <http://dx.doi.org/10.1103/PhysRevE.64.041108>.

BéNICHOU, O.; LOVERDO, C.; MOREAU, M.; VOITURIEZ, R. Intermittent search strategies. *Review of Modern Physics*, The American Physical Society, v. 83, p. 81–129, 2011. ISSN 0034-6861,1539-0756. Available at: <http://doi.org/10.1103/RevModPhys.83.81>.

CHECHKIN, A. V.; GONCHAR, V. Y.; KLAFTER, J.; METZLER, R. Fundamentals of lévy flight processes. In: ____. *Fractals, Diffusion, and Relaxation in Disordered Complex Systems*. John Wiley and Sons, Ltd, 2006. chap. 9, p. 439–496. ISBN 9780470037140. Available at: <https://onlinelibrary.wiley.com/doi/abs/10.1002/0470037148.ch9>.

CHECHKIN, A. V.; METZLER, R.; GONCHAR, V. Y.; KLAFTER, J.; TANATAROV, L. V. First passage and arrival time densities for lévy flights and the failure of the method of images. *Journal of Physics A: Mathematical and General Physics*, Institute of Physics, v. 36, p. L537–L544, 2003. ISSN 0305-4470,0022-3689. Available at: <http://doi.org/10.1088/0305-4470%2F36%2F41%2FL01>.

CHEN, J. From the central limit theorem to heavy-tailed distributions. *Journal of Applied Probability*, Applied Probability Trust, v. 40, p. 803–806, 2003. ISSN 0021-9002. Available at: <http://doi.org/10.2307/3215954>.

CLAUSET, A.; SHALIZI, C. R.; NEWMAN, M. E. J. Power-law distributions in empirical data. *SIAM Review*, Society for Industrial and Applied Mathematics, v. 51, p. 661–703, 2009. ISSN 0036-1445,1095-7200. Available at: <http://doi.org/10.1137/070710111>.

COX, D. *The Theory of Stochastic Processes*. 1. ed. Chapman and Hall/CRC, 2017. ISBN 1138460346,9781138460348. Available at: <http://gen.lib.rus.ec/book/index.php?md5=c56d4d941044b7fdfaf2b976ca4b58ba>.

DARWIN, C. *The Origin of Species (1859)*. Pickering and Chatto (Publishers) Ltd, 1992. ISBN 1851963057. Available at: <http://gen.lib.rus.ec/book/index.php?md5=5e38dc35f6107930d2bbae9497e655a3>.

DENISOV, S. I.; HORSTHEMKE, W.; HÄNGGI, P. Steady-state lévy flights in a confined domain. *Phys. Rev. E*, American Physical Society, v. 77, p. 061112, Jun 2008. Available at: <https://link.aps.org/doi/10.1103/PhysRevE.77.061112>.

DENNERY, P.; KRZYWICKI, A. *Mathematics for physicists*. Dover ed. Dover Publications, 1996. (Dover books on mathematics). ISBN 9780486691930,0486691934. Available at: <http://gen.lib.rus.ec/book/index.php?md5=75ff2f92e67f4ffa69de3331464f432e>.

DENTZ, M.; CORTIS, A.; SCHER, H.; BERKOWITZ, B. Time behavior of solute transport in heterogeneous media: transition from anomalous to normal transport. *Advances in Water Resources*, Elsevier Science, v. 27, p. 155–173, 2004. ISSN 0309-1708. Available at: <http://doi.org/10.1016/j.advwatres.2003.11.002>.

DOI, M. Second quantization representation for classical many-particle system. *Journal of Physics A: Mathematical and General Physics*, Institute of Physics, v. 9, p. 1465–1477, 1976. ISSN 0305-4470,0022-3689. Available at: <http://doi.org/10.1088/0305-4470%2F9%2F9%2F008>.

DOI, M. Stochastic theory of diffusion-controlled reaction. *Journal of Physics A: Mathematical and General*, IOP Publishing, v. 9, n. 9, p. 1479–1495, sep 1976. Available at: <https://doi.org/10.1088%2F0305-4470%2F9%2F9%2F009>.

DYBIEC, B.; GUDOWSKA-NOWAK, E.; CHECHKIN, A. To hit or to pass it over—remarkable transient behavior of first arrivals and passages for lévy flights in finite domains. *Journal of Physics A: Mathematical and Theoretical*, IOP Publishing, v. 49, n. 50, p. 504001, nov 2016. Available at: <https://doi.org/10.1088%2F1751-8113%2F49%2F50%2F504001>.

EDWARDS, A. M.; PHILLIPS, R. A.; WATKINS, N. W.; FREEMAN, M. P.; MURPHY, E. J.; AFANASYEV, V.; BULDYREV, S. V.; LUZ, M. G. E. da; RAPOSO, E. P.; STANLEY, H. E. Revisiting lévy flight search patterns of wandering albatrosses, bumblebees and deer. *Nature*, Nature Publishing Group, v. 449, p. 1044–1048, 2007. ISSN 0028-0836,1476-4679. Available at: <http://doi.org/10.1038/nature06199>.

EINSTEIN, A. Über die von der molekularkinetischen theorie der wärme geforderte bewegung von in ruhenden flüssigkeiten suspendierten teilchen. *Annalen der Physik*, John Wiley and Sons, v. 322, p. 549–560, 1905. ISSN 0003-3804,1521-3889. Available at: <http://doi.org/10.1002/andp.19053220806>.

EMLEN, J. M. The role of time and energy in food preference. *American Naturalist*, University of Chicago Press, v. 100, p. 611–617, 1966. ISSN 0003-0147,1537-5323. Available at: <http://doi.org/10.2307/2459299>.

FELLER, W. *An Introduction to Probability Theory and Its Applications, Vol. 2*. 2. ed. Wiley, 1971. ISBN 0471257095,9780471257097. Available at: <http://gen.lib.rus.ec/book/index.php?md5=5ee1e3564baa8470668e6a8a28c7e416>.

FICK, D. A. Ueber diffusion. *Annalen der Physik*, John Wiley and Sons, v. 170, p. 59–86, 1855. ISSN 0003-3804,1521-3889. Available at: <http://doi.org/10.1002/andp.18551700105>.

FOGEDBY, H. C. Lévy flights in quenched random force fields. *Physical Review E*, The American Physical Society, v. 58, p. 1690–1712, 1998. ISSN 1539-3755,1550-2376. Available at: <http://doi.org/10.1103/physreve.58.1690>.

GARBACZEWSKI, P.; STEPHANOVICH, V. Fractional laplacians in bounded domains: Killed, reflected, censored, and taboo lévy flights. *Phys. Rev. E*, American Physical Society, v. 99, p. 042126, Apr 2019. Available at: <https://link.aps.org/doi/10.1103/PhysRevE.99.042126>.

GETOOR, R. K. First passage times for symmetric stable processes in space. *Transactions of the American Mathematical Society*, American Mathematical Society, v. 101, p. 75–75, 1961. ISSN 0002-9947,1088-6850. Available at: <http://doi.org/10.1090/S0002-9947-1961-0137148-5>.

G.H., W. *Aspects and applications of the random walk*. NH, 1994. (Random Materials and Processes). ISBN 0444816062,9780444816061. Available at: <http://gen.lib.rus.ec/book/index.php?md5=792513c4fe6a4d4fa0bbd799e324f3d0>.

G.K., Z. *Human Behavior and the Principle of Least Effort*. AW, 1949. Available at: <http://gen.lib.rus.ec/book/index.php?md5=d7363402de1969ffad3f0ae2cfa30b1c>.

GOODENOUGH, J.; MCGUIRE, B.; JAKOB, E. *Perspectives on Animal Behavior*. 3. ed. Wiley, 2009. ISBN 0470045175,9780470045176. Available at: <http://gen.lib.rus.ec/book/index.php?md5=588bca90cc32e58004e9d0d0dd6d7c81>.

GRASSBERGER, P.; SCHEUNERT, M. Fock-space methods for identical classical objects. *Fortschritte der Physik*, v. 28, n. 10, p. 547–578, 1980. Available at: <https://onlinelibrary.wiley.com/doi/abs/10.1002/prop.19800281004>.

GóRSKA, K.; PENSON, K. A. Lévy stable two-sided distributions: Exact and explicit densities for asymmetric case. *Physical Review E*, The American Physical Society, v. 83, p. 061125, 2011. ISSN 1539-3755,1550-2376. Available at: <http://doi.org/10.1103/PhysRevE.83.061125>.

HAAG, G. *Modelling with the Master Equation : Solution Methods and Applications in Social and Natural Sciences*. Springer, 2017. ISBN 978-3-319-60300-1,3319603000,978-3-319-60299-8. Available at: <http://gen.lib.rus.ec/book/index.php?md5=2c1bec164e56574d8dc329da90fa28fc>.

HALLAM, L. J. G. (auth.)and T. G.; (EDS.), S. A. L. *Mathematical Ecology: An Introduction*. 1. ed. Springer-Verlag Berlin Heidelberg, 1986. (Biomathematics 17). ISBN 978-3-642-69890-3,978-3-642-69888-0. Available at: <http://gen.lib.rus.ec/book/index.php?md5=1392cc237d14cf76c4d6bfa983e60d2c>.

HUMPHRIES, N. E.; WEIMERSKIRCH, H.; QUEIROZ, N.; SOUTHALL, E. J.; SIMS, D. W. Foraging success of biological levy flights recorded in situ. *Proceedings of the National Academy of Sciences*, National Academy of Sciences, v. 109, p. 7169–7174, 2012. ISSN 0027-8424,1091-6490. Available at: <http://doi.org/10.1073/pnas.1121201109>.

HUMPHRIES, N. E.; WEIMERSKIRCH, H.; SIMS, D. W. A new approach for objective identification of turns and steps in organism movement data relevant to random walk modelling. *Methods in Ecology and Evolution*, v. 4, n. 10, p. 930–938, 2013. Available at: <https://besjournals.onlinelibrary.wiley.com/doi/abs/10.1111/2041-210X.12096>.

IINO, R.; KUSUMI, A. Single-fluorophore dynamic imaging in living cells. *Journal of Fluorescence*, Springer, v. 11, p. 187–195, 2001. ISSN 1053-0509,1573-4994. Available at: <http://doi.org/10.1023/a%3A1012297000742>.

ISAACSON, S. A. Relationship between the reaction–diffusion master equation and particle tracking models. *Journal of Physics A: Mathematical and Theoretical*, IOP Publishing, v. 41, n. 6, p. 065003, jan 2008. Available at: <https://doi.org/10.1088%2F1751-8113%2F41%2F6%2F065003>.

KAMPEN, N. V. *Stochastic Processes in Physics and Chemistry*. 3rd ed. ed. Elsevier, 2007. (North-Holland personal library). ISBN 9780444529657,0444529659. Available at: <http://gen.lib.rus.ec/book/index.php?md5=78da212d8fe17e2f7632fc20933dc6a9>.

KIRCHNER, J. W.; FENG, X.; NEAL, C. Fractal stream chemistry and its implications for contaminant transport in catchments. *Nature*, Nature Publishing Group, v. 403, p. 524–527, 2000. ISSN 0028-0836,1476-4679. Available at: <http://doi.org/10.1038/35000537>.

KLAFTER, J.; SOKOLOV, I. M. Anomalous diffusion spreads its wings. *Physics World*, v. 18, p. 29–32, 2005. ISSN 0953-8585,2058-7058. Available at: <http://doi.org/10.1088/2058-7058%2F18%2F8%2F33>.

KWASNICKI, M. Eigenvalues of the fractional laplace operator in the interval. *Journal of Functional Analysis*, v. 262, n. 5, p. 2379 – 2402, 2012. ISSN 0022-1236. Available at: <http://www.sciencedirect.com/science/article/pii/S0022123611004344>.

MACARTHUR, R. H.; PIANKA, E. R. On optimal use of a patchy environment. *American Naturalist*, University of Chicago Press, v. 100, p. 603–609, 1966. ISSN 0003-0147,1537-5323. Available at: <http://doi.org/10.2307/2459298>.

MANDELBROT, B. The pareto-lévy law and the distribution of income. *International Economic Review*, John Wiley and Sons, v. 1, p. 79–106, 1960. ISSN 0020-6598,1468-2354. Available at: <http://doi.org/10.2307/2525289>.

MANTEGNA, R. N.; STANLEY, H. E. *An introduction to econophysics: correlations and complexity in finance*. 0. ed. Cambridge University Press, 2000. ISBN 9780521620086,0521620082. Available at: <http://gen.lib.rus.ec/book/index.php?md5=dfe41b3351c63731ab5dc9f3e7520666>.

MATTIS, D. C.; GLASSER, M. L. The uses of quantum field theory in diffusion-limited reactions. *Rev. Mod. Phys.*, American Physical Society, v. 70, p. 979–1001, Jul 1998. Available at: <https://link.aps.org/doi/10.1103/RevModPhys.70.979>.

METZLER, R.; KLAFTER, J. The random walk's guide to anomalous diffusion: a fractional dynamics approach. phys rep. *Physics Reports*, v. 339, 01 2000.

METZLER, R.; KLAFTER, J. The restaurant at the end of the random walk: Recent developments in the description of anomalous transport by fractional dynamics. *J. Phys. A: Math. Gen*, v. 3737, 08 2004.

MOIVRE, A. de. *The doctrine of chances; or, A method of calculating the probabilities of events in play*. 3rd. ed. New York, Chelsea Pub. Co., 1967. (AMS Chelsea Publishing). ISBN 0821821032,9780821821039. Available at: <http://gen.lib.rus.ec/book/index.php?md5=db729b0b7a6fee996deaf1429806a68c>.

MUZY, P.; SALINAS, S.; SANTANA, A.; T, T. A. Mario Schönberg e a introdução do espaço de Fock na física estatística clássica. *Revista Brasileira de Ensino de Física*, scielo, v. 27, p. 447 – 462, 09 2005. ISSN 1806-1117. Available at: <http://www.scielo.br/scielo.php?script=sci_arttext&pid=S1806-11172005000300023&nrm=iso>.

NETO, P. J. R. *Análise da Dinâmica Energética de Buscas Aleatórias*. Phd Thesis (PhD Thesis) — UFPE, 2012.

NEWMAN, M. Power laws, pareto distributions and zipf's law. *Contemporary Physics*, Taylor and Francis Group, v. 46, p. 323–351, 2005. ISSN 0010-7514,1366-5812. Available at: <http://doi.org/10.1080/00107510500052444>.

NOLAN, J. Stable distribution: Models for heavy-tailed data. 01 2014.

NOLAN, J. P. *Stable Distributions - Models for Heavy Tailed Data*. Boston: Birkhauser, 2018. In progress, Chapter 1 online at http://fs2.american.edu/jpnolan/www/stable/stable.html.

PARETO, V. *Course of Political Economy at the University of Lausanne*. F. Rouge, Pichon, 1896/97. Available at: <http://gen.lib.rus.ec/book/index.php?md5=46274ff9eb60de84d1dfe47a692f760d>.

PENG, C.-K.; MIETUS, J.; HAUSDORFF, J. M.; HAVLIN, S.; STANLEY, H. E.; GOLDBERGER, A. L. Long-range anticorrelations and non-gaussian behavior of the heartbeat. *Physical Review Letters*, The American Physical Society, v. 70, p. 1343–1346, 1993. ISSN 0031-9007,1079-7114. Available at: <http://doi.org/10.1103/PhysRevLett.70.1343>.

PENSON, K. A.; GÓRSKA, K. Exact and explicit probability densities for one-sided lévy stable distributions. *Phys. Rev. Lett.*, American Physical Society, v. 105, p. 210604, Nov 2010. Available at: <https://link.aps.org/doi/10.1103/PhysRevLett.105.210604>.

PINTO, C. M.; LOPES, A. M.; MACHADO, J. T. A review of power laws in real life phenomena. *Communications in Nonlinear Science and Numerical Simulation*, Elsevier Science, v. 17, p. 3558–3578, 2012. ISSN 1007-5704. Available at: <http://doi.org/10.1016/j.cnsns.2012.01.013>.

RAMOS-FERNáNDEZ, G.; MATEOS, J.; MIRAMONTES, O.; COCHO, G.; LARRALDE, H.; AYALA-OROZCO, B. Lévy walk patterns in the foraging movements of spider monkeys (ateles geoffroyi). *Behavioral Ecology and Sociobiology*, Springer, v. 55, p. 223–230, 2004. ISSN 0340-5443,1432-0762. Available at: <http://doi.org/10.1007/s00265-003-0700-6>.

REIF, F. *Fundamentals of statistical and thermal physics*. 1. ed. McGraw-Hill Science/Engineering/Math, 1965. (McGraw-Hill Series in Fundamentals of Physics). ISBN 0070518009,9780070518001. Available at: <http://gen.lib.rus.ec/book/index.php?md5=be43aa10c84cbf4b1695d72144ff88ea>.

ROSS, S. *A First Course in Probability*. 5. ed. Prentice Hall PTR, 1997. Available at: <http://gen.lib.rus.ec/book/index.php?md5=413502a3902ad6f4a891b7644b563ae8>.

SAKURAI, J. J. *Modern quantum mechanics*. Rev. ed. Addison-Wesley Pub. Co, 1994. ISBN 9780201539295,0201539292. Available at: <http://gen.lib.rus.ec/book/index.php?md5=135c77b33b4d32d809c3e39335dd6ae2>.

SHLESINGER, J. K. G. Z. M. Lévy walks in dynamical systems. *Physica A: Statistical Mechanics and its Applications*, Elsevier Science, v. 200, p. 222–230, 1993. ISSN 0378-4371. Available at: <http://doi.org/10.1016/0378-4371%2893%2990520-e>.

TäUBER, U. C.; HOWARD, M.; VOLLMAYR-LEE, B. P. Applications of field-theoretic renormalization group methods to reaction–diffusion problems. *Journal of Physics A: Mathematical and General Physics*, Institute of Physics, v. 38, p. R79–R131, 2005. ISSN 0305-4470,0022-3689. Available at: <http://doi.org/10.1088/0305-4470%2F38%2F17%2FR01>.

VISWANATHAN, G.; BARTUMEUS, F.; BULDYREV, S.; CATALAN, J.; FULCO, U.; HAVLIN, S.; LUZ, M.; LYRA, M.; RAPOSO, E.; STANLEY, H. Lévy flight random searches in biological phenomena. *Physica a-Statistical Mechanics and Its Applications*, v. 314, p. 208–213, 11 2002.

VISWANATHAN, G.; RAPOSO, E.; LUZ, M. da. Lévy flights and superdiffusion in the context of biological encounters and random searches. *Physics of Life Reviews*, Elsevier Science, v. 5, p. 133–150, 2008. ISSN 1571-0645. Available at: <http://doi.org/10.1016/j.plrev.2008.03.002>.

VISWANATHAN, G. M.; AFANASYEV, V.; BULDYREV, S. V.; MURPHY, E. J.; PRINCE, P. A.; STANLEY, H. E. Lévy flight search patterns of wandering albatrosses. *Nature*, Nature Publishing Group, v. 381, p. 413–415, 1996. ISSN 0028-0836,1476-4679. Available at: <http://doi.org/10.1038/381413a0>.

VISWANATHAN, G. M.; BULDYREV, S. V.; HAVLIN, S.; LUZ, M. da; RAPOSO, E. P.; STANLEY, H. E. Optimizing the success of random searches. *Nature*, v. 401, p. 911–914, 1999.

VISWANATHAN, G. M.; LUZ, M. G. E. da; RAPOSO, E. P.; STANLEY, H. E. *The Physics of Foraging: An Introduction to Random Searches and Biological Encounters*. Cambridge University Press, 2011. ISBN 1107006791,9781107006799. Available at: <http://gen.lib.rus.ec/book/index.php?md5=12e75db686c94a603fd2744e3461fba5>.

ZOIA, A.; ROSSO, A.; KARDAR, M. Fractional laplacian in bounded domains. *Phys. Rev. E*, American Physical Society, v. 76, p. 021116, Aug 2007. Available at: <https://link.aps.org/doi/10.1103/PhysRevE.76.021116>.

ZOLOTAREV, V. M.; UCHAIKIN, V. V. *Chance and Stability. Stable Distributions and their Applications*. Walter de Gruyter, 1999. (Modern Probability and Statistics). ISBN 9067643017,9789067643016. Available at: <http://gen.lib.rus.ec/book/index.php?md5=bf957d0c659535f5322a000c69905b2d>.

APPENDIX A – GENERAL CONSTRUCTION OF THE HAMILTONIAN-LIKE OPERATOR FOR A SET OF RANDOM DIFFUSING PARTICLES

In this Appendix we discuss, in general terms, the derivation of the Hamiltonian-like operator H defined from the Schrödinger-like equation,

$$\frac{\partial}{\partial t}|\psi(t)\rangle = -H(\{a_j^\dagger, a_j\})|\psi(t)\rangle, \tag{A.1}$$

for a system of classical non-interacting identical particles diffusing randomly on a one-dimensional finite domain of discrete sites $j = 0, 1, ..., N$. We consider that the number of particles at a given site j is $n_j = 0, 1, 2, .., N_p$, with the total number of particles constrained to $N_p = \sum_j n_j$. We also define the vector $\mathbf{n} \equiv (n_1, n_2, ..., n_{N)}$ and, whenever convenient, we use below the notation $\mathbf{n}^{(k,j)} = (n_1, n_2, \ldots, n_{k-1}, n_{k+1}, \ldots, n_{j-1}, n_{j+1}, \ldots, n_N)$, so that $\mathbf{n} = (\mathbf{n}^{(k,j)}, n_k, n_j)$. The quantity $P(\mathbf{n}, t)$ is the probability density for a given set $\mathbf{n}$ of occupation numbers of particles in time t. Single-particle transitions can be represented in the master equation [Mattis and Glasser 1998, Baez and Biamonte 2018, Isaacson 2008, Grassberger and Scheunert 1980]

$$\begin{aligned}\frac{\partial P(\mathbf{n},t)}{\partial t} &= \sum_{j,k} D_{kj}\Big[(n_k+1)\,P(\mathbf{n}^{(k,j)}, n_k+1, n_j-1, t) \\ &\quad -n_k\,P(\mathbf{n},t)\Big],\end{aligned} \tag{A.2}$$

in which the transition rate for a particle to jump from site j to site k is proportional to the number of particles, with proportionality constant $D_{kj} = D_{jk}$ (symmetrical jumps) and $D_{jj} = 0$. (Simultaneous multiple-particle transitions occur with vanishing probability.) In a representation of Fock states $\{|\mathbf{n}\rangle\}$, the state of the system in time t reads

$$|\psi(t)\rangle = \sum_{\mathbf{n}} P(\mathbf{n},t)\,|\mathbf{n}\rangle, \tag{A.3}$$

where each set $\mathbf{n}$ in the sum above has total number of particles N_p, so that

$$\begin{aligned}\frac{\partial}{\partial t}|\psi(t)\rangle &= \sum_{\mathbf{n}}\sum_{j,k} D_{kj}\Big[(n_k+1)P(\mathbf{n}^{(k,j)}, n_k+1, n_j-1, t) \\ &\quad -n_k\,P(\mathbf{n},t)\Big]|\mathbf{n}\rangle.\end{aligned} \tag{A.4}$$

Now, by using Eq. (A.5)

$$\begin{aligned}a_j^\dagger|k\rangle &= |n_0, n_1, ..., n_k, ..., n_j+1, ..., n_N\rangle, \\ a_j|k\rangle &= n_j|n_0, n_1, ..., n_k, ..., n_j-1, ..., n_N\rangle,\end{aligned} \tag{A.5}$$

we write

$$a_j^\dagger a_k |\mathbf{n}^{(k,j)}, n_k+1, n_j-1\rangle = (n_k+1)|\mathbf{n}\rangle, \tag{A.6}$$

which implies

$$\begin{aligned}
\frac{\partial}{\partial t}|\psi(t)\rangle &= \sum_{\mathbf{n}}\sum_{j,k} D_{kj}\Big\{a_j^\dagger a_k P(\mathbf{n}^{(k,j)}, n_k+1, n_j-1, t) \\
&\quad |\mathbf{n}^{(k,j)}, n_k+1, n_j-1\rangle - a_k^\dagger a_k P(\mathbf{n},t)|\mathbf{n}\rangle\Big\} \\
&= \sum_{j,k} D_{kj}\Big\{a_j^\dagger a_k \sum_{\mathbf{n}} P(\mathbf{n}^{(i,j)}, n_k+1, n_j-1, t) \\
&\quad |\mathbf{n}^{(k,j)}, n_k+1, n_j-1\rangle - a_k^\dagger a_k \sum_{\mathbf{n}} P(\mathbf{n},t)|\mathbf{n}\rangle\Big\} \\
&= \Big\{\sum_{j,k} D_{kj}\left(a_j^\dagger a_k - a_k^\dagger a_k\right)\Big\}|\psi(t)\rangle.
\end{aligned} \tag{A.7}$$

By comparing this result with Eq. (A.8),

$$\frac{\partial}{\partial t}|\psi(t)\rangle = -H(\{a_j^\dagger, a_j\})|\psi(t)\rangle, \tag{A.8}$$

and using that $D_{kj} = D_{jk}$ and $D_{jj} = 0$, we obtain the Hamiltonian-like operator,

$$H = \sum_{j,k} D_{kj}\left(a_j^\dagger a_k - a_k^\dagger a_k\right). \tag{A.9}$$

We note that the first term in H can be assigned to the jump of a particle from site k to j with probability D_{kj}. The number operator (second term) arises due to the algebra of the raising and lowering operators, and are ultimately related to the conservation of the total number of particles in a jump transition. In the case of absorbing boundary conditions at the sites $j = 1$ and $j = N$ (see the main text of the thesis below Eq. (5.4)), with $D_{kk} = 0$, $D_{kj} = P_{kj}$ if $j \neq 1$ and $j \neq N$, and $D_{kj} = 0$ if $j = 1$ and $j = N$, Eq. (A.9) becomes Eq. (5.2).

APPENDIX B – ILLUSTRATIVE CALCULATION FOR A SMALL SYSTEM OF 6 SITES

In this Appendix we provide an illustrative example of the calculation of the Hamiltonian-like matrix H, Eq. (5.5), and the associated forms Q, J and $U(0,t)$ in the simple case of a small system with $N = 5$ (i.e., only six sites available to the Lévy flier, $j = 0, 1, ..., N$). We consider, for instance, the case of the Cauchy flier with $\alpha = 1$. The integral (5.4) for $\alpha = 1$ reads

$$I_{\alpha=1}(a) = \frac{\arctan(a)}{\pi}, \tag{B.1}$$

from which the off-diagonal elements of the Hamiltonian matrix can be obtained as

$$[H_{\alpha=1}]_{mn} = [\arctan(|m-n|-1) - \arctan(|m-n|)]/\pi, \tag{B.2}$$

if $m \neq n$, $m \neq 1$, $n \neq 1$, $m \neq 6$ and $n \neq 6$. The other matrix elements are calculated from the first, third and fourth lines of Eq. (5.3) combined with Eqs. (5.4) and (B.1). We thus obtain the Hamiltonian matrix for $\alpha = 1$,

$$H_{\alpha=1} = \begin{pmatrix} 0 & -1/2 & -1/4 & -0.148 & -0.102 & 0 \\ 0 & 1 & -1/4 & -0.102 & -0.045 & 0 \\ 0 & -1/4 & 1 & -1/4 & -0.102 & 0 \\ 0 & -0.102 & -1/4 & 1 & -1/4 & 0 \\ 0 & -0.045 & -0.102 & -1/4 & 1 & 0 \\ 0 & -0.102 & -0.148 & -1/4 & -1/2 & 0 \end{pmatrix}.$$

We observe that the columns $n = 1$ and $n = 6$ are null due to the absorbing sites at the boundary positions $j = 0$ and $j = N = 5$, respectively. Further, we also note that the sum of each column of $H_{\alpha=1}$ is null (we show above only the first three decimal places), as a consequence of the sum to unit of the total probability for the random particle to be anywhere in the bounded interval. By using the Jordan decomposition method [Dennery and Krzywicki 1996], the matrices $Q_{\alpha=1}$ and $J_{\alpha=1}$ can be built from the eigenvalues and eigenvectors of $H_{\alpha=1}$, yielding

$$Q_{\alpha=1} = \begin{pmatrix} 1 & 0 & 0.575 & -0.270 & 0.138 & 0.05 \\ 0 & 0 & -0.247 & 0.579 & -0.554 & -0.327 \\ 0 & 0 & -0.329 & 0.303 & 0.416 & 0.625 \\ 0 & 0 & -0.329 & -0.303 & 0.416 & -0.625 \\ 0 & 0 & -0.247 & -0.579 & -0.554 & 0.327 \\ 0 & 1 & 0.575 & 0.270 & 0.138 & -0.05 \end{pmatrix}$$

and

$$e^{-tJ_{\alpha=1}} = \begin{pmatrix} 1 & 0 & 0 & 0 & 0 & 0 \\ 0 & 1 & 0 & 0 & 0 & 0 \\ 0 & 0 & e^{-0.485t} & 0 & 0 & 0 \\ 0 & 0 & 0 & e^{-0.968t} & 0 & 0 \\ 0 & 0 & 0 & 0 & e^{-1.219t} & 0 \\ 0 & 0 & 0 & 0 & 0 & e^{-1.327t} \end{pmatrix}.$$

The first two columns in $Q_{\alpha=1}$ represent the eigenvectors $|1,0,0,0,0,0\rangle$ and $|0,0,0,0,0,1\rangle$, which indicate that, once the boundary site $j=1$ or $j=6$ is reached, the particle is absorbed and cannot leave this position. On the other hand, the matrix $J_{\alpha=1}$ is diagonal, with elements given by the eigenvalues of $H_{\alpha=1}$. Again, due to the presence of the boundary absorbing sites two eigenvalues are null, which correspond to the unit values in the first two columns of $\exp(-tJ_{\alpha=1})$. The other eigenvalues of $H_{\alpha=1}$ can be read off from the decay constants in the exponentials above. Finally, the evolution operator as a function of time t is obtained from the matrix product $U_{\alpha=1}(0,t) = Q_{\alpha=1}\exp(-tJ_{\alpha=1})Q^{-1}_{\alpha=1}$, Eq. (5.1), where $Q^{-1}_{\alpha=1}$ denotes the inverse matrix of $Q_{\alpha=1}$. Any relevant quantity can be calculated from the time evolution operator. For example, in the specific case with $j = j_0 = 2$ and Eqs. (B.3)-(B.4)

$$|\psi(t)\rangle = U(0,t)|\psi(0)\rangle, \tag{B.3}$$

$$P(j,t) = \langle j|\psi(t)\rangle = \langle j|U(0,t)|\psi(0)\rangle. \tag{B.4}$$

leads to the following exponential decay,

$$\begin{aligned} P_{\alpha=1}(j_0,t) &= \langle j_0|U_{\alpha=1}(0,t)|j_0\rangle = 0.320\,e^{-0.485t} \\ &+ 0.180\,(e^{-0.968t} + e^{-1.219t}) \\ &+ 0.393\,e^{-1.327t}. \end{aligned} \tag{B.5}$$

We finally mention that the above procedure can be applied to any other value of $\alpha \in (0,2]$ by using Eqs. (5.3)-(5.5).